Technical Report No. 143

4951-1-T

STUDIES IN DIGITAL COMMUNICATIONS

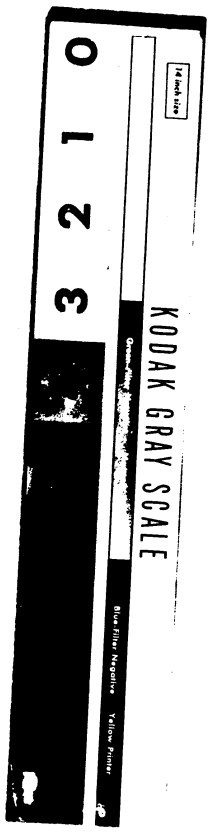

PART I: FEASIBILITY OF ASYNCHRONOUS MULTIPLEXING

PART II: PERFORMANCE OF HIGH-SPEED DIGITAL COMMUNICATIONS OVER TROPOSCATTER LINKS

by

M. P. Ristenbatt
K. A. Haines

COOLEY ELECTRONICS LABORATORY

Department of Electrical Engineering
The University of Michigan
Ann Arbor

Contract No. DA-36-039 sc-89168
U. S. Army Electronics Material Agency
Fort Monmouth, New Jersey

August 1963

ACKNOWLEDGMENTS

A number of people contributed to the work reported herein. Mr. Timothy Felisky conducted the early work in implementing the single channel extremal coding on the computer, and also built the analog extremal coding system. Credit is due Mr. Stephen Weinstein for early work in the buffer analysis of the asynchronous multiplexing system. Also Mr. Weinstein did initial work for the troposcatter problem. Both Mr. Felisky and Mr. Weinstein left our employ before this report was written.

Mr. T. G. Birdsall was invaluable as a technical advisor throughout this work. In addition he conducted the computer experiments for the initial buffer analysis that was run early in the program. We gratefully acknowledge the contribution of Mr. James Daws who was responsible for the equipment and computer operations during the latter half of the program. Credit is also due Mr. Robert Carlsen who formulated the problem of determining sync behavior under fading.

We also owe thanks to the members of the Signal Corps Communications Security Division for providing necessary technical and operational information.

TABLE OF CONTENTS

TABLE OF CONTENTS (Cont.)

LIST OF ILLUSTRATIONS

LIST OF ILLUSTRATIONS (Cont.)

LIST OF ILLUSTRATIONS (Cont.)

LIST OF TABLES

LIST OF SYMBOLS FOR PART I

α_o	=	Probability of a buffer being empty directly after a clock pulse
b(k, N', a)	=	Binomial distribution function for k events in N' samples, each independent event having a probability of a
β_k	=	Probability density for buffer occupancy, i.e., probability that k buffer stages will be filled directly before the clock pulse
c	=	Critical value of N' for which a F.O.F. of > .01 exists in the buffer
F.O.F.	=	Freezout fraction, i.e., fraction of total extrema frozen out by the buffer
$f_1(t)$	=	Probability density function for the length of type 1 talk bursts
$f_2(t)$	=	Probability density function for the length of type 2 talk bursts
k	=	Number of extrema generated in a clock pulse interval
L	=	Mean talk burst duration
M	=	Buffer size, i.e., number of slots which may contain samples simultaneously in the buffer
n	=	Number of resumptions of a talker without intervening talk bursts by his communicant
N	=	Number of sources comprising the multichannel link
N'	=	Number of sources in simultaneous talk bursts
p	=	Probability that a talker will be in talk burst
p(k, u)	=	Probability of a total of k extrema generated by N parallel sources in a time interval, τ
$p_1(t)$	=	Probability density function for the length of resumption pauses
$p_2(t)$	=	Probability density function for the length of response pauses
Q	=	Mean type 2 talk burst length
r	=	A random number selected from a random number generator
R	=	Average extrema rate for a single source
R'	=	Extrema rate for a single source in a talk burst
S/N	=	Rms average signal power to noise power ratio
t	=	Real time in seconds
t_F	=	Average time that $u > u_c$ is maintained
T_{f1}	=	Length of type 1 talk burst
T_{f2}	=	Length of type 2 talk burst
T_{p1}	=	Length of resumption pause
T_{p2}	=	Length of response pause
τ	=	Clock pulse interval, i.e., interval between times at which samples are

selected from the buffer and transmitted

u = Short term average extrema rate

u_c = Critical value of u for which a F.O.F. of > .01 exists in the buffer. This is related to c by Eq. 7

LIST OF SYMBOLS FOR PART II

α	=	Absolute voltage signal-to-noise threshold
B	=	IF bandwidth (before discriminator)
D	=	Deviation ratio; ratio of the peak allowable frequency deviation of the FM carrier to baseband bandwidth.
DCPSK	=	Differentially coherent phase-shift keying
δf	=	Rms frequency deviation produced by a single channel about its particular binary subcarrier
ΔF	=	Rms frequency deviation for a multichannel system about the FM carrier
E_b/N_o	=	Ratio of mean signal energy to noise power per cycle
E'_b/N_o	=	Ratio of short term signal energy to noise power per cycle
f(t)	=	Amplitude output of the dual diversity summing device
f_b	=	Bandwidth of the fading signal
f_o	=	Highest frequency in FM baseband
FSK	=	Frequency-shift keying
k	=	Critical fading level, expressed as a fraction of the voltage mean
k_1	=	Threshold ratio for a single channel system
k_2	=	Threshold ratio for a two-channel system
k_3	=	Equivalent threshold ratio for a two-channel system to be used as a single channel threshold ratio
m	=	Order of diversity
m(t)	=	Signal level uncorrupted by fading
$n_i(t)$	=	Internal noise signal on the ith channel
$p[x_i(t)]$	=	Probability density of the fading signal amplitude $x_i(t)$
$p_2(t)$	=	Power signal-to-noise ratio for a two-channel system
PCM	=	Pulse code modulation
P_E	=	Probability of bit error as a function of R
P_{EF}	=	Probability of bit error with fading
PSK	=	Phase-shift keying
$P_i(f_bT, f_bt_o, k)$	=	Probability of one or more fades of length greater than or equal to t_o during an observation time T on channel i

LIST OF SYMBOLS FOR PART II (Cont.)

$P(f_b T, f_b t_o, k)$	=	Probability of one or more fades of length greater than or equal to t_o during an observation time T. The critical fade ratio is k
$P_{1,2}(f_b T, f_b t_o, k)$	=	Probability of one or more fades of length greater than or equal to t_o, during an observation time T, for a two channel switched diversity system
$P'(0)$	=	Average time density of occurrence of a fade (may be interpreted as the probability of a fade in the time interval $1/f_b$)
$P'_{1,2}(0)$	=	Probability of a fade in the interval $1/f_b$ for a two channel switched diversity system
R	=	Ratio of the short time mean signal energy to twice the noise power per cycle
S/N	=	Rms signal power to noise power ratio
σ_n	=	Rms noise level
t_o	=	Length of a critical fade
T	=	Observation time
TW	=	Time bandwidth product
τ	=	Baud time (duration of elementary telegraph waveform)
$v_i(t)$	=	Signal voltage-to-rms noise ratio for an i-channel system
V_x^2	=	Expected value of x^2
V_y^2	=	Expected value of y^2
$x_i(t)$	=	Signal amplitude variations caused by fading on the ith channel
y	=	A Rayleigh distributed random variable

ABSTRACT

Part I describes experiments and calculations aimed at demonstrating the feasibility of asynchronous time multiplexing for multichannel speech. This multiplexing method was proposed and an initial evaluation done in a predecessor contract. The work here generally served to elaborate on the theoretical analysis and predictions made previously, and demonstrated them in the laboratory. The experiments tested various aspects of the method, and culminated in a realistic multichannel experiment with extremal coded speech signals.

The major feasibility demonstrations were done by using a digital computer with A-D equipment. However, an analog extremal coding system was built in order to demonstrate the equipment simplicity.

The work here showed that asynchronous time multiplexing is feasible, under the conditions treated, for systems having as few as 24 sources. It was concluded that the advantage of this method over sychronously multiplexed PCM is about 2.7 for 100 sources, and 2.1 for 24 sources. Increases in this advantage should be possible with system improvements. The speech quality with this advantage is not distinguishable, with casual listening, from that of the usual PCM.

The feasibility demonstrations here indicate that there are no evident technical reasons preventing application of asynchronous time multiplexing. We feel this method should eventually supplant the synchronous multiplex method whenever bandwidth is sufficiently important to warrant the change.

Part II is a theoretical evaluation of the critical issues when sending high speed digital data over troposcatter radio links. Troposcatter fading causes errors, assuming synchronization, and also influences the difficulty of maintaining synchronization. The first issue is fairly well treated in the literature, and the literature results are summarized here. The major effort was devoted to evaluating the effect of the fading on maintaining synchronization.

The technique involved here was to apply previously reported level crossing data for Rayleigh fading processes, which were run on an analog computer. These basic Rayleigh fading results were then adapted to both a switched diversity and an equal gain diversity case. This provided the probability of exceeding certain fade lengths in given observation intervals.

It was found that if digital synchronization equipment can tolerate fades of the order of 50 milliseconds, synchronization should be no problem over a troposcatter link under the conditions assumed. However, if the equipment can only tolerate fades of the order of a few milliseconds, the synchronization will not be effective.

These results indicate both a general technique for evaluating the synchronization problem under fading conditions, and indicate the required equipment capabilities in order to operate successfully with digital data over troposcatter links.

PART I: FEASIBILITY OF ASYNCHRONOUS MULTIPLEXING

This work on asynchronous multiplexing essentially extends work which was done on the predecessor contract (DA 36-039 sc-87172) and which was reported in Ref. 1.

The idea of asynchronous multiplexing resulted from an investigation designed to find more efficient ways of sending digital speech over a common facility. The present method for doing this is to use synchronously multiplexed PCM.

In this section we will first review the asynchronous system, and then describe experimental results of running a buffer in a manner proposed by the original assumptions and predictions. Next we will describe multichannel experiments and analyses designed to demonstrate feasibility of asynchronous multiplexing. Finally we will describe two methods by which single channel extremal codings were experimentally implemented.

1. REVIEW OF ASYNCHRONOUS MULTIPLEXING SYSTEM

During the predecessor contract on this work, a time multiplexing system for digitalized speech sources was proposed which we have called asynchronous multiplexing. We will now consider the basic factors in asynchronous multiplexing, review the system, and note the summary of a previous analysis and prediction.

1.1 Basic Factors in Asynchronous Multiplexing

If a number of speech sources are to be multiplexed on a common digital channel (or trunk), a standard method is to use synchronous time multiplexing of the PCM samples. Synchronous operation refers to the fact that each connected source is given a single channel slot within a frame. With such synchronous multiplexing the connected speech source is sampled regularly at the Nyquist sampling rate.

This operation has two disadvantages. (1) If the speech sources using the common facility are telephone communicators, each source uses his allotted part of the channel less than one-half of the time, because each is in a two-way conversation. (2) The regular sampling used with such synchronous multiplexing provides enough samples to insure that all information is transmitted. However, a great deal of the time, redundant samples carrying very little or no information are transmitted.

As a result of work done on the predecessor contract, it was proposed that an appropriate irregular sampling of each speech source be utilized, and that each speech source

seek access to the transmission link only when it has a sample to transmit. In other words, since the samples from each source occur irregularly, it is proposed that the samples from all the sources be allowed to enter the channel asynchronously without prior arrangement.

Such asynchronous time multiplexing may be regarded as a form of "demand matching" (Filipowsky Ref. (2) and (3)), where a source has access to the channel only when it has information to transmit. This means both reducing redundancy of the single source and smoothing the nonuniform flow of information from the multiple sources. In an ideal multichannel case, demand matching would allow the channel to handle all the information from all of the sources. Further, all the information would be statistically stable enough so that the channel could operate at a uniform rate (without a buffer), even though the individual sources created information at a sporadic rate. In practice one cannot realize this ideal. Not all of the information can be transmitted (a situation usually called freezeout), and the information rate of the total ensemble of sources is not perfectly constant so that some buffering is required.

Work on an irregular sampling for speech, which permits realization of the asynchronous time multiplexing described here, is reported in Mathews (4) and Spogen, et al., (5). This sampling method has been called "extremal coding" or "selective amplitude sampling" (SAS). The two major aspects of extremal coding are: (1) the samples occur irregularly, and (2) the average rate of occurrence is about one-fifth that of the Nyquist sampling rate .

1.2 General Description of Asynchronous Multiplexing System

Figure 1 shows a block diagram of the transmitter side of the proposed asynchronous time multiplex system. Irregular analog samples (which occur only when a source is active) have access to an M-sample buffer after digital encoding. The irregular sampling allows: (1) sampling which reduces redundancy from that of regular sampling and (2) a more uniform flow of total samples from the N sources. A sample is removed from the buffer every τ seconds (synchronously).

If the buffer is full, an arriving sample will be "frozen out" or rejected. If the buffer is empty throughout a transmission interval τ, the channel will be "idle" for this interval (data that does not require real time transmission could be inserted in such idle time).

Any irregular sampling (of analog waveforms) must be accompanied by time information. As originally proposed, it was assumed that the number of sources, N, be sufficiently high that the time between transmitted samples will be small, and only "buffer-delay-time" need be sent in order for the receiver to locate accurately the time placement of samples (shown in Fig. 1). Since this system runs asynchronously, a "source identification" must also accompany each sample.

As mentioned, the system envisaged incorporated "extremal coding" as a particular irregular sampling method. Extremal coding refers to the process of sampling the waveform

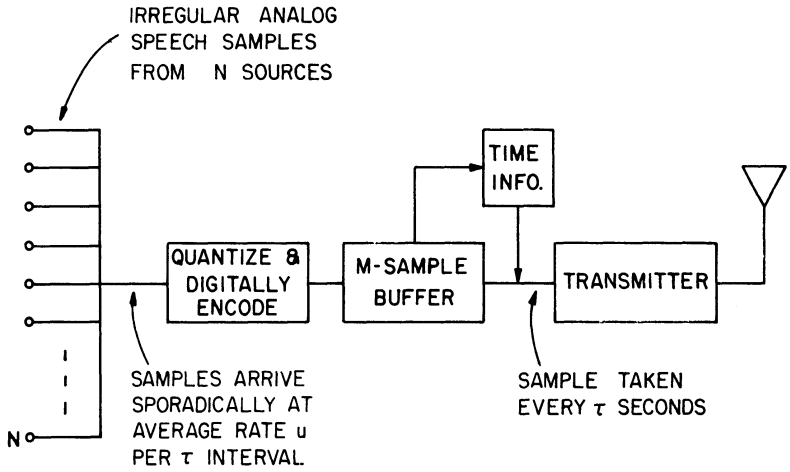

Fig. 1 Transmitter Block Diagram of Asynchronous Time Multiplex System

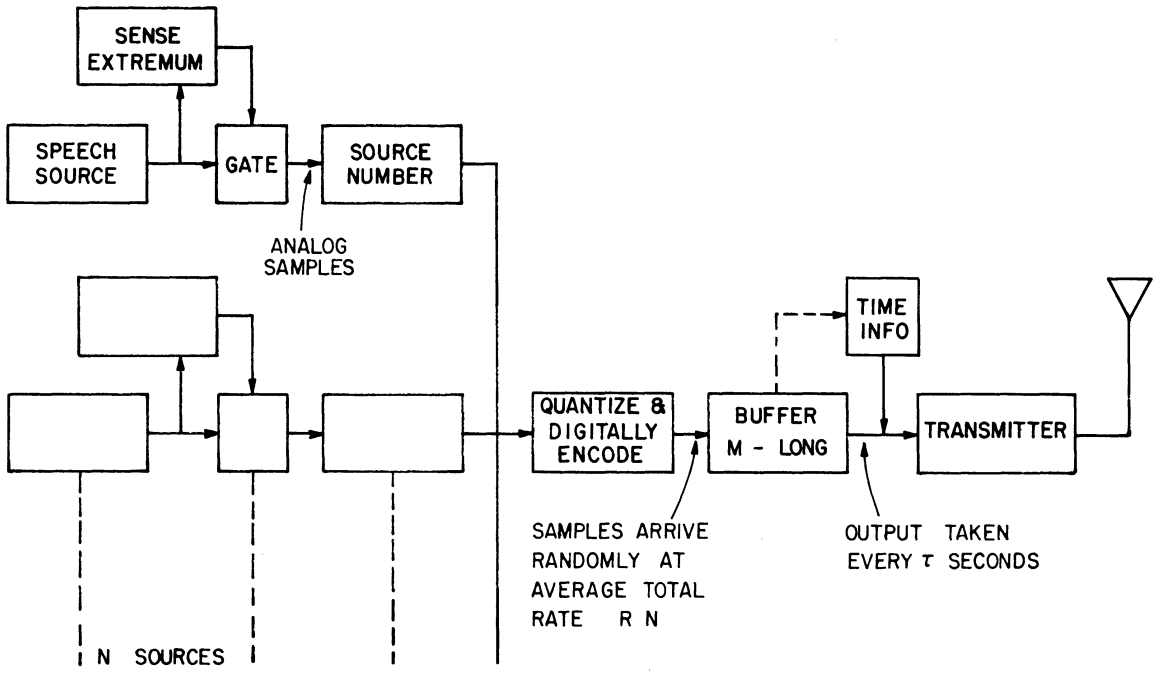

Fig. 2. Block diagram of asynchronous time multiplexing using extremal coding.

only at local "extrema" (local maximum or minimum), and sending only these values. At the receiver end one may fit a waveform to these quantized irregularly-spaced samples (or "boxcar" and filter the irregular samples). This method has been shown to yield very good speech in experimental tests, Ref. (4) and (5). It represents a useful sampling method for running a multichannel situation asynchronously.

When extremal coding is considered, the general block diagram of Fig. 1 is replaced by the more specific one of Fig. 2. The first function is to sense the extrema, and allow only amplitudes at extrema to pass through a gate. A source identification must next be inserted.

The amplitudes of the extrema are then digitally quantized and coded by a common unit. This information feeds the buffer asynchronously. Parameters will be chosen so that only "buffer delay" time information need be sent.

1.3 Summary of Previous Analyses and Prediction

Using the extremal coding referred to above, at the end of last year's work a prediction was made for the expected improvement over synchronous systems. In this section we wish to simply review this prediction and the reasoning behind this prediction. Later in this section we will portray a more sophisticated analysis and prediction. The new prediction will differ somewhat from the previous prediction, but not radically.

The prediction presented last year was based first on choosing a certain number of connected sources (which determined both the total rate and the amount of time information that needed to be sent), secondly on choosing the average extrema rate from each source (which is determined by the coding and the resulting quality), and finally on the assumption that the distribution of the occurrences of the multichannel extrema in any clock pulse interval is Poisson (which is necessary in order to apply the previous buffer analysis). The numbers chosen for last year's analysis were as follows. A 100 channel system was assumed. This relatively large value was chosen in order to be assured of a Poisson distributed extrema distribution function whose mean value is independent of time, and also so that one need only send time information denoting the amount of buffering. The extrema rate was based on the results in Refs. 4 and 5, wherein it was concluded that an extrema rate of about 1500 for an active source is reasonable. Next a design value for the fraction of extrema frozen out had to be chosen. This freeze out fraction was chosen to be .0005 which was assumed reasonable for extremal coding. It was also necessary to assume some average fraction of time during which all of the connected sources were active. This average fraction or "on" time was taken to be about one-half.

To emphasize the major assumptions, then, the basic extrema rate was associated with "active" sources and this was taken to be 1500 extrema per second. Enough sources were included in the system so that exactly half of them were active or generating extrema at any time. It was further assumed that the Poisson distribution applied to this combined average rate and activity state. Also a freeze out fraction of .0005 was used.

Under the foregoing assumptions, it was concluded that the bit rate could be reduced by a factor of 3 using the asynchronous system. This factor of 3 was associated with a small estimated drop in the quality of the speech, which is of course related to the quality of the extremal coding method. It was estimated, based on data which is published in the literature, that a quantization signal-to-noise ratio of 21 db could be realized with this system. Since present military systems use 6 bits at 8 kc for an estimated 26 db quantization signal-to-noise ratio, it is predicted that extremal coding will entail about a 5 db signal-to-noise ratio loss. However based on experiments which were done in this laboratory, this is in the range where

the difference in quality is hard to detect by listening.

It was an expressed object of this year's work to perform whatever experiments and analyses were necessary in order to justify or correct the prediction which was made using the above previous gross model. In order to do this it was necessary to perform certain multi-channel experiments. Also single channel experiments were required in order to ascertain what minimum extrema rates could be achieved for a given listening quality. Both the multi-channel experiments and the results of the extremal coded channel will be reported in the following sections. The number of parallel channels is reduced from 100 and some of the previous assumptions are no longer held to be valid. First we will describe an experiment which corroborated the previous analysis of the buffer.

2. EXPERIMENTAL ACTION OF A 16 LONG BUFFER

The first experiment demonstrating the feasibility of asynchronous multiplexing consisted of running an experimental buffer (in a computer) under the conditions assumed in the analysis done last year (described above). The objective of this experiment was to corroborate the mathematical analysis done previously (Refs. 1 and 7). Also, results could be found with this experiment which were unattainable theoretically.

Note that the input to the buffer in this experiment consisted of events which were generated according to a Poisson statistic; hence this test did not test the validity of the Poisson assumption. Also, the experiment here utilized a constant "average rate of extrema" (a constant u). This assumption is not always valid, especially when the number of parallel channels is reduced substantially below 100 as in section 3.

This buffer experiment was programmed on a computer and used the Monte Carlo technique. The output from a random source available in the computer was operated on by a transfer function in order to go from the equally-distributed probability to a Poisson statistic.

2.1 Experimental Results

As mentioned, a Monte Carlo simulation of a 16-long buffer was run on a computer, in this case an IBM 709[1] in order to ascertain buffer aspects not amenable to analysis. The simulation effected a buffer where the input in each τ interval was determined by a Poisson random generator, and one sample, if available, was removed at the end of each τ interval. The Poisson random generator was effected by suitably grouping random digits from an equally-likely random generator. Such an equally-likely generator is available as a standard computer subroutine.

Freezeout conditions were noted by the occurrence of buffer content exceeding buffer length (16) in any τ interval. After a given buffer occupancy was recorded, samples were limited to 16, one sample was removed, and the next input was called for. The probability density of buffer occupancy (β_k) for u = 0.8 and 0.9 (see footnote 2) is shown in Fig. 3.

This data resulted from 20 runs of 1000 τ intervals for each of four initial buffer

[1] An IBM 7090 has replaced this IBM 709; later experiments were done on the 7090.

[2] As noted in Refs. 1 and 7, the u equals the average rate (taken across sources) of occurrence of samples in time τ.

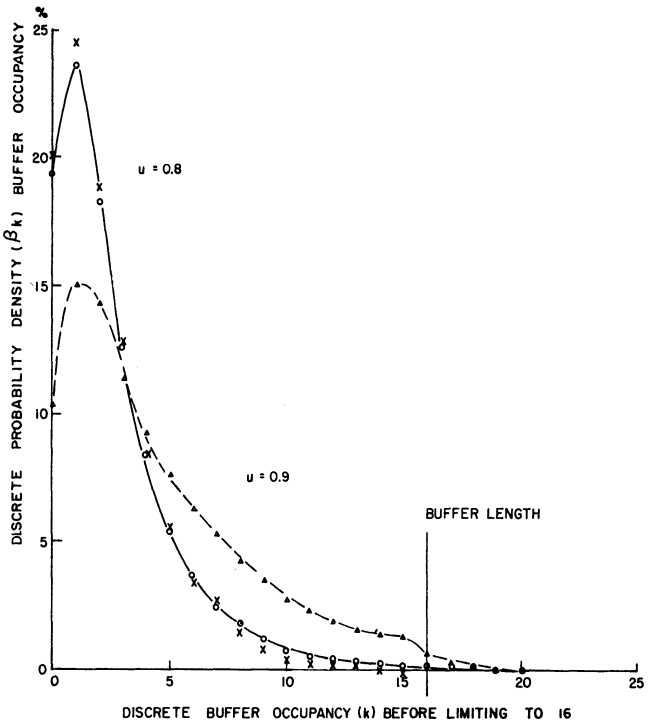

Fig. 3. Discrete probability density of buffer occupancy.

contents: 0, 5, 10, and 15 samples. Since the average, over 20, histograms of these results were essentially alike for the four different starting conditions, the results of these four were in turn averaged. It is these averages which are plotted in Fig. 3. An important conclusion is that averages over 1000 intervals are "steady-state" averages for u = 0.8 or 0.9. This is true since the averaged experimental values for each of the four initial contents are close to the theoretical β_k values (shown by x's in Fig. 3). Note that Fig. 3 should be read as a histogram; the points are connected only to aid in separating the two conditions.

The ordinate values of these curves show that the idle time, which is approximately $(1 - \mu)$, is as expected, and that the most likely buffer occupancy is one sample, which was predicted by the analysis of Ref. 1. The computer data also indicated freezeout behavior as predicted by the analysis; however, the freezeout data is not statistically significant since it's such a negligible percentage (< 0.05 percent).

Another Monte Carlo experiment was run to determine how many τ intervals are required for the buffer to recover to average occupancy after full load (where freezeout may have occurred). With initial contents of 15, the histogram of occupancy was noted for each of the first 120 τ intervals. One thousand sample points are used for each histogram. Selected positions from these are shown in Fig. 4.

It can be seen that, for u = 0.8, the buffer recovers to average conditions at about 80 τ intervals after full load. These curves depict the transient occupancy conditions after full load.

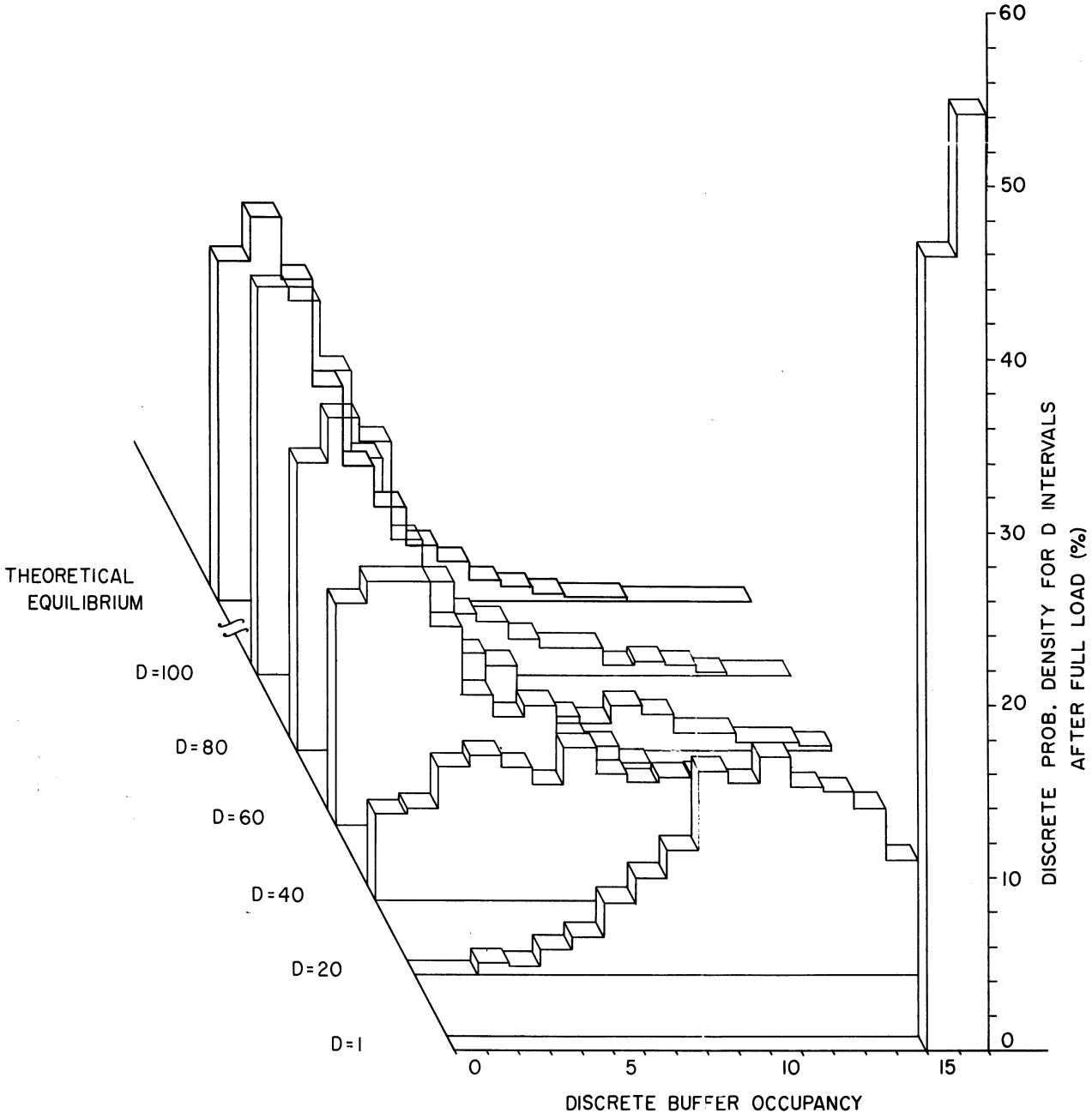

Fig. 4. Probability density of buffer occupancy after full load.

The above Monte Carlo results, along with the analysis done last year, show that under the given assumptions low freezeout can be obtained for modest buffer length if the input is Poisson distributed.

We will now describe a series of multichannel experiments whose purpose was to test the assumptions and parameter values assumed above. In effect, these experiments resulted in a more sophisticated analysis technique for the multichannel system.

3. MULTICHANNEL EXPERIMENTS

In last year's analysis (Ref. 1), discussed in section 1.3, it was assumed that the number of sources (N) involved is large enough so that one can consider the number of "active" channels as being independent of time. As the number of sources decreases, it is clear that the number of sources which provide extrema simultaneously fluctuates, and these fluctuations cannot be ignored as N becomes small. This is obvious in the limiting case for N = 1. The primary differences between the analysis (and experiments) which follow and last year's analysis stems from this fact of here accounting for the fluctuating number of "active" sources. A second difference discussed in section 3.2.1 is that the previously used F.O.F. (freeze out fraction) of .0005 is increased substantially.

Each source provides extrema only when the talker is actually talking. We will call these periods of activity "talk bursts." Basically a talk burst is related to the time during which energy above a certain minimum level is being transmitted. In the experiments done below, an end of "talk burst" was assumed whenever no extrema occurred for 50 milliseconds or more. Thus in this analysis, talk bursts do not include pauses greater than 50 msec between phrases or words, nor do they include those periods when the talker is listening to his communicant. Obviously this means that a source is in talk burst periods less than one-half of the time. In the following analysis, it is assumed that each source generates extrema by some stationary process during the time in which the user is actually engaged in a talk burst. There are no extrema generated at other times.

The distribution function for the number of extrema per clock pulse interval (τ) when N' sources are in simultaneous talk bursts is shown to be approximately Poisson in Section 3.1. In Section 3.2 the effects of freezeout on a voice specimen are described; then use is made of the results of Section 3.1 to choose values of sampling rate, $1/\tau$, for a parallel channel system by considering an analysis based on talk bursts. A 24 channel system experiment is described in Section 3.3 and the effects of the buffer on an actual voice specimen which comprises one of the channels of this multichannel system are examined.

3.1 The Extrema Distribution Function

As noted the previous analysis assumed that the extrema distribution function may be approximated as Poisson for the multichannel system (Ref. 1). This implies that the probability of "k" extrema occurring in any clock pulse interval (τ) is independent of the outcomes of all other clock pulse intervals, and is given by

$$p(k, u) = e^{-u} \frac{u^k}{k!}, \tag{1}$$

where: $p(k, u)$ = probability of k extrema among the sources in a time interval τ,

u is the average number of extrema per clock pulse interval.

In the previous analysis this assumption was applied to an assumed fraction of the total N connected sources (N/2 sources were assumed active at any given time). Since the analysis here accounts for a varying number (N') of "sources in simultaneous talk burst," we are interested in testing the Poisson assumption for N' talkers in simultaneous talk bursts.

The validity of this Poisson assumption was investigated in computer experiments where N' took on values ranging from 2 to 24. Note that, if N' is of the order of 24, the N connected sources are of the order of 50. We will now describe the experiments which tested the Poisson assumption.

The experiment was carried out as follows: first an analog voice specimen was sampled at a 40 kc rate (the 40 kc choice is described in the next section). Then, via a computer program (see Section 4.1) the "extrema" of these 40 kc samples were found. At this point all intervals greater than 50 msec containing no extrema were removed from the data, leaving only periods of talk bursts. It was the occurrence of the extrema that was tested for Poissonness. Thus the occurrence or lack of occurrence of an extrema was retained from the original samples, while the level information, being of no consequence for this experiment, was discarded. The remaining data were then split up into sections, and these (presumedly independent) sections were used to implement N' "simultaneous talkers in talk burst."

After performing the above operations on the original voice specimen, a total of 216,000 of the resulting samples (hereafter referred to as sample slots) were used to provide an equivalent multichannel specimen of length $5.4/N'$ seconds over which the statistics could be found.

A computer program allowed probability densities to be constructed for each value of N'. This process is depicted in Fig. 5. Basically this consists of dividing the total 40 kc "slots" into N' parallel groups. This is done in a straightforward "sequential" way. The number of times in which k extrema occur in corresponding slots is then counted. This directly gives an experimental measure of $p(k, u)$, the probability of getting k extrema in any clock pulse interval of length $1/40 \times 10^3$ for N' simultaneous talkers. The parameter u is defined as the average number of extrema generated by the N' channel system in a clock pulse interval.

The details of this computer program are given in Appendix A. The results are shown in Figures 6 and 7. The actual extrema distribution function for the number of extrema per clock interval is shown along with the corresponding Poisson distribution value given (previously) by Equation (1).

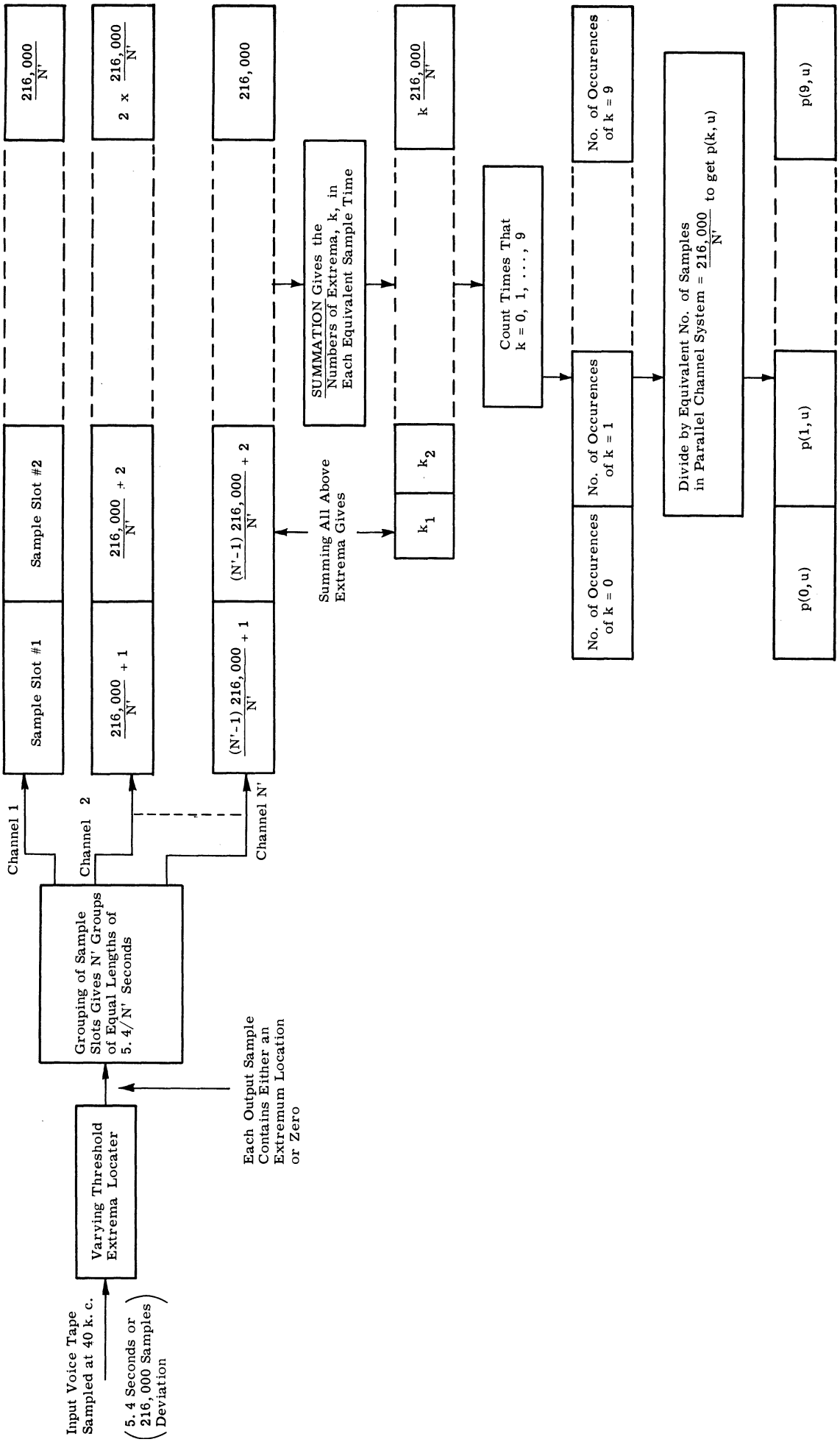

Fig. 5. Calculation of extrema probability, $p(\kappa, u)$

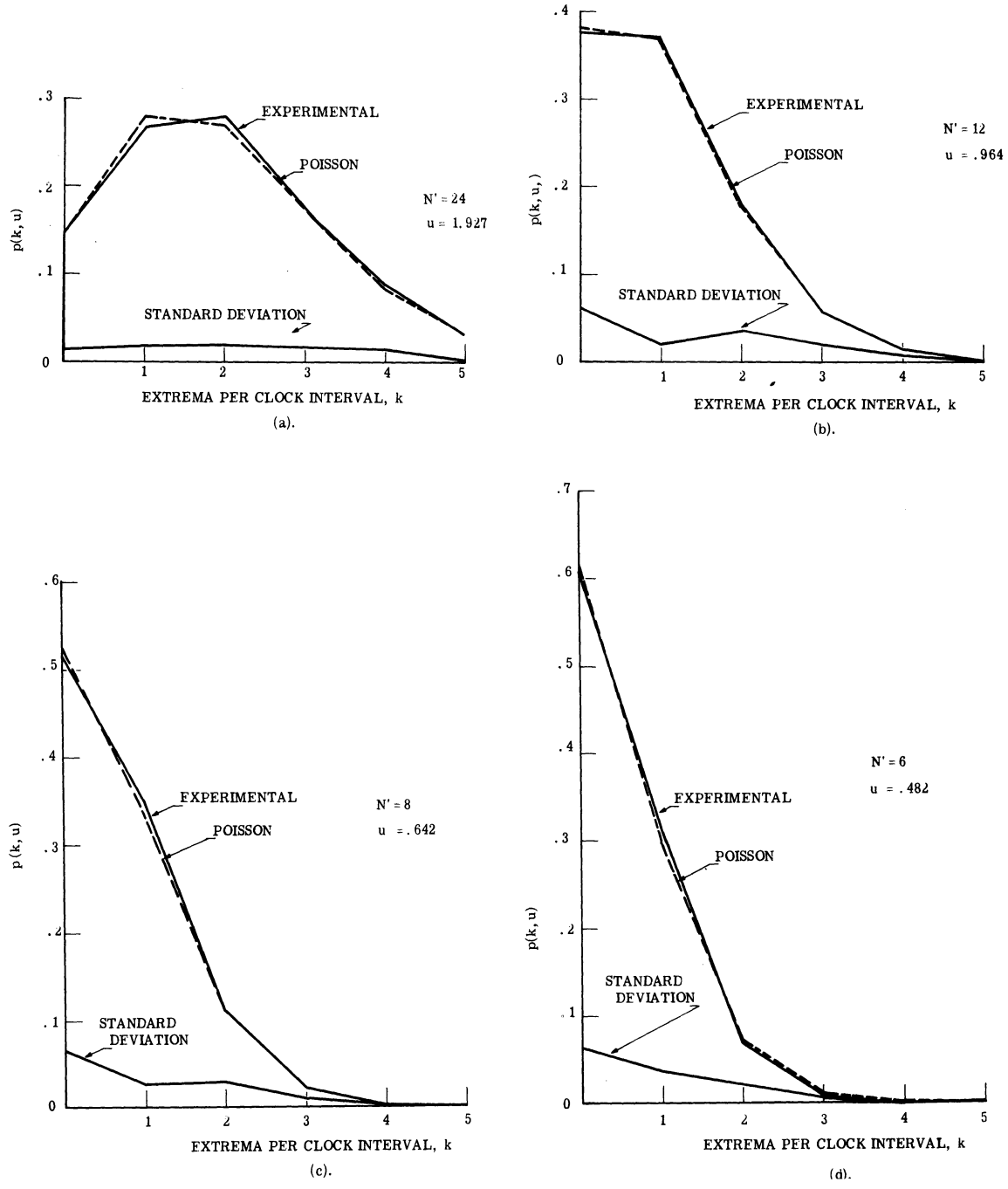

Fig. 6 Experimental results for distribution of extrema from N' simultaneous talk bursts. (a) N' = 24, u = 1.927, (b) N' = 12, u = .964, (c) N' = 8, u = .642, (d) N' = 6, u = .482.

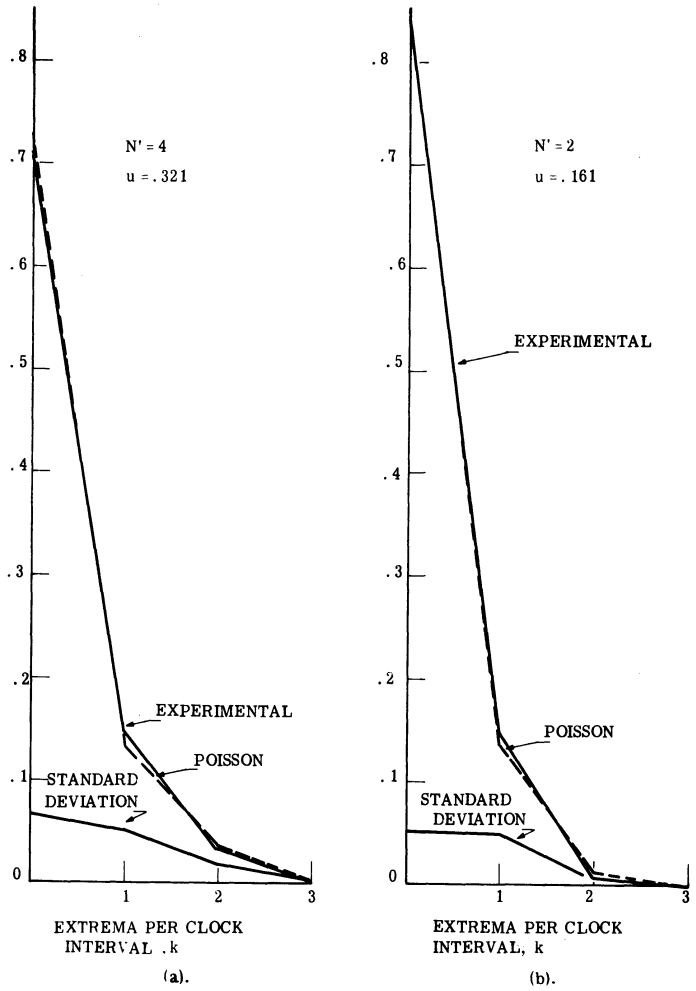

Fig. 7 Experimental results for distribution of extrema from N' simultaneous talk bursts. (a) N' = 4, u = .321, (b) N' = 2, u = .161.

For both the experimental distribution function and the Poisson distribution function, the value of u is taken as .0803 N'. This value is arrived at as follows. The total number of extrema for the entire 216,000 samples was computed and the sum divided by 216,000, giving a value of .0803. This then corresponded to the average number of extrema generated by a single channel in talk burst. If all channels are independent, as was assumed, then the average number of extrema generated by N' channels in simultaneous talk burst is simply u = .0803 N'.

Using this value of u, Eq. 1 becomes

$$p(k, .0803\ N') = e^{-.0803\ N'} \frac{(.0803\ N')^k}{k!} \qquad (2)$$

As seen in Figures 6 and 7 the results indicate that the extrema distribution function is close to Poisson for all values of N' considered. Although it has not been plotted in the figures, it is interesting to note that the binomial distribution function is as good a match to the experimental results as is the Poisson distribution function for N' = 24 and 12. In addition, the binomial distribution is almost exactly equivalent to the experimental results for N = 2, 4, 6, and 8. The binomial distribution function for this u is given by:

$$b(k, N', .0803) = \binom{N'}{k} (.0803)^k (1 - .0803)^{N'-k}, \quad (3)$$

where: k is the number of extrema per clock interval.

Even though the figures indicate that the distribution functions are approximately Poisson for the relatively large averaging time of 5.4/N' seconds (216,000/N' clock pulse intervals), they do not necessarily indicate that the events (extrema) are independent for each clock pulse interval. It seems intuitive in fact, that for the single channel case (N' = 1), the events in each clock pulse interval are not independent. If there is a dependence relationship, then the process could still be viewed as being stationary in every respect except that its expected value varies. Hence its nonstationarity appears in this special way.

An averaging over shorter time intervals was carried out in order to investigate this stationarity question in more detail. For each value of N', the total specimen of 5.4/N' seconds was broken down into several smaller specimens of 22.5 msec (900 clock pulse intervals) each. This would give 10 such smaller specimens from the original specimen when N' is 24, and 120 when N' is 2. For each value of N', distribution functions were calculated for each of the smaller specimens and a standard deviation was computed of these distributions about the mean values of the original specimen. These standard deviations are shown in Figures 6 and 7. Large standard deviations would indicate that the events in each of the smaller specimens cannot be assumed to be independent from all of the other smaller specimens. From the figures it appears that for larger values of N', the ratios of the standard deviations to the mean values are quite small, and as N decreases these ratios become larger as expected. When the original voice specimen was replaced by a random extrema generator which provided independent outputs, a standard deviation was computed by the above method for N' equal 24. It is worth noting that these standard deviations were no less than those obtained when a voice specimen was used. Although it would be desirable to perform these experiments on even smaller sized specimens of about 90 clock pulse intervals each (2.25 msec) in order to investigate the stationarity of the process even further, the above comparison indicates that the process can be assumed to be stationary for N' greater than about 8.

On the strength of the above experimental results it can be assumed that the extrema location statistics of parallel channels of speech engaged in simultaneous talk bursts are equivalent to those of a Poisson generator. This result both bears on the following experiments (to be described) and on the previous analysis. If N (number of channels) is sufficiently high so that the variation of N' (number of simultaneous talkers) can be neglected, as was assumed in the previous analysis of section 1.3, then the above results verify that the extrema distribution function is Poisson for the N channel system.

The way in which the above results influence further experiments will become clear in the next section.

3.2 Parameter Selection for Asynchronous Multiplexing

As mentioned, the analysis presented herein differs mainly from the prior analysis in that here we account for the varying number of simultaneous talkers. In this section we will first describe a freezeout experiment which permits us to select tolerable freezeout conditions. Then, based on these conditions, other system parameters are derived.

3.2.1 Effects of Freezeout. First we wish to examine the freezeout situation. In the previous analysis (Ref. 1) it was assumed that an F.O.F. (freezeout fraction) of .0005 was tolerable. This was chosen then because a synchronous multiplex system (TASI---see Ref. 1) operated with a .001 F.O.F. However the TASI system caused consecutive samples to be frozen out. It can be shown that this causes average freezeout lengths of .03 seconds. This is an appreciable part of a syllable length, which averages about 150 msec. In the asynchronous multiplex system here, the frozen out extrema are selected from all parallel channels somewhat at random. Therefore the probability that several consecutive extrema from the same channel are frozen out is negligible. Primarily for this reason the chosen value of .0005 is much too conservative.

In order to arrive at a more reasonable "just tolerable F.O.F.," the following experiment was conducted. The computer selected the extrema from a voice tape by a varying threshold technique which provided good speech reproduction (see Section 4.1). Then each of these extrema was retained or discarded depending on the selection of a random sample from a group of numbers. As an example, if a F.O.F. of .10 was the desired freezeout value, each extremum was discarded when numbers from 0 to 9 were selected from amongst the numbers from 0 to 99. Otherwise the extrema were retained and recombined by a curve fitting technique to provide a new voice tape. Those F.O.F.'s investigated were, .01, .02, .05, .10, .20, and .40. These operations are illustrated in Fig. 8.

Aural examinations of the voice tape with these F.O.F.'s gave a good indication of the effects of these F.O.F.'s on the quality of the voice reproduction. From these results it appears that a F.O.F. of .01 is just barely perceptible. This value is therefore taken as a "just tolerable F.O.F." Values of F.O.F. greater than .10 seriously deteriorate the quality of the speech reproduction.

An interesting observation is that even with values of F.O.F. up to .40, the speech is intelligible if the system low pass cutoff frequency is raised from its normal value of 100 cycles to a value of about 400 cycles. Of course the fidelity of the voice reproduction is decreased. However, in actual telephone channels the low cutoff is 200 to 300 cps.

3.2.2 Choice of the Clock Pulse Interval, τ. We will now describe the method of choosing parameters for the asynchronous multiplexing system. In effect this amounts to arriving at a design value for the clock pulse interval τ. This clock pulse interval must not be

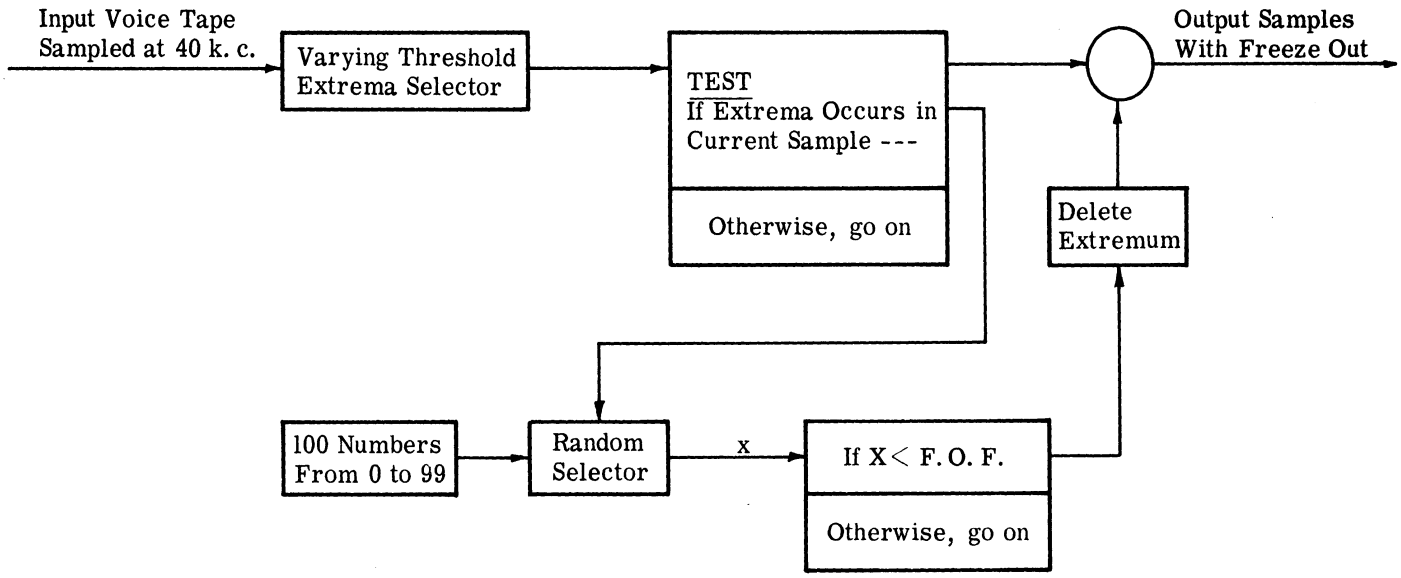

Fig. 8. Block diagram of computer experiment for freezeout fraction.

so large that an intolerable amount of freezeout will occur, nor must it be so small that the multichannel system has no information to transmit during many intervals. Since N' (the number of simultaneous talkers) is varying, the freezeout fraction of course also varies. Therefore, in addition to stating a just tolerable freezeout, one must state how much of the time this freezeout will be exceeded.

We may find the clock interval τ by choosing the following parameters:

(1) A "just tolerable F.O.F." will be exceeded only 1 percent of the time. This number was chosen as being a conservative value.

(2) The probability that a talker will be in talk burst, p = .4. This estimate is based upon the definition of a talk burst used here, and the measured statistics reported in Refs. 8 and 9.

(3) R', the rate of generation of extrema for a single talker while in a talk burst is 2300 extrema per second. This value of R' was taken from measurements of a previous experiment.

(4) A 16 stage buffer will be used.

(5) The distribution function for parallel channels in talk burst is Poisson (see Section 3.1).

Assumption (1) implies that a critical number of channels in simultaneous talk bursts, N', which gives a "just tolerable F.O.F." is exceeded with a probability of no greater than .01. Denote this critical value of N' as c. Since all channels are independent, c may be found from a solution of the cumulative binomial distribution, which gives the probability that there are more than c events out of N possible, if each has a probability p.

$$B(c, N, p) = .01 = \sum_{N'=c}^{N} \frac{N!}{N'!(N - N')!} p^{N'} (1 - p)^{N-N'} \qquad (4)$$

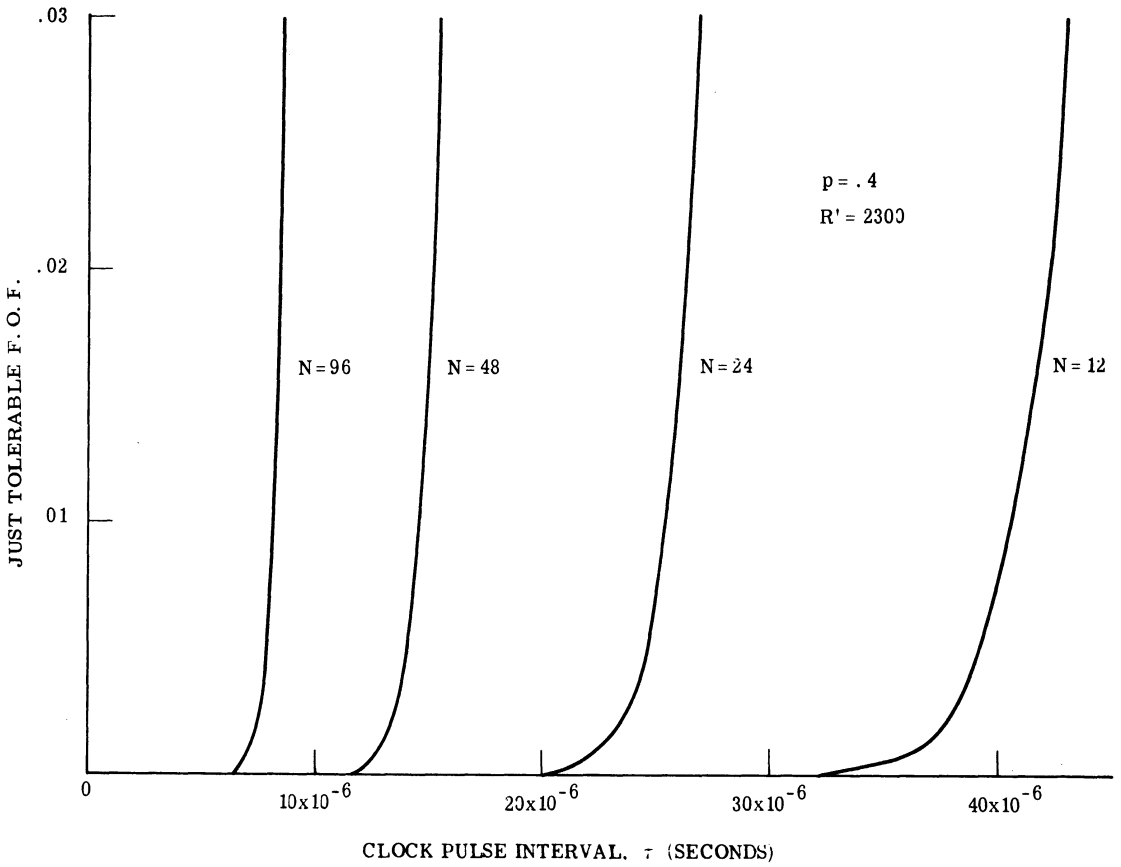

Fig. 9. Just tolerable F. O. F. versus clock interval τ

Since all buffering analysis centers around u, the ratio of average buffer input rate to average output rate, we can translate the varying N' situation into varying u by using the relation:

$$u = R' N' \tau \tag{5}$$

where: R' = extrema rate for a single source in a talk burst

N' = number of simultaneous talkers in talk burst

τ = length of a clock pulse period interval

If N' = c (critical value of N'), then the critical u (u_c) is given by:

$$u_c = R' c\tau. \tag{6}$$

We can now relate the critical value of u_c which is exceeded less than one percent of the time, to the value of τ through Eqs. 4 and 6. Since the extrema distribution has been shown to be Poisson, the analysis of Fig. 30 of Ref. 1 holds, and may be used to relate u_c to F.O.F. Thus we can relate values of τ to just tolerable F.O.F. for various values of N (connected channels). This relationship is plotted in Fig. 9.

In this figure, the just tolerable freezeout fraction is plotted versus the clock interval τ for various values of N, given that the just tolerable F.O.F. is exceeded only one percent of the time. For all values of N shown, the slope of the curve is so great that there is not much difference (in the related τ interval) between a tolerable F.O.F. of .01 and .03. This indicates that there is not much dependence of τ on the actual value of tolerable F.O.F. As mentioned,

Fig. 9 uses the freezeout method of calculation depicted in Fig. 30 of Ref. 1. This figure in Ref. 1 is based on the following calculation:

$$\text{F.O.F.} = \frac{u_c - 1 + e^{-u_c \alpha_o}}{u_c} \tag{7}$$

where: u_c = critical u described above

α_o = a parameter which is calculated by the analysis of Ref. 1, and is equal to the probability that the buffer is empty directly after a clock pulse.

An assumption inherent in using the results of Fig. 30 is that u remains essentially constant for a large enough time to allow the buffer to reach a steady state. We can investigate this by examining the amount of time that u is greater than u_c. The average duration of time that u greater than u_c is maintained, can be calculated by the following binomial equation (Bullington, et al., Ref. 8):

$$t_F = L \sum_{k=c}^{N} \frac{1}{k} \frac{B(k, N, P)}{B(c, N, P)}, \tag{8}$$

where: t_F = average time that u greater than u_c is maintained

L = mean talk burst duration.

The resultant values of t_F are shown on the curves of Fig. 9 when L = 3 seconds. L of 3 seconds is a typical value estimated from the data of Ref. 8. It can be seen from Fig. 9 that t_F is equivalent to enough clock pulse intervals τ to cause a 16 stage buffer to reach a level which is at least equal to the steady state level for u_c. As an example, when N = 24 and $\tau = 25 \times 10^{-6}$ seconds in figure 9,

$$\frac{t_F}{\tau} = \frac{.27 \times 2300 \times 24}{.6} = 24{,}800 \text{ clock intervals.} \tag{9}$$

In Section 2.3 it was seen that only about 1000 clock intervals were required for the buffer to reach steady state.

The multichannel system simulation of the next section was carried out on a 24 channel system. When a just tolerable F.O.F. of .01 (a conservative figure) is assumed in Fig. 9, the resulting τ is:

$$\tau_{24} = \frac{1}{39{,}600} \approx \frac{1}{40{,}000} \text{ seconds.} \tag{10}$$

This value of τ was used both in the 24 channel simulation of Section 3.4, and in the tests for Poissonness described in the previous section.

In conclusion, a just tolerable F.O.F. may be selected from the above results, and

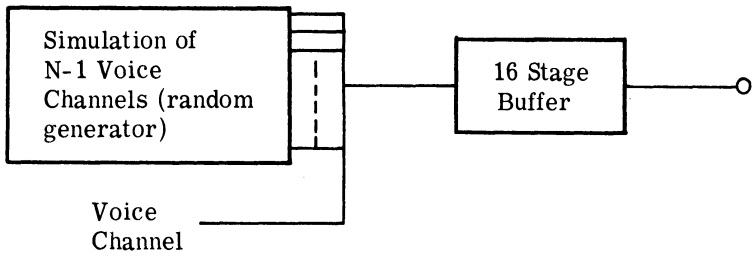

Fig. 10. Depiction of multichannel system simulation.

may then be used to select proper values for clock pulse intervals for any desired conditions of asynchronous multiplexing.

3.3 Multichannel System Simulation

In this section an over-all experiment is described which in effect represents a culmination of the previous work and results. This experiment essentially simulated an N channel system via a digital computer. This is accomplished by artificially simulating N-1 of the channels by a random extrema generator. These extrema are fed into a 16 stage buffer along with the extrema from the actual voice specimen of the Nth channel. The effects of the buffer freezeout on this Nth channel are then examined. A block diagram of this process is shown in Fig. 10. The details of the computer program are included in Appendix A.

The random extrema generator is a Poisson generator (see Section 3.1) whose mean extrema rate varies directly as the number of channels, N', which are engaged in simultaneous talk bursts. A sample of the random process N' may be acquired by using statistics from a study by Murphy and Norvine, Ref. 9, as discussed in the following paragraph. The random extrema generator then provides k extrema each clock pulse interval according to the probability density function;

$$p(k, N') = \ell^{-\tau R'N'} \frac{(\tau R'N')^k}{k!} \tag{11}$$

where: N' is a function of time, and R' = 2300.

We will first portray the method of implementing the random extrema generator in accordance with Eq. 11. Then the results of the experiment will be discussed.

3.3.1 Simulation of N' Channels in Simultaneous Talk Burst. In order to consider an N' channel simulation we must first discuss a single speech channel. A single channel may be synthesized by using the probability density curves of Ref. 9. Basically this involves the selection of simple algebraic formulae which may be used by the computer to generate pauses and talk bursts periods by a single talker, and which reasonably match the experiment data of

Ref. 9. In order to use the results of this data we must understand the relationship between our "talk bursts" (defined in Section 3), and "talkspurts" as used in the experimental study of Ref. 9. Talkspurts are defined as, ". . . speech by one party, including his pauses, which is preceded and followed, with or without intervening pauses, by speech from the other party . . . ." This implies that talkspurts may be made up of more than one talk burst. As noted before, a pause within a talkspurt occurs whenever speech energy is absent for 50 milliseconds or more. This in effect denotes the talk bursts. In our analysis, two kinds of talk bursts exist. The first kind is a talk burst which is preceded and followed by pauses and talk bursts of the other speaker. The second kind is either followed or preceded (or both) by a pause and then by one or more talk bursts of the same speaker. The first kind of talk burst includes all monosyllabic replies. Those pauses between talk bursts of the same speaker are defined as resumption pauses. Thus a sequence of resumption pauses and talk bursts of type 2 comprises a talkspurt. Those pauses between talkspurts of different speakers are defined as response pauses.

In order to synthesize the single channel system, we must choose algebraic expressions whose plots adequately match the experimental data of Ref. 9 for the talk bursts, the pauses, and the resumption probabilities (the probability of resumptions within a talkspurt). The algebraic expressions presented herein, which are finally arrived at after a trial and error type of curve fitting, use general functions of the type $t^n \exp(-at^x)$. They are reasonably simple, have mean values which correspond to the experimental data, and peak at approximately the correct places. We have chosen the probability density function for length of Type 1 talk bursts whose plot is the solid curve of Fig. 11. Figure 12 shows the assumed curve for lengths of Type 2 talk bursts, the solid curve of Fig. 13 the curves for lengths of response pauses, and the solid curve of Fig. 14 the curve for lengths of resumption pauses. The solid curve of figure 15 depicts the assumed curve for probability of resumptions within a talkspurt. It will now be shown that these solid curves approximately match the data compiled in Ref. 9, and given by the broken lines in the respective curves, and the additional figure 16.

The solid curves for response pauses, resumption pauses, and probability of resumptions in Figs. 13, 14, and 15 obviously match the broken lines taken from Ref. 9 and require no more comment. It then remains to validate the talk burst curves of Figs. 11 and 12 by use of the measured data on Fig. 16.

The broken line of Fig. 11 for Type 1 talk bursts is taken directly from the data of Ref. 9 by combining the two curves of Fig. 16. We may then assume that the solid curve for Type 1 talk bursts in Fig. 11 adequately matches the broken curve derived from Ref. 9. The mean value for the curve for Type 2 talk bursts of Fig. 12 is arrived at in the following manner. Consider these facts taken from the data of Ref. 9:

The mean length of Type 1 talk bursts (see Fig. 11) = .82 secs.

The mean response pause length (see Fig. 13) = .41 secs.

The mean resumption pause length (see Fig. 14) = .73 secs.

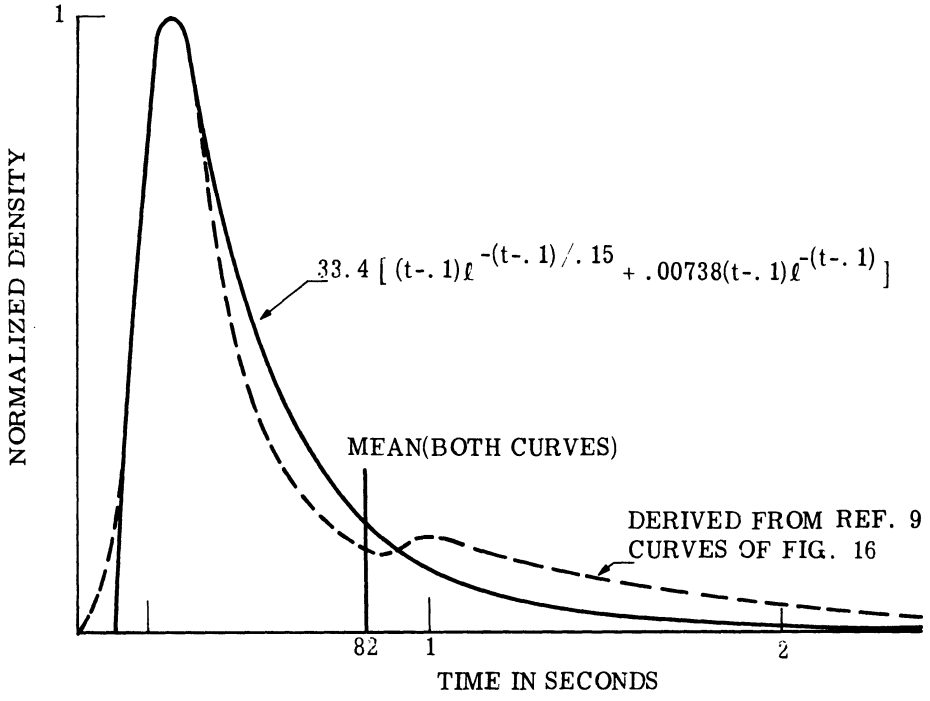

Fig. 11. Lengths of talkbursts (Type 1).

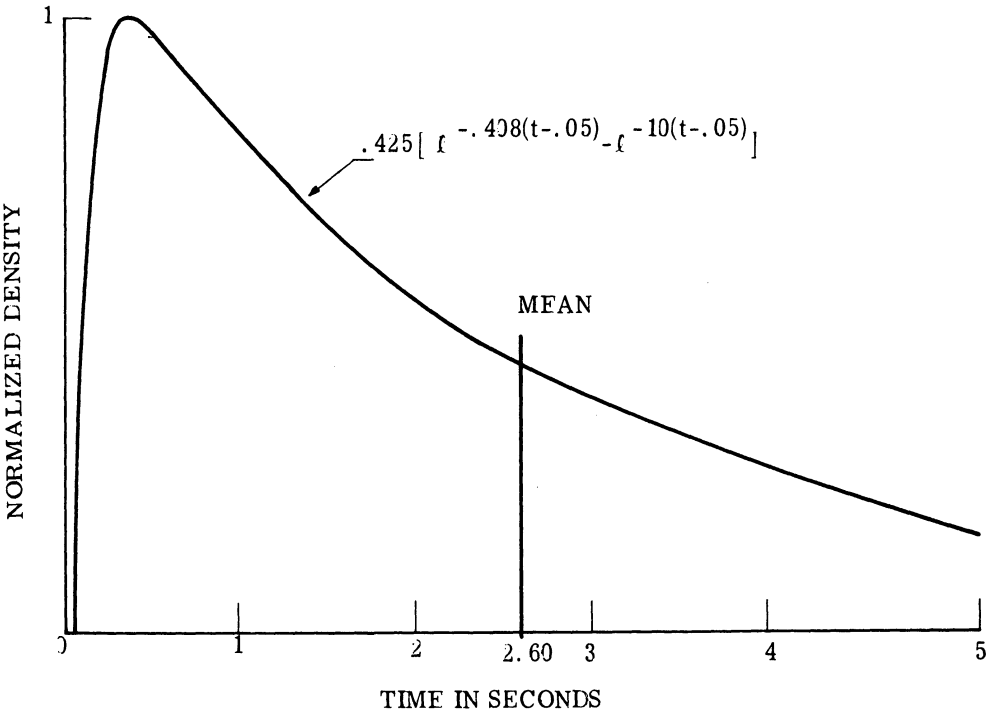

Fig. 12. Lengths of talkbursts (Type 2).

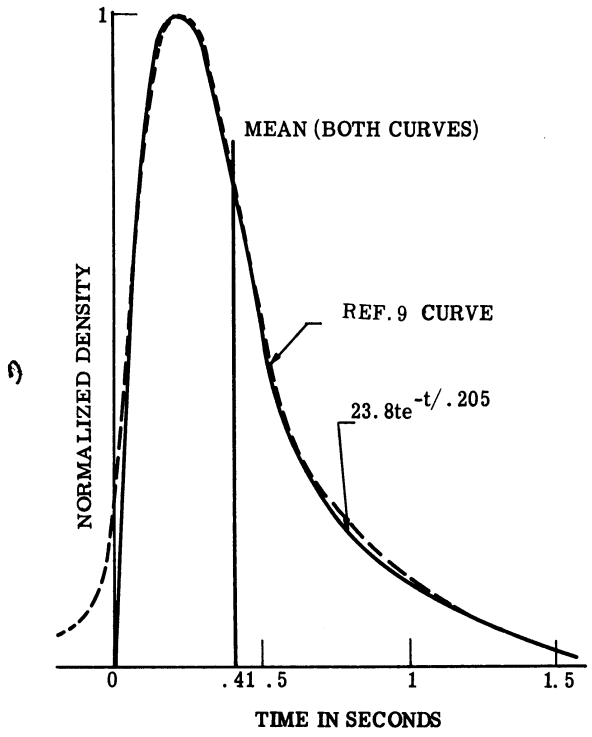

Fig. 13. Response Pauses

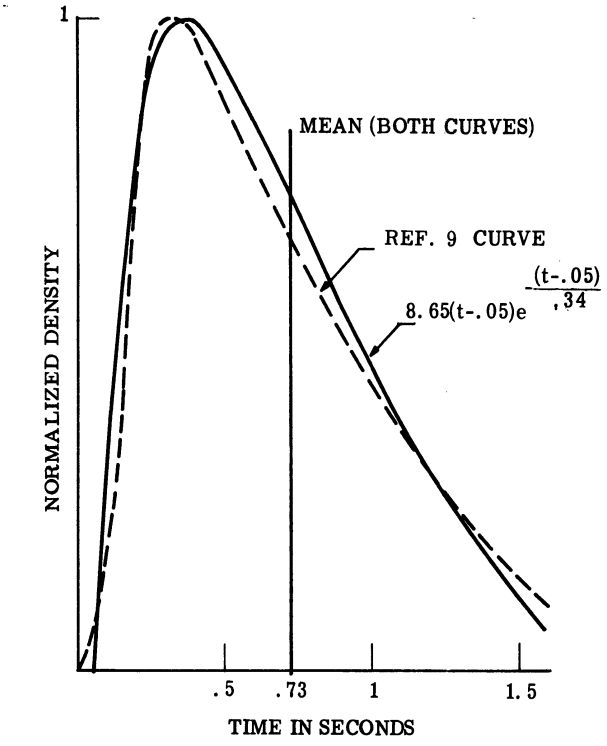

Fig. 14. Resumption pauses

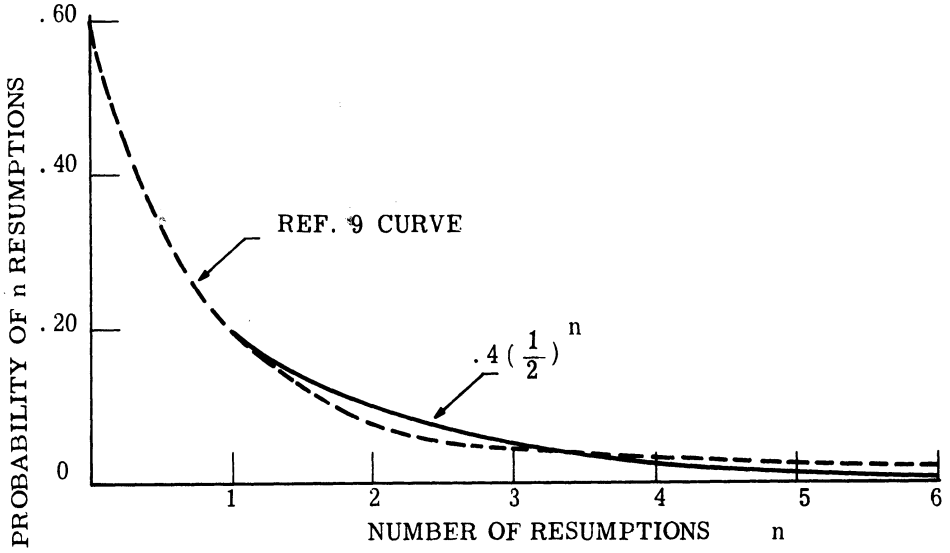

Fig. 15. Probability of resumptions in talkspurts.

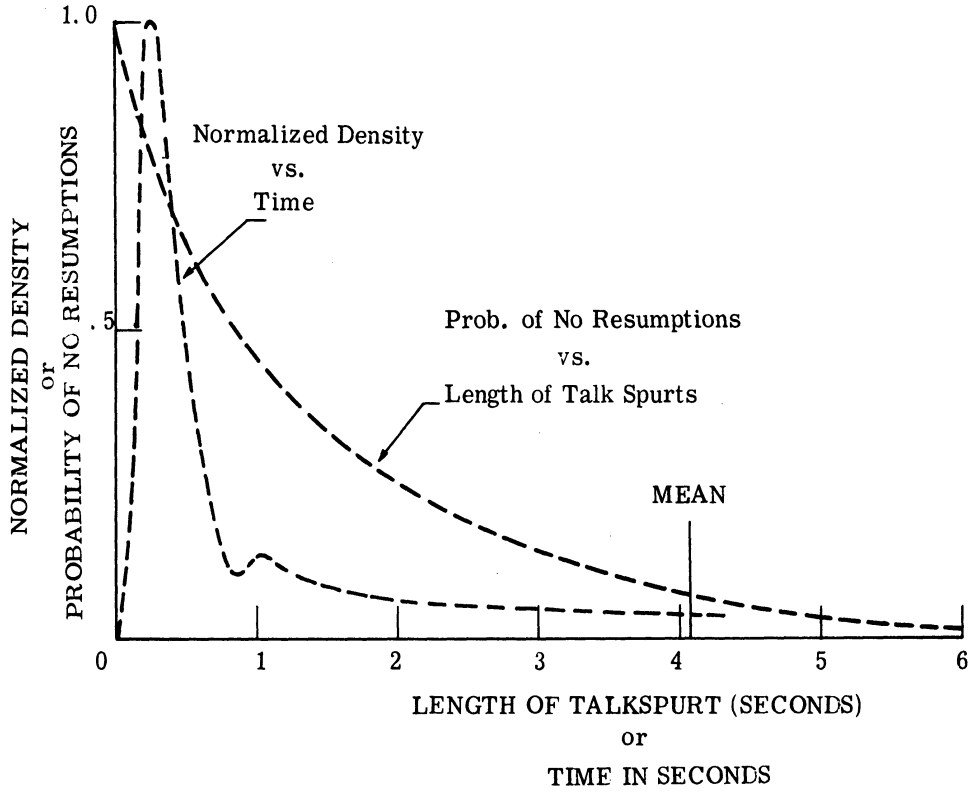

Fig. 16. Probability distribution for length of talkspurts containing no resumptions, and probability distribution for length of talkspurts.

The probability of a Type 1 talk burst, i.e., a talk burst with no resumptions (see Fig. 15) = .6

The mean talkspurt length (see Fig. 16) = 4.14 secs.

Using these facts and the solid curve of Fig. 15 for resumption probability, we may evaluate a mean Type 2 talk burst length, Q, from the equation

$$.6(.82) + 4 \sum_{n=1}^{\infty} \left(\frac{1}{2}\right)^n [(n+1)Q + n(.73)] = 4.14 \tag{12}$$

where: Q = mean Type 2 talk burst length

n = the number of resumptions.

A solution of Eq. 12 yields

$$Q = 2.60 \text{ secs.}$$

As a check on the values taken from Ref. 9 and on the resultant value of Q, the resultant probability that a talker will be in talk burst, p, should be about .4 as in Section 3.2.2. This value is

$$p = \frac{.6(.82) + .4 \sum_{n=1}^{\infty} \left(\frac{1}{2}\right)^n (n+1)\, 2.60}{2(4.14 + .41)} = .396 \tag{12a}$$

This corresponds well with the design value of .4.

In summarizing, we note that all probability density functions which produce the solid curves of Figs. 11, 12, 13, and 14 are valid and may be used to synthesize a single channel. Only the mean value of the second type of talk burst is known, and for lack of more information, we shall assume the probability density function producing the curve of Fig. 12 to be valid.

The solid curves referred to above have the following algebraic form. For talk bursts of Type 1,

$$f_1(t) = 33.4(t - .1)\left[e^{-(t-.1)/.15} + .00738\, e^{-(t-.1)}\right]. \tag{13}$$

For talk bursts of Type 2,

$$f_2(t) = .426\left[e^{-.408(t-.05)} - e^{-10(t-.05)}\right]. \tag{14}$$

For resumption pauses,

$$p_1(t) = 8.65\,(t - .05)\, e^{-(t - .05)/.34} \tag{15}$$

For response time pauses,

$$p_2(t) = 23.8\, t\, e^{-t/.205} \tag{16}$$

These are the equations, then, which were instrumented in the computer to "generate" the various talk bursts and pauses.

Figure 17 illustrates the method of selecting talk bursts for each channel. Random numbers, designated as, r, are selected from the random number generator. When these values are equated to the integrals of the density functions, talk burst and pause times lengths T_{f_1}, T_{f_2}, T_{p_1}, and T_{p_2} are calculated which correspond to the respective functions f_1, f_2, p_1, and p_2. Note in the figure that the talker of interest, talker A, must pause to wait for replies by talker B, during which time extrema are not being transmitted by the system. Only during talk burst periods of T_{f_1} and T_{f_2} for talker A is this single channel influencing the multichannel value of N'.

For each of the N-1 channels, the digital computer randomly selects pause and talk burst intervals. N' is then a function of time and is acquired simply by calculating the number of channels in simultaneous talk burst as indicated in Fig. 18. This resultant value of N' is then used in equation (11) to obtain the number of extrema in each clock pulse interval. These extrema are fed into the buffer with the extrema from the voice tape. If the buffer is full, extrema from the voice tape may be frozen out. It is this freezeout effect that is of interest in the results of the actual test discussed in the next paragraph.

3.3.2 Results of a 24 Channel System Test. From Section 3.2.2 the clock pulse interval for this 24 channel system is selected as τ = 1/40,000 seconds. When a typical voice tape input was subjected to this system, as shown in Fig. 18, very few extrema were frozen out in a run of about 7.4 seconds. The effect of this freezeout was of course undetectable.

The behavior of the random variable N' for the 23 channels (N-1) is shown in Fig. 19. From this figure it is obvious that the fluctuations of N' about the mean value of 9.8 (this mean value was obtained for the entire 7.4 second test) are quite large indicating that we cannot approximate this system with a constant value of N', and that an analysis such as the talk burst analysis described herein is necessary. Note that the experimental mean value of N' of 9.8 is in good correspondence with the theoretical design value of:

$$\begin{aligned} \text{average } N' &= p \times N \\ &= 0.4 \times 24 = 9.6 \end{aligned} \tag{17}$$

The buffer occupancies experienced in this test are shown in Fig. 20.

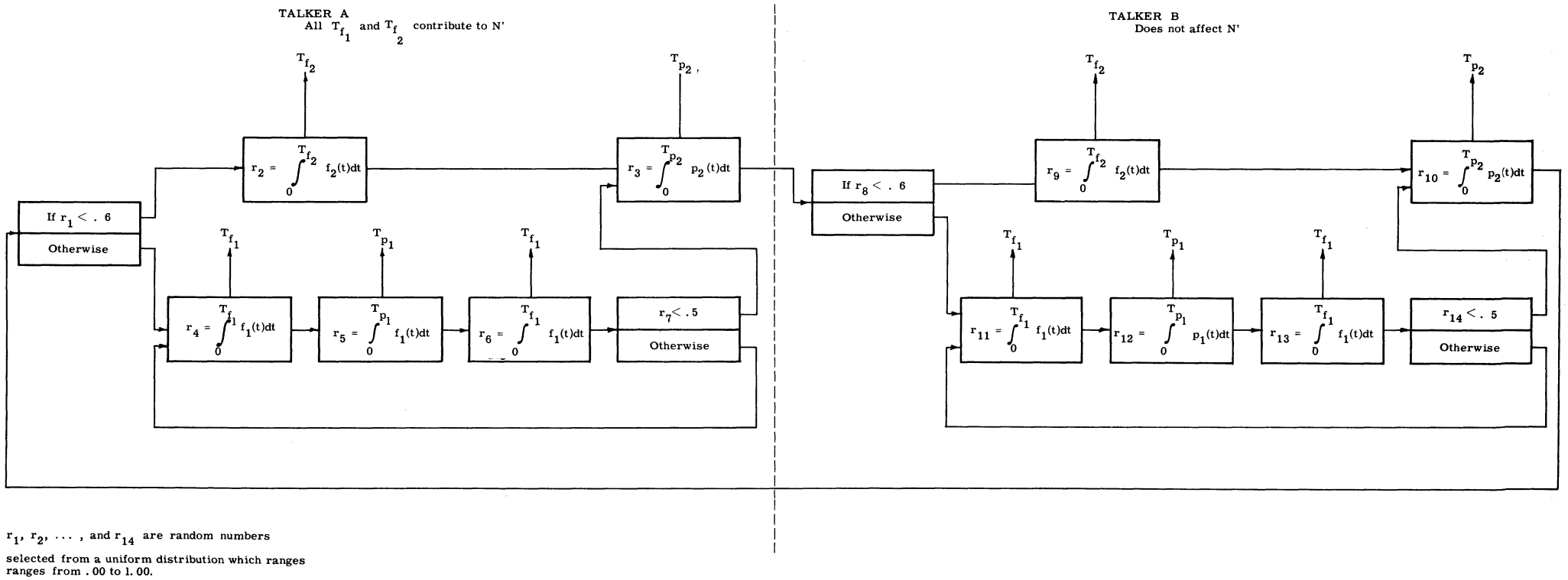

Fig. 17 Block diagram of computer experiment for generation of talk bursts and pauses for a single channel.

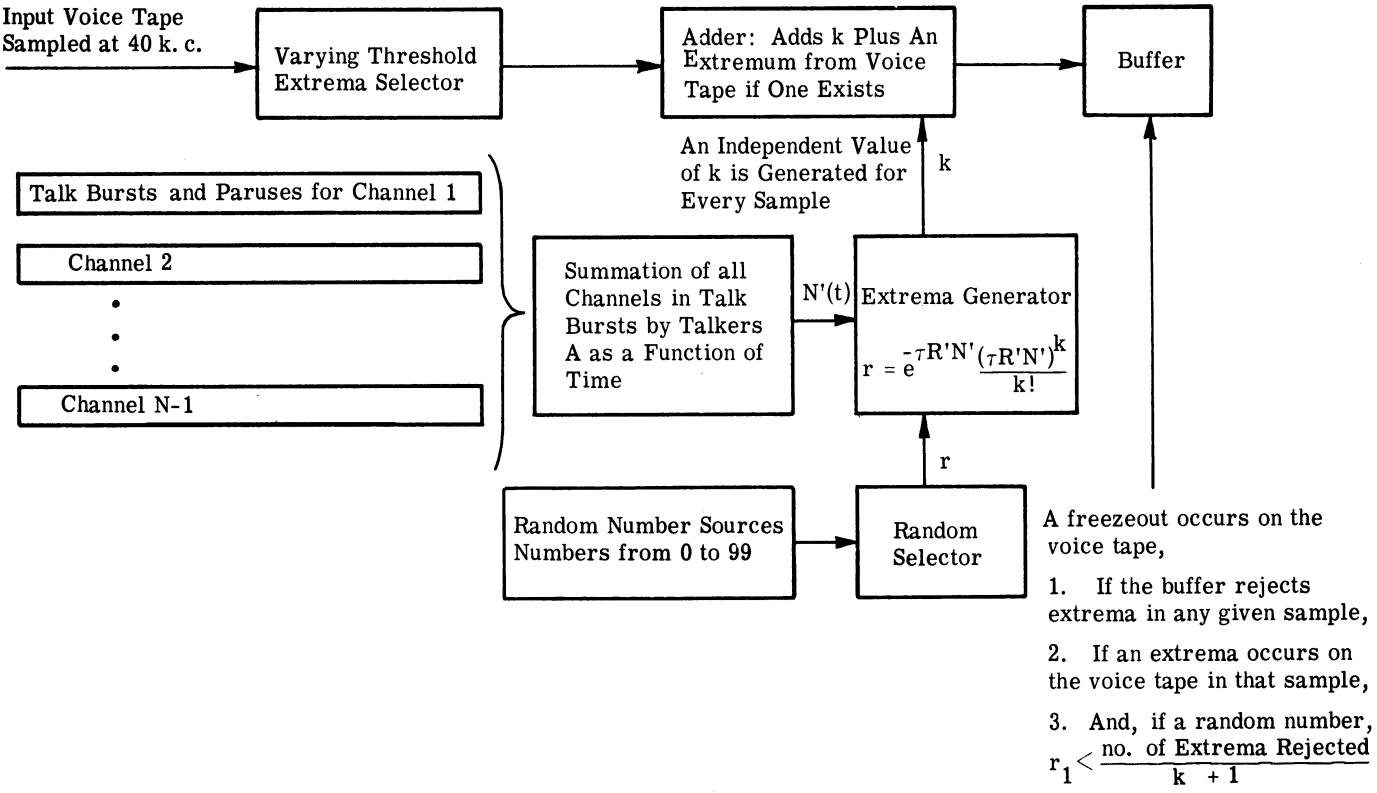

Fig. 18. Effect of the buffer on a single channel

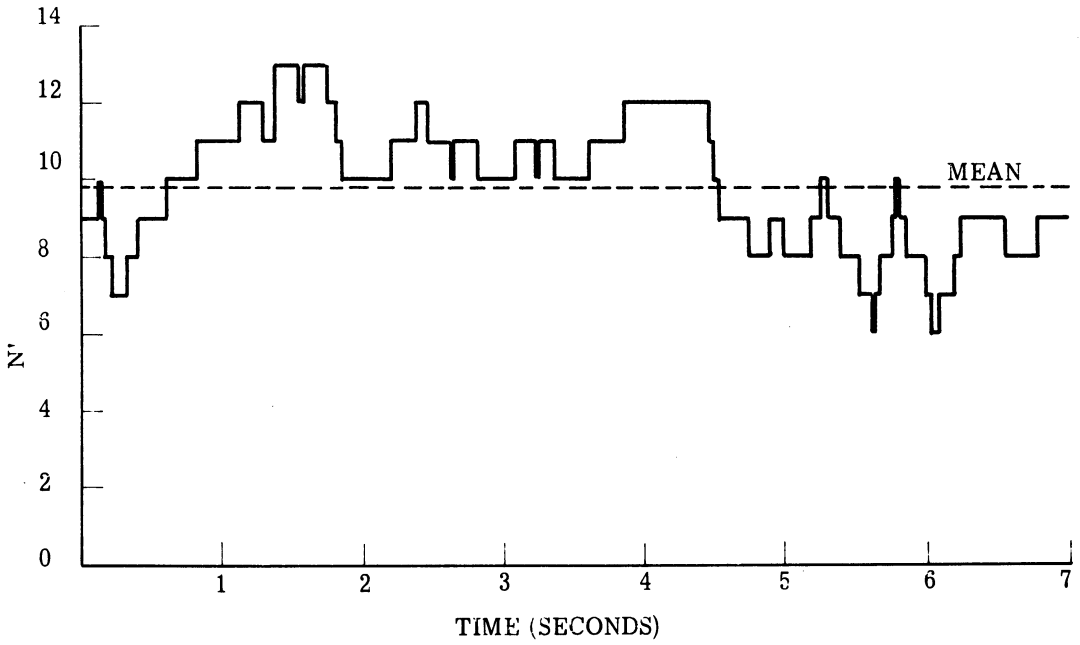

Fig. 19. Channels in simultaneous talkbursts as a function of time.

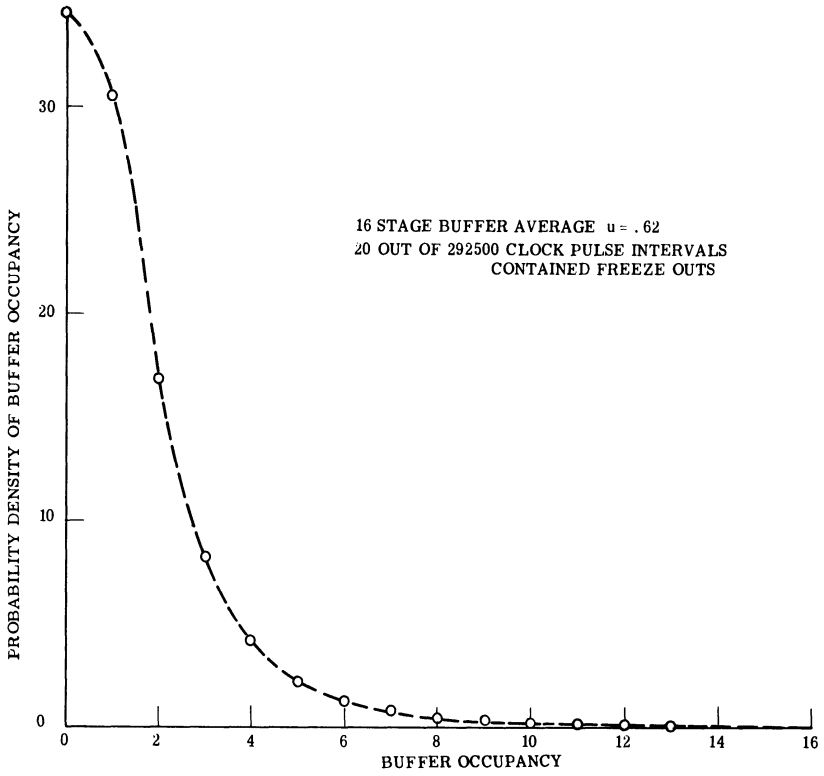

Fig. 20. Buffer occupancies

3.4 System Evaluation and Conclusions

We now wish to compare the asynchronous multiplexed system as analyzed here to a companded PCM system, as was done previously in Ref. 1 (See section 1.3).

First we need to consider the "bits per sample" for this system. As noted in Ref. 1, the three items in each sample are: (1) the amplitude of extrema; (2) the source number; and (3) time information. It has been found that 6 bits of amplitude information are sufficient. The time information, however, requires some comment.

In our computer extremal coded studies (described in the next section) the input samples were taken at a 20 kc rate. This corresponds to a time quantization of 0.5×10^{-4} seconds. In an actual system the extrema will be detected without time quantization, but it will experience a quantized delay in the buffer. We shall base our estimate of time information on the following assumption: finding extrema from samples taken at $1/\Delta t$ is roughly equivalent to detecting true extrema and allowing time jitter of Δt. This would mean, using our experimental figure, that time need be encoded only to within 0.5×10^{-4} seconds. As a precaution, we will adopt a safety factor of 2, and estimate the required time accuracy to be 0.25×10^{-4} seconds.

Since we are assuming a 16 stage buffer, and since the time information varies with τ, it is seen that the required time "bits" are given by:

$$\text{Time bits} = \log_2 \left[16 \times \frac{\tau}{0.25 \times 10^{-4}} \right] \qquad (18)$$

We can now note the complete number of bits required per sample of information:

Quantity	Bits Required
Amplitude of Extremum	6
Source Number	$\log_2 N$
Time Information	$\log_2 \left[16 \times \frac{\tau}{0.25 \times 10^{-4}}\right]$

The digit rate for the asynchronous multiplexed system can be stated as:

$$R = \text{digit rate} = \frac{6 + \log_2 N + \log_2 [16 \times \tau / 0.25 \times 10^{-4}]}{\tau} \tag{19}$$

As noted before, the τ can be read from Fig. 9 for a given value of tolerable freeze-out and channel number, N. It is worthwhile to review the major assumptions inherent in using Fig. 9 to obtain τ. They are:

1. The selected tolerable F.O.F. occurs at most 1 percent of the time.
2. The extrema rate for talk bursts (R') is about 2300 extrema per second.

The other factors involved are noted in Section 3.2.2.

We can compare the rate of Eq. 19 with $4.8 \times 10^4 \times N$ bits per second for companded PCM. This should provide comparable quality speech reproduction.

A bit rate ratio may be defined as:

$$\frac{\text{Digit rate for companded PCM}}{\text{Digit rate for asynchronous multiplexed system}} = \frac{\tau \times 48 \times 10^4 \times N}{6 + \log_2 [16 \times \tau / 0.25 \times 10^4]} \tag{20}$$

This is a measure of the estimated improvement in channel capacity of asynchronous multiplexed system over companded PCM. This ratio is plotted in Fig. 21 versus the number of channels N for a tolerable freezeout of $0.0\bar{1}$ and 0.03. Note that Fig. 21 takes no account of the fact that the time information will be quantized. Thus fractional time bits are used in plotting Eq. 20. From the curves it appears that the bit rate advantage is greater than 2 so long as N is greater than 20. For 100 channels it is estimated that the bit rate advantage is at least 2.5.

We can now summarize the results of these multichannel experiments. First of all, from the Poisson test described in Section 3.1 it was found that the extrema generated by a fixed number (greater than 6) of talkers in simultaneous talk bursts are Poisson distributed and stationary. Thus if the fluctuations of the number of talkers in simultaneous talk bursts is truly insignificant, the extrema distribution function is Poisson with a fixed mean value.

From the freezeout experiments described in Section 3.2.1 it was learned that when 1 percent of the extrema in a good quality voice production are randomly deleted the effects

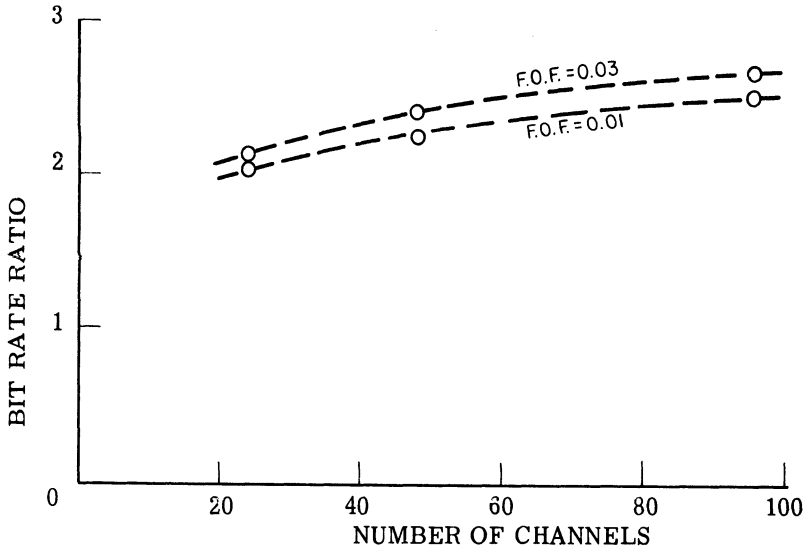

Fig. 21. Bit rate compared to companded P. C. M.

are insignificant. At 3 percent the effects are barely noticeable. Therefore, it is estimated that choosing a 3 percent tolerable freezeout, to occur no more than 1 percent of the time, is a conservative criterion for freezeout.

Finally, the multichannel system simulation of Section 3.3 demonstrated the feasibility of operation with as few as 24 channels with the parameters described above. As noted, the estimated bit rate saving for 24 channels (over PCM) is about 2.

All of the above analysis has been based on fairly conservative interpretations of the experiments accomplished. There are two factors which may improve the bit rate advantage of asynchronous multiplexing, in the future, over that shown above. First of all, with some development the extrema rate may be reduced from 2300 (for talk bursts) to something like 2000. Laboratory results have already achieved lower rates (Ref. 4), but practical techniques have not yet yielded sufficient quality at the lower rates. Secondly, the freezeout parameters chosen here may turn out to be more conservative than necessary. More experiments are required to ascertain this. An estimated value which may be achieved in the future for the bit rate ratio of a 100 channel system is about 3.2.

4. IMPLEMENTATION OF EXTREMAL CODING OF SPEECH

As noted in Section 2 above, the essential idea here is that an existing coding which is proposed in Mathews (Ref. 4) and Spogen (Ref. 5), has been adopted here for use in this asynchronous multiplexing method. The actual quantitative degree of bit saving in using this asynchronous method over synchronous PCM for a given quality depends of course on the success of implementing a certain quality with this extremal coding. For a number of reasons it was necessary in this work to implement single channel extremal coding channels in order to study the quality which was available. One big reason for requiring this is that the conditions here are not the same as those under the work of Refs. 4 and 5.

As noted before in Section 2, the essential idea in extremal coding is to select those positions on the waveform which are extrema and send only those samples. Consequently the chief problem in implementing a channel in the transmitter is to write certain rules under which the extrema will be selected. For example the noise problem appears here. One must select "rules" such that extrema will not be sent when only noise is present. In the transmitter then the essential idea is to adopt a framework or a means of selecting extrema. It may be noted that in Ref. 4 a variety of sophisticated techniques was used on the computer to select the extrema. In the work of Ref. 5, a more elementary method of selecting the extrema (in analog fashion) was used.

In the extremal coding "receiver" the essential idea is to accept the irregularly arriving samples, put them in their proper position, and then fit a waveform between these irregularly occurring samples. In actual equipment the most elementary way of fitting a wave-form between irregularly occurring samples is to "box car" the samples and then filter the results. This gives some valid approximation to the actual waveform. However one can get more sophisticated than this by fitting a standard type wave between the irregular samples; this was done when the computer method was used.

During this year, the single channel extremal coded experiments were implemented by two methods: (1) by use of the digital computer, and (2) by means of an analog prototype extremal coder and receiver. The digital computer method was used as the primary experimental method, in which a number of things were to be tried. The primary idea with the analog method was to demonstrate that one can obtain reasonable quality with an existing piece of equipment. In other words in the analog method one would hope to make use of all the things which are learned via the more experimental computer method.

As mentioned before the objective of these single channel codings were as follows: 1) to determine the effect of particular implementation methods on quality, 2) to determine the

effect of freezeout on quality (See 3.2.1), and 3) to give us some experience with the type of quality that extremal coding can afford versus given extrema rates. If one had to rely simply on statements made in the literature about listening quality one would not be in the same position as if one can do the listening in the laboratory. Finally it was necessary to have actual experimental results in order to perform the multichannel experiments described in the previous section. In particular when running the simulated 24 channel situation, it was necessary to have as input actual extrema statistics. Furthermore when making the Poisson test actual extrema statistics were used.

As mentioned we have run both computer experiments and analog experiments which implement extremal coding. In the computer case two different sets of "rules" were tried for implementation of the transmitter detection of extrema, and a "waveform fit" was applied to the receiver samples. In the analog case the transmitter selected extrema by a fairly straightforward derivative method with a window, and in the receiver the samples were boxcarred and then filtered. We will first describe the computer experiment and results below and then the analog experiment and results.

4.1 Computer Implementation of a Single Extremal Coded Source.

Because the digital computer is a flexible instrument, it has become the practice in recent years to use it as an experimental tool. That is, instead of constructing equipment to perform particular functions in digital communications, one simply writes programs to treat the digitized samples in the fashion which equipment would treat it. Thus, in effect, one has achieved a more or less idealized experiment which serves a very useful laboratory function. The chief idea is that, by using such a flexible method, one can obtain the upper bounds on experimental performance. Then one should try to implement actual equipment to match the simulated results as closely as possible.

In implementing the computer experiment one first puts the analog voltage through a digital-to-analog converter. This digital-to-analog converter must both sample and quantize the analog voltage, and also put the information on a magnetic tape in a form suitable for acceptance by an IBM 7090 computer. Note that a magnetic tape input is virtually required because one needs high input rates in order to do this type of experimenting. If one had to punch cards for each input sample the amount of card punches and the speed of card punching would prohibit efficient or sensible use of this technique.

Although the samples are inserted into the computer via this A-D method, the program is put in via cards. The program then performs the experiment simulation on each individual sample of data.

The experimental procedure is depicted in Fig. 22. First the analog speech is put through the special A-D converter.[3] The resultant digital tape is then put on an IBM 7090. After

[3]Although the A-D function here is elementary, the actual equipment is fairly sophisticated. This is because the digital tape must be properly formatted for acceptance by the digital computer. Hence a number of timing, synchronizing, and control functions are required.

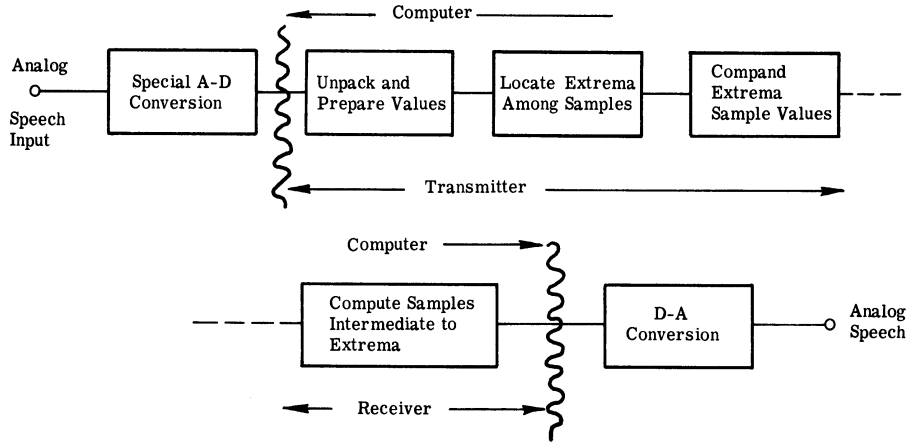

Fig. 22. Basic block diagram of computer implementation.

reading the input tape the computer examines the input sample values and determines the sample extreme values. At the sampling rate of 20 kc, it was estimated that the sample extrema are sufficiently close to the actual extrema so that his effect should not limit the quality.

After the extrema are located, the computer will erase the intermediate samples. The signal now stored in the computer corresponds to the extremal coded signal (pulses representing the sample time and sample value of the extrema). This signal can now be companded and coded for transmission. In the computer, the companding operation will employ logarithmic companders.

A more complete block diagram of the entire computer experiment is shown in Fig. 23. Here both the actual "simulation" operations, and the measurements (shown in dashed lines) are shown. Practically all of the functions shown here have been discussed, and need not be repeated. Note that the "freezeout" function shown in Fig. 23 is used only when testing the effect of freezeout (as described in Section 3.2).

The various measurements shown in Fig. 23 will be discussed later when portraying the experimental results.

The procedure used for finding and identifying the extrema will now be treated. There were essentially two basic methods for finding the extrema via the computer method. One of these is called the "constant threshold" and the other is the "varying threshold method."

A basic objective, with extremal coding, is to get the best possible quality for the least number of transmitted extrema. Thus, not all minor "bumps" in a speech waveform are desired, since such extrema would elevate the extrema rate without a commensurate increase in quality. The thresholds mentioned are simply means of separating the desired extrema from the minor undesired ones, and also distinguishing actual speech extrema from noise.

Under ideal conditions extrema could be detected by noting all zero-crossings of the derivative of the waveform. Because of both minor bumps and noise in the waveform, however, it is desirable to make the derivative of the waveform pass through some "window" before noting an extrema. In other words, instead of noting zero-crossings (zero window) of the derivative waveform, one requires the derivative to pass through from the plus side to the minus side

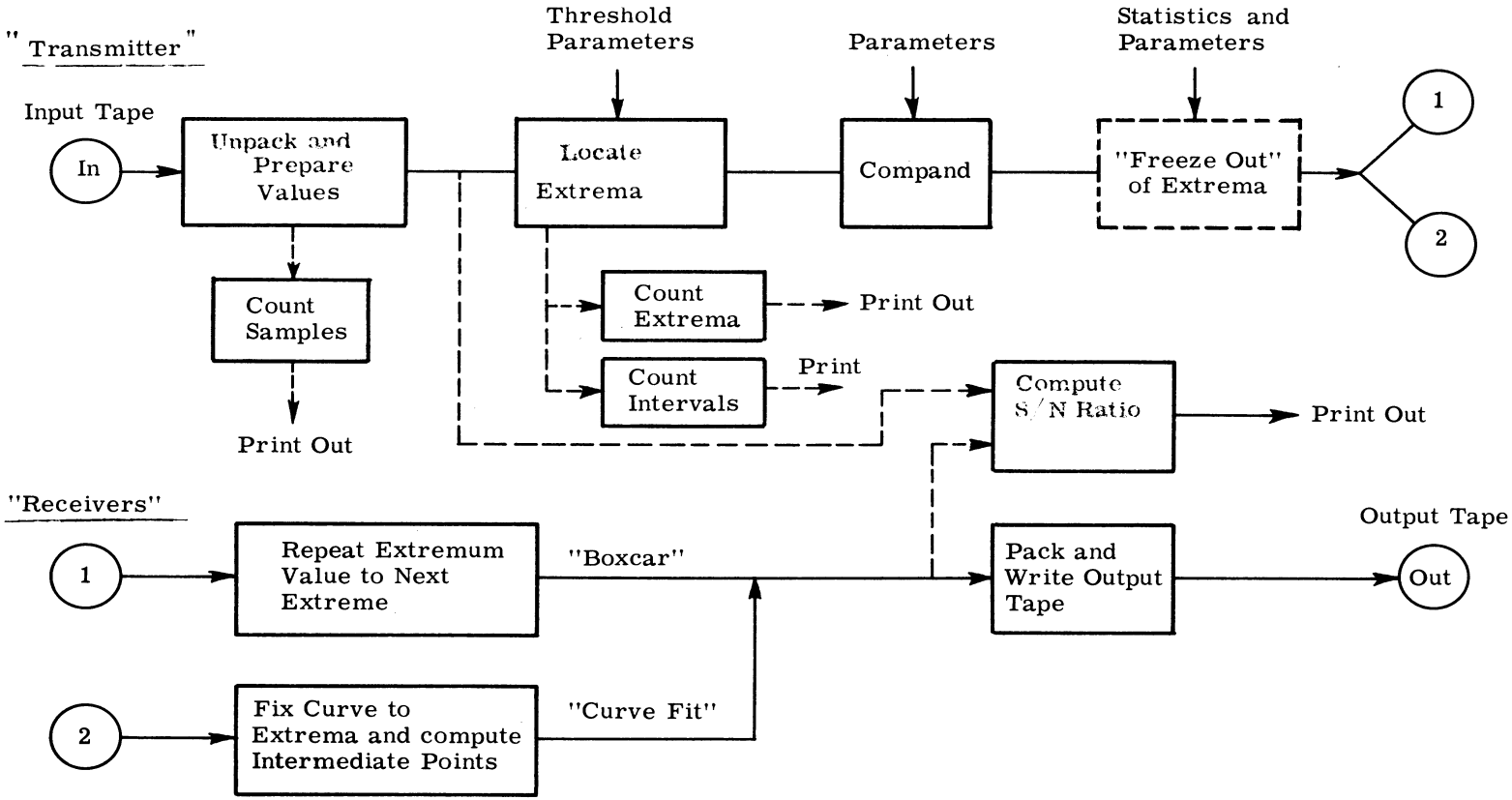

Fig. 23. Block diagram of extremal coding computer simulation.

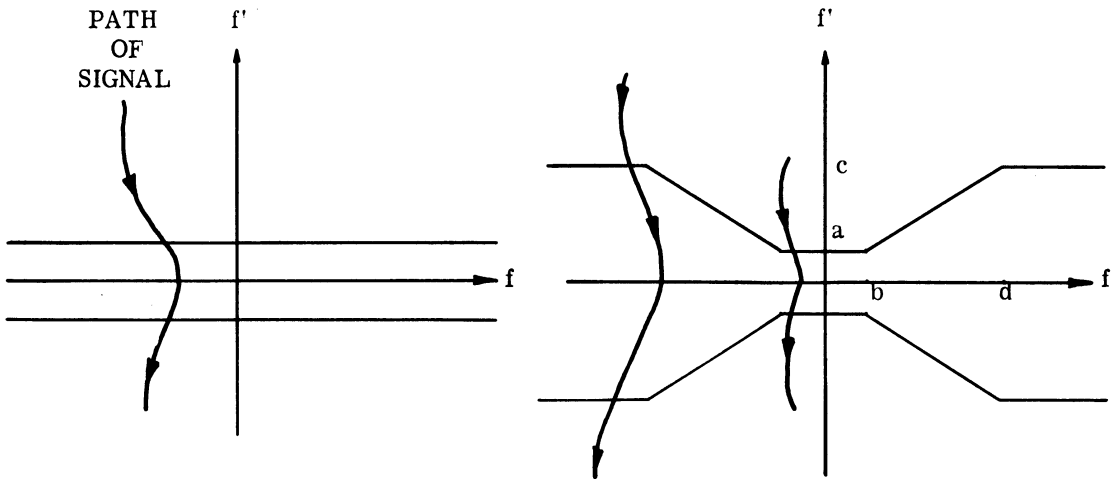

(a) CONSTANT THRESHOLD (b) VARYING THRESHOLD

Fig. 24. Sketches of thresholds in extrema selection

of a window, or vice-versa, as shown in Fig. 24a. When the signal and its derivative combine so as to go through the window, then an extrema will be found in the intervening portion. An alternative to this window would be to construct a varying window, as shown in Fig. 24b. In using this varying threshold, the major idea is to cause the threshold to vary with amplitude of the wave. Thus when the waveform is large this threshold requires a large change in derivative before an extremum is detected. This threshold was used in an attempt to get better quality for a given rate of extremum. As will be seen later these varying thresholds tried here did not improve the quality-rate relation noticeably.

The particular variable threshold will be denoted by (a, b), (c, d), based on Fig. 24b. This specifies the breakpoints in the varying window. In all cases tried the same slope was used but the constant values were varied. The slope of the window was determined by the equation:

$$\text{slope} = \frac{f_i - f_{i-1}}{|f_i + f_{i-1}|} \cong \frac{f_i'}{|f_i + f_{i-1}|} = 0.08 \qquad (20a)$$

where: f_i = amplitude of ith sample

f_i' = digital derivative

The most frequent window used was given by (5, 32), (40, 256).

To emphasize, then, if one used zero-crossings instead of some window such as shown in Fig. 24, the resultant extrema rate would be too high for the resultant quality. The procedure for finding the extrema can now be outlined:

1. Sample speech at 20 kc in order to get the extrema located with this accuracy.
2. Find the derivative by taking $(a_{i+1} - a_i)$, the difference between two consecutive samples.
3. Select a "center clip" section or "center window." Naturally as the window is "widened" the quality will tend to deteriorate; if the window is narrowed the quality will tend to improve.
4. An extremum will be identified each time the derivative waveform passes through the center window. If the derivative enters and emerges from the same side, no extrema will be noted. If a derivative passes through, then the extrema is identified as that sample which is the highest (or the lowest) during the time the derivative is within the window.

In a communications situation, it is these extrema which are sent over the link. In the experiments here we completed the system by forming a "receiver." This also was done in the computer. The "receiver" consists of taking the given extrema values (and their locations) and calculating the values of intervening regular samples according to some law.

With both threshold methods of detecting the extrema, the receiver method consisted of placing the extrema at the proper place and then fitting a waveform to the extrema samples. This was done by using the interpolation waveform suggested by Ref. 4. This amounts to taking the extrema and fitting the function:

$$F(x) = x^2(3 - 2x) \qquad 0 < x \leq 1 \tag{21}$$

where: $F(0) = 0$, $F(1) = 1$

as the interpolation waveform. The time interval between the two extrema of interest is normalized to equal 1. Then intervening sample values are calculated, assuming the first extrema is at the origin. By this means the sample values intermediate to the extrema sample values were determined, and this was used to form the "output" waveform.

A slight embellishment in the receiver consisted of artifically bringing the waveform down to zero if there were 50 consecutive time slots (at the 20 kc rate) without an extremum. This was the means chosen to bring the waveform to zero when the speech was off. Some such "rule" has to be made, and simply represents a receiver modification. It should be understood that this does not increase the transmitted samples.

A description of the computer program for this extremal coding case is given in Appendix C.

4.1.1 Experimental Results. We will now depict the experimental results that were achieved by using these computer methods. First we will make some general statements about

the method of constant rate and variable rate and about the rate versus listening quality. Then we will show time plots of various segments of the waveform to both indicate the excellent reproduction of the waveform by this simple method, and also to indicate those trouble spots which do occur. Thirdly we will discuss the table showing the signal-to-noise ratio versus the rate (for each of the records); finally we will show the average extremal time interval distribution between extrema.

It may be remembered from the introduction that the analysis of last year assumed that extremal coding of sufficient quality could be obtained at about the rate of 1600 extrema per second. Also, this figure was associated with the time that a channel is "active." This figure was based on the work of Refs. 4 and 5. In the amount of time which was available for experimentation here, we were not able to get reasonable enough quality at rates of 1600 extrema per second. In should be recognized that methods used in Ref. 4 allowed a large number of fairly sophisticated computer techniques to increase the "quality-extrema rate" ratio. Here we were relatively restricted because we used only those computer methods which can obviously be implemented rather simply by analog equipment.

We were able to obtain quite acceptable quality under the given conditions at extrema rates of about 2000 to 2100, corresponding to "active" time, or "talkspurts." Our best estimate of the "talk burst" rate[4] (which takes out all pauses between extrema which are longer than 50 milliseconds) is about 2300 extrema per second. Although this increase from effectively 1600 to 2100 of course decreases the advantage of the asynchronous multiplexing over that predicted earlier, the loss is not too great as was seen in Section 3.4.

During the experiments which were done it was found that there was essentially no difference in quality between the constant threshold and the varying threshold, depicted in Fig. 24. Although the waveform action was changed slightly, as will be seen later, the changes were not significant either in the signal-to-noise calculation or in the listening results.

It appears that the most disturbing distortion which is characteristic of the extremal coding is at the low frequencies. This is caused by the fact that one is fitting a standard waveform between the irregularly spaced extrema. Most of the "distortion energy" will come in those cases where there is a relatively long stretch between the extrema so that the waveform may be slightly incorrect for some period of time. It was found that one can improve greatly the quality (or reduce the distortion) of extremal coded speech by keeping the low frequency cutoff at 250 cycles or above. It may be noted that this low frequency cutoff aspect of extremal coding is very appropriate with telephone lines. Therefore extremal coding should be able to afford quality which is barely distinguishable from normal telephone line speech. This can be corroborated by listening tapes which were made from our experiments.

---

[4] Talk bursts and talkspurts were defined in Section 3·3·1· Essentially talkspurts include both talk bursts and pauses of a single party

In the experiments which are being reported here there were essentially two separate cases. The first case consisted of three sentences of speech at a given volume input. Due to some indications in those results a later set of experiments were run at a higher volume. At this higher volume the speech was "read faster" than the previous. That is, the same three sentences were used but these sentences were read in a fast "radio announcer" fashion so as to provide a higher average rate. The motive here was to obtain an action which is more characteristic of "talk burst" activity (rather than talkspurt—see Sec. 3.3.1). This was successful, since only a few pauses had to be removed.

To conclude these general remarks then, we were able to obtain very acceptable speech especially suited for telephone lines at a talk burst rate of 2300 extrema per second, or an over-all active (talkspurt) rate estimated to be about 2100 extrema per second. Although this rate is not as low as the experimental rate reported when this coding was proposed this rate is reasonable when one considers that we were restricted here to relatively unsophisticated rules in implementing the transmitter and receiver. However, even with these simple rules we believe that the rate can be reduced from this if one spends some time in development. Based on the experiments done to date, we believe that one can achieve talk burst rates of about 2000 extrema per second.

Time Charts

In order to show the time behavior of the effectiveness of extremal coding, Figs. 25 and 26 show some typical input and output curve shapes of speech plotted by the computer. In these figures the "stars" indicate the input sample values and the continuous line shows the sketched path of the output sample values. By comparing the line indicated by the stars with the solid one can see how the output departs from the input. In general the output follows the input with good fidelity.

All the charts in Figs. 25 and 26 came from the speech experiment value which yielded the 2100 extrema per second (about 2300 per talk burst). As mentioned before this sample sounds very good and is ralatively indistinguishable from telephone channels whose lower cutoff is something like 200 cycles per second. It may be noted that at higher rates one can obtain still better fidelity between the output and the input. For example Fig. 27, which shows a sample of part of a recording which would be at the rate of 2900 extrema per second shows that the output follows the waveform with good fidelity even over wide swings.

Figure 28 serves to indicate the essential difference between using the constant threshold and the varying threshold in the time plane. As one would expect, the varying threshold begins to miss some of the extrema which are farther away from zero. This will result in the action between "240" and "250" in Fig. 28. The top portion, Fig. 28a, was obtained with the constant threshold, while the bottom, Fig. 28b, was obtained with a commensurate varying threshold. It can be seen that the action throughout the entire time sequence is about the same

(a)

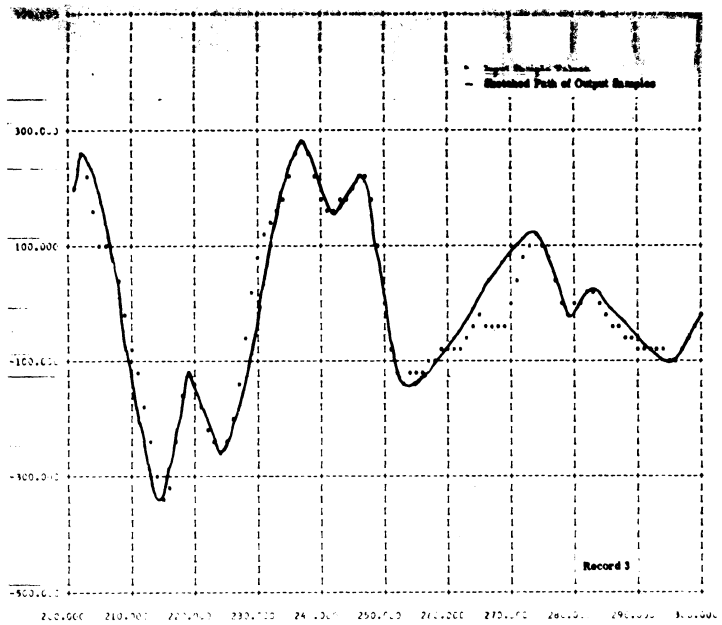

(b)

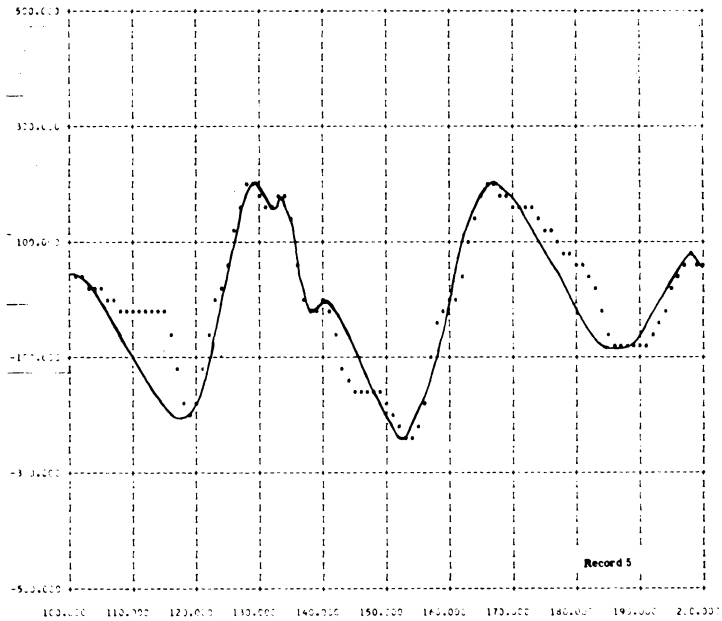

(c)

Fig. 25. Time charts of input and output for computer implementation. ($\pm$ 5 constant threshold.)

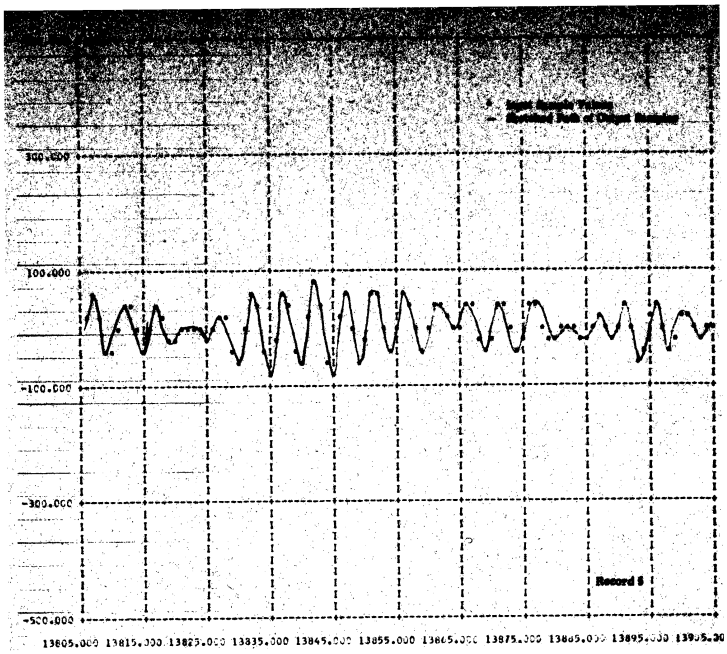

(a)

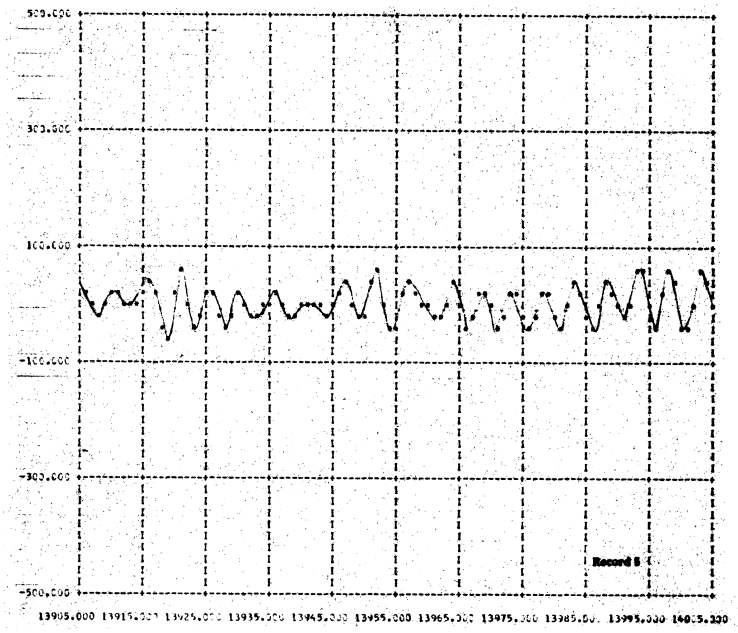

(b)

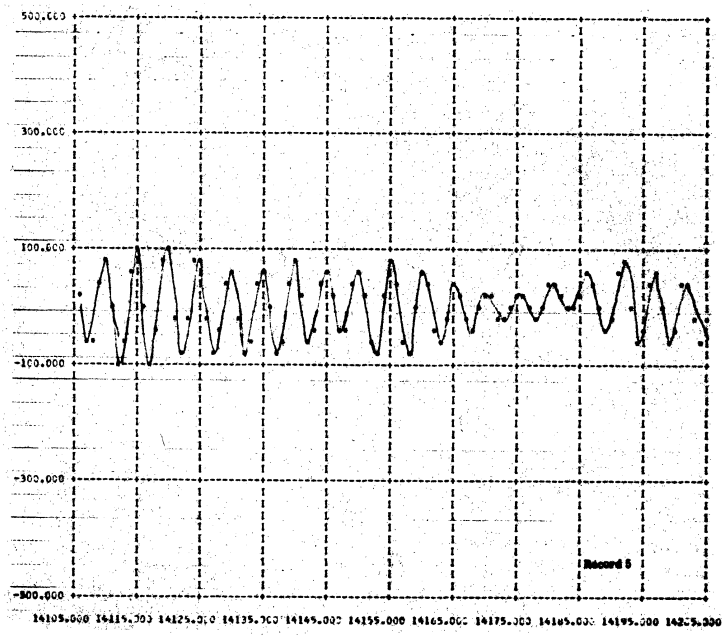

(c)

Fig. 26. Time charts of input and output for computer implementation. ($\pm$ 5 constant threshold.)

(a)

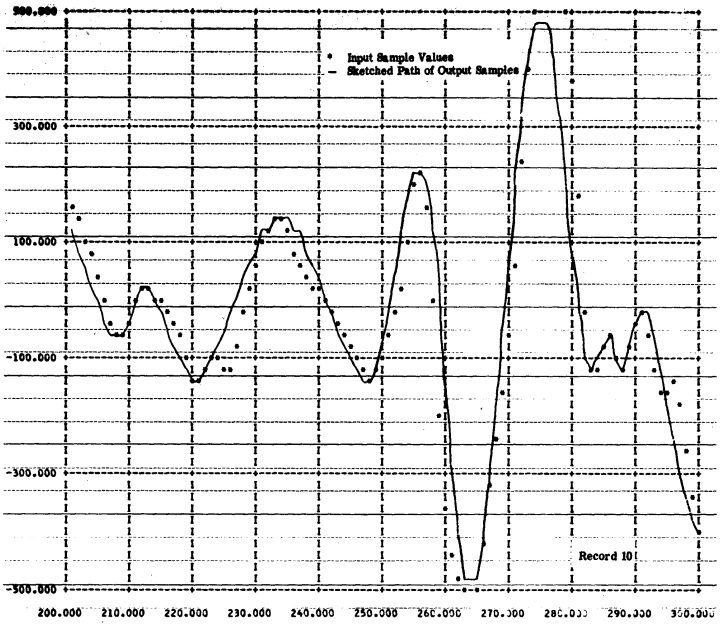

(b)

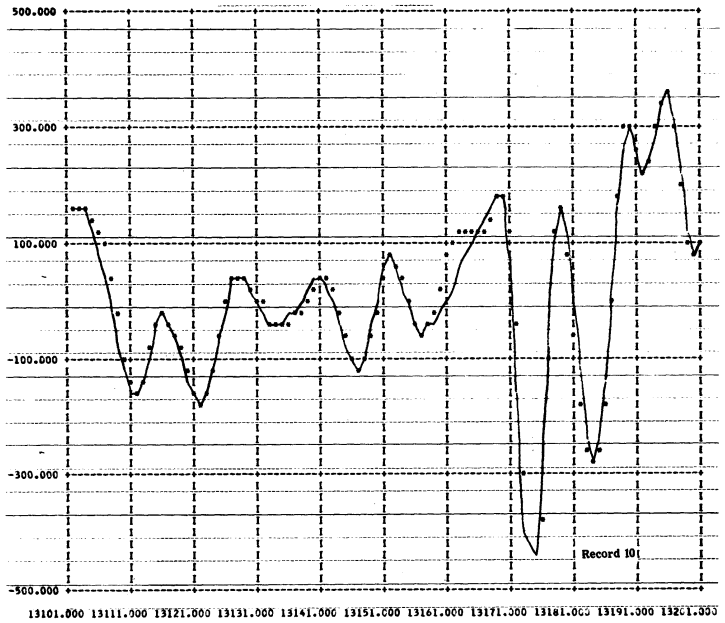

(c)

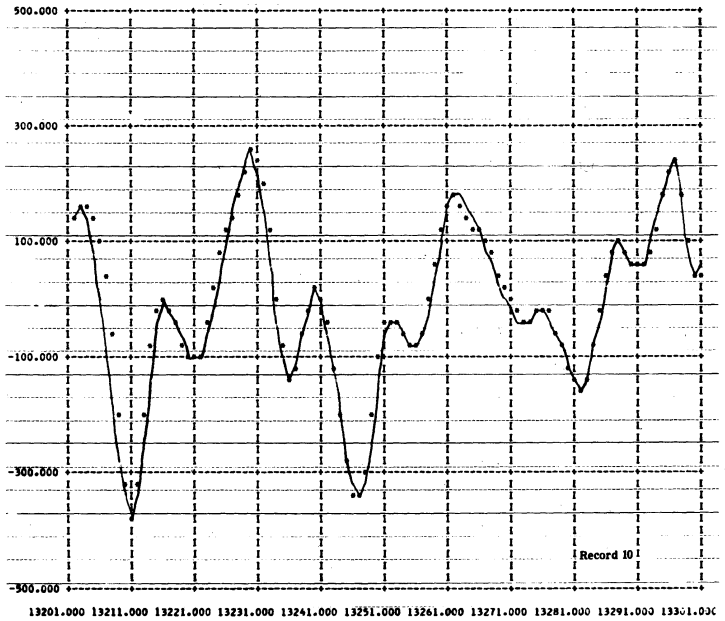

Fig. 27. Time charts of input and output for computer implementation with higher rate. (No. 5 in Table II.)

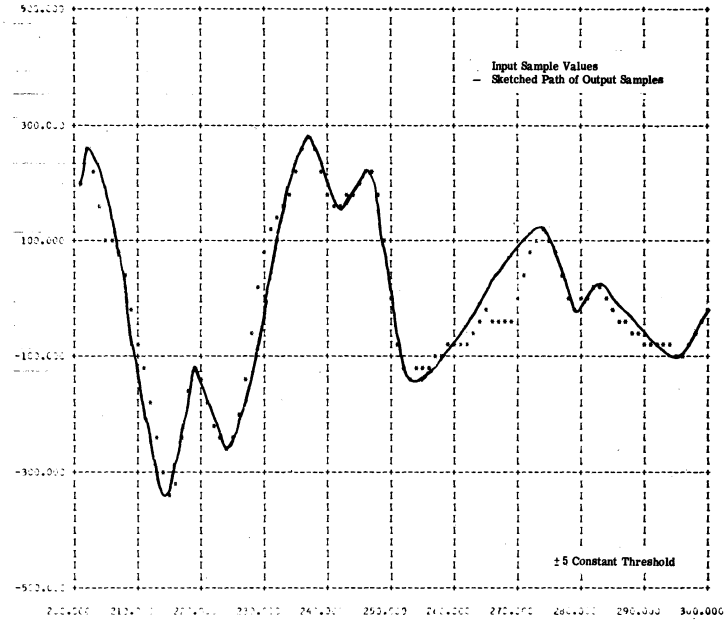

(a)

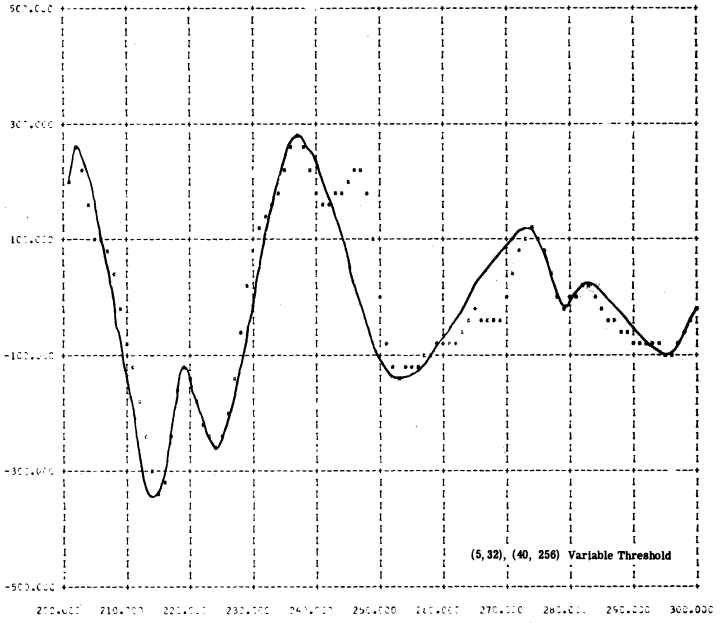

(b)

Fig. 28. Time chart of input and output for the constant threshold case, and the variable threshold case.

(a)

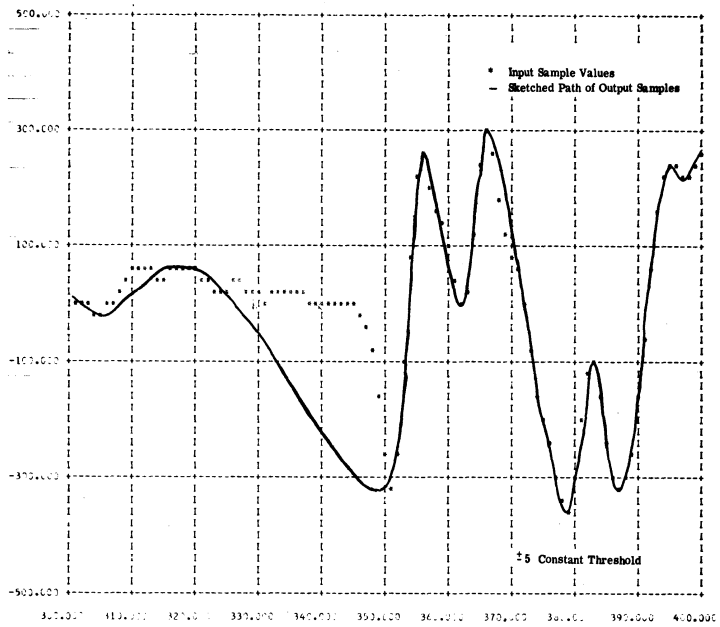

(b)

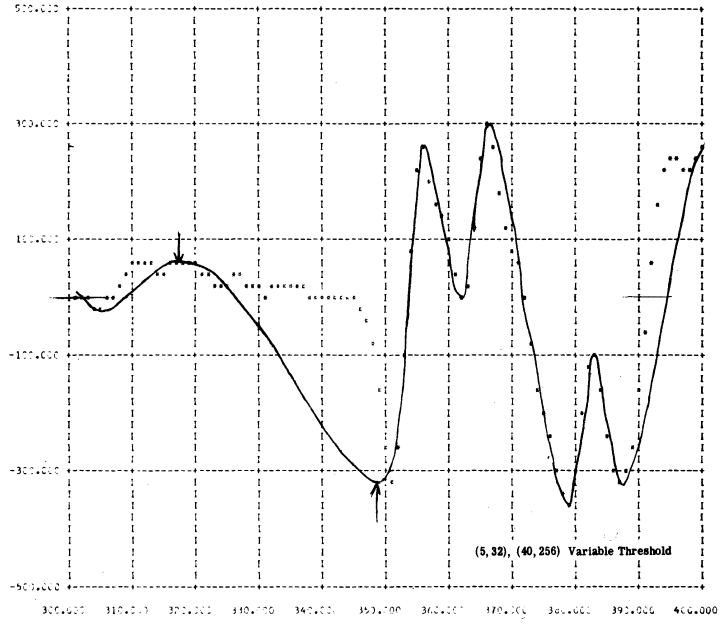

Fig. 29. Time chart of input and output denoting a common distortion with extremal coding.

for both cases except in the area of 240-250; one extrema is missed by the varying threshold. Of course, if such extrema are not very important to the quality of speech it would be desirable to eliminate them. However in this case, and in many cases like this, missing extrema of this nature introduce undesired distortion.

Probably the most flagrant and consistent type of error which this type of coding makes is shown in Fig. 29. Here between 320 and 350 it is seen that the fitted output waveform departs quite drastically from the input waveform. The action here is characterized by the fact that the input waveform is spending some time around the origin, and then moving away at a steep rate. Since the "extremal" sensing used here has no way of knowing when the waveform departs from zero, it fits a waveform between the two extrema as shown. This is the most flagrant source of error in the coding system used here. Probably the most profitable way to improve the quality-extremal rate ratio is to find a simple and effective way to counter this problem. It may be noted that this happens in both the constant and varying threshold while the lower one results from a varying threshold. Note also that one can again see how an extrema is missed by the varying threshold case by comparing the right side of these graphs.

We can see other examples of the effect of this "zero departure" difficulty with the extremal coding by looking at previous figures. For examples in Fig. 25 it occurs between 100 and 110 in the upper one and also between 260 and 270 in the lower one.

Signal-to-Noise Results

Another way in which the efficacy of extremal coding can be evaluated is to calculate a signal-to-noise ratio derived from the distortion. In our case the average signal-to-noise ratio was derived by using:

$$\text{Average } (S/N)_{db} = 10 \log_{10} \frac{\sum_i f_{in}^2(t_i)}{\sum_i \left[f_{out}(t_i) - f_{in}(t_i) \right]^2} \tag{22}$$

As mentioned previously two sets of experiments are being discussed in this report. The results of the first set are shown in Table I.

In this case the speech sample of three sentences comprised 16 "records." A "record" corresponds to an amount of data which approximately fills the computer storage. Since the computer cannot process the data in real time, the data must be divided into such segments.

Table I essentially shows the S/N and the corresponding extrema rate per second on a record-by-record basis. Both constant and varying thresholds are shown in this table. Note that one can compare the rate of extrema with the rate of zero-crossing of the derivative that would occur if the window were zero. With regard to the signal-to-noise ratio in db stated

Record No.	Rate of Derivatives Crossing Zero (no window)	1. Derivative Window at Constant 5		2. Varying Derivative Window (5,32), (40, 256)		3. Derivative Window at Constant ± 10	
		Rate	S/N	Rate	S/N	Rate	S/N
2	3460	2118	10.44	1746		1777	9.3
3	4240	3248	3.75	2997	2.14	2670	2.7
4	4590	3541	11.13	3318	9.79	3018	8.9
5	4560	3597	10.35	3397	9.337	3132	9.6
6	4600	2686	11.30	2500	9.43	2230	9.7
7	3450	2343	12.06	2153	10.08	1808	8.9
8	5750	1005	8.26	1005	8.26	888	7.3
99	5250	1	-0.065	1	-0.065	0	---
10	4350	2748	1.69	2559	-0.02	2561	0.86
11	4080	2639	-18.85	2333	-20.26	2219	-19.2
12	3560	2349	6.77	2023	5.56	1831	5.7
13	4600	73	9.32	71	8.016	32	5.0
14	5930	15	-0.155	15	-0.155	0	---
15	4660	1920	4.95	1804	4.25	1381	4.6
16	3940	2946	5.22	2670	3.841	2585	4.5
17	4760	2033	10.76	2004	9.	1721	9.0
	4520	2079		1912		1601	

Table I. Comparison of extrema rate and S/N results for constant and varying derivative windows.

here, it should be noted that a signal-to-noise ratio of 10 in this calculation is very good. This calculation is done in the computer by comparing the output sample to the input sample. Some of the noise spectrum will be filtered out in the output and will not be entirely effective in producing distortion in the speech. This is especially true at the lower end where, as mentioned before, keeping the low frequency cutoff at about 250 cycles per second significantly reduces the distortion of the extremal coded speech. Therefore it must be cautioned that these values should be used as relative numbers and not for comparison with other speech results obtained under entirely different conditions.

The time charts in Figs. 25 and 26 were taken from the run labelled No. 1 in Table I. The threshold in this case was constant, and set at "5." The value 5 refers to a basic quantum in the digitized input. Since the input is quantized with 10 bits to ±512 levels, the 5 here means that the derivative has to be within ±5 basic units before an extrema is detected.

The quality statements made earlier also referred to this run No. 1. It was stated that about 2100 extrema are required for the average "active" speech (talkspurt), and this was estimated to correspond to 2300 for a talk burst rate. From listening it was found that the quality of this tape was quite good.

In a second set of experiments a series of tests were run at a higher volume, where the speech was also occurring at a higher rate. The extent of the more rapid speech rate is illustrated by the fact that the same three sentences used before now only comprise 12 records

instead of 16. The extrema rate for the speech here is appropriate for "talk burst" rates.

The results of this second set of experiments are shown in Table II below. Comparing the results here to those of Table I it may first be noted that the extrema rate is higher here since they are approximately "talk burst" rates.

Record No.	(4190) 4. ±10 Constant Window		(4141) 5. Variable Derivative Window (5,32), (40,256)		(4328) 6. Variable Derivative Window (10,64), (40,256)		(5479) 7. Variable Derivative Window (20,128), (60,384)		(5897) 8. Variable Derivative Window (20,128), (80,512)		(5590) 9. ±20 Constant Window	
	Rate	S/N	Rate	S/N	Rate	S/N	Rate	S/N	Rate	S/N	Rate	S/N
2	All Noise		All Noise		All Noise		All Noise		All Noise		All Noise	
3	1937	8.34	1799	6.72	1683	6.27	1434	4.78	1434	4.78	1511	5.57
4	3396	7.1	3637	6.22	3264	5.92	2586	4.49	2586	4.49	2622	5.04
5	3445	4.61	3775	4.38	3316	3.73	2579	1.78	2579	1.78	2615	2.05
6	3322	1.01	3616	0.69	3256	.35	2590	-1.49	2590	-1.49	2608	-1.38
7	2507	10.168	4468	11.0	2465	9.85	1584	+7.09	1584	7.09	1587	7.10
8	3117	10.81	3668	11.4	3084	10.19	2310	7.82	2310	7.82	2319	7.99
9	2666	11.15	3511	10.5	2577	9.92	1743	7.69	1743	7.69	1773	8.09
10	2884	7.09	3014	6.6	2762	6.13	2125	3.63	2125	3.63	2152	3.86
11	1989	8.28	2649	9.27	1917	7.90	1186	5.50	1186	5.50	1195	5.62
12	1380	10.047	1998	8.76	1270	8.37	793	6.95	793	6.95	817	7.28
13	3204	-0.314	3487	-0.42	3099	-.89	2408	-2.83	2408	-2.83	2423	-2.77
14	1671	10.19	2042	10.7	1621	9.63	1183	7.08	1183	7.08	1195	7.19
Average	26265	7.44	3138	7.15	2526	6.45	1817	4.37	1875	4.37	1901	4.64

Note: Tape 53 with 1.6 volt peak audio.

Table II. Comparison of Rate and Signal-to-Noise Ratio Results for Talk Burst Rates.

The chief reason for increasing the volume was to increase the input audio signal-to-noise ratio. However it was found that this increase did not improve the quality-extremal rate ratio. Thus it was shown that the audio input S/N was not limiting the quality.

Finally, we wish to note the plot of the distribution between extrema. This is shown in Fig. 30. This graph shows the distribution of run No. 1 (constant threshold) and also No. 4. For comparison the distribution given by Ref. 4 is shown. This information in this distribution is used as a guide to indicate methods of improving the quality-extremal rate ratio. To increase the quality per rate it appears necessary to move the peak of this distribution to the right to correspond with the literature results.

4.1.2 Conclusions. In conclusion then the above series of results and accompanying listening tests indicate that ordinary telephone quality is obtainable at talkspurt rates of about 2100 extrema per second, which corresponds to talk burst rates of about 2300 extrema per second. Although these are the results accomplished within the amount of time available for this effort, we feel that even better quality may be obtained for a lower rate after some further development. As mentioned above, a potential improvement lies in detecting when the waveform remains constant for a period, and then artificially introducing an extremum at such a point.

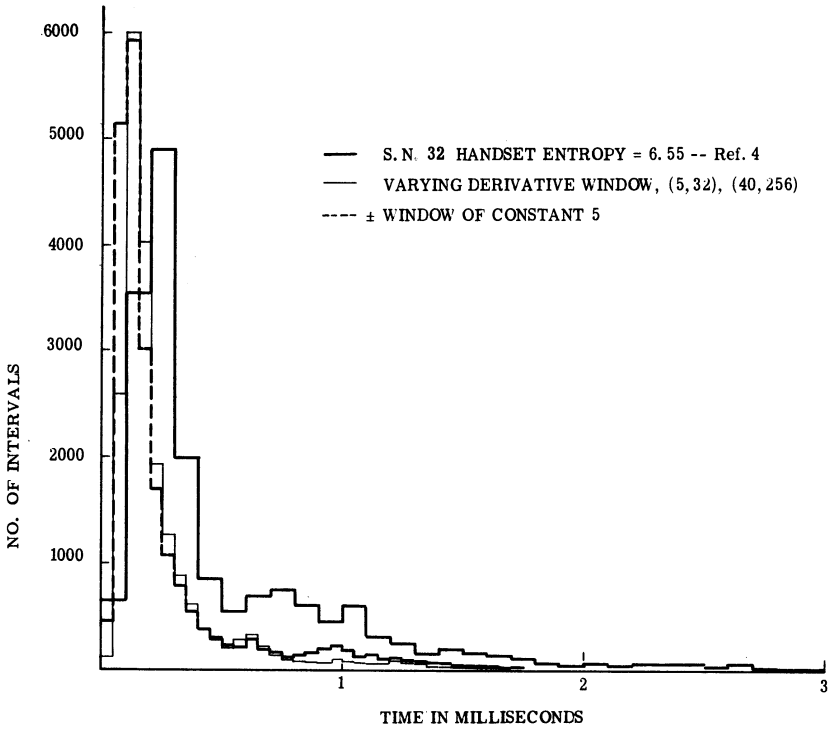

Fig. 30. Probability distribution of time between extrema for various conditions.

This concludes the results of the computer implementation of the signal channel extremal coding.

4.2 Implementation of Extremal Coded Channel by an Analog Method

In the asynchronous multiplexing system of interest here the function which is new and novel is the detecting of extrema, and the reconstruction of the waveform from extrema. In the previous section we described the computer method of implementing an extremal coded channel. The objective here was to demonstrate and build one prototype of an extremal coder and simple receiver. It was felt that since this is the unique portion of the entire system that this requires some prototype demonstration. The buffering operation and other aspects of this asynchronous multiplexing method are considered to be relatively straightforward applications of existing methods and techniques. The work here, then, represents essentially a fairly sophisticated extremum detector combined with a fairly simple receiver. The receiver simply consists of a "boxcar" circuit, which holds a constant value at the last sample voltage until the next sample arrives. This irregular step-like waveform is then filtered to provide the output.

A functional block diagram of the extremal coder and of the boxcar receiver is shown in Fig. 31. Although there are several ways in which the detection of the extrema may be performed, the simplest way is to differentiate the input signal and detect the zero-crossings of the differentiated wave. A pulse, then, at each zero-crossing is used to trigger a sampling gate, which samples the signal at the time of the detected extremum. Threshold and clipping operations (as in previous computer case) would be included to eliminate unnecessary or noise-caused extrema. A series of pulses, of heights representing the amplitude values of the extrema and located at the times they occur, is the output of this basic coder.

The circuit which was devised to implement this extremal coding is shown in Fig.

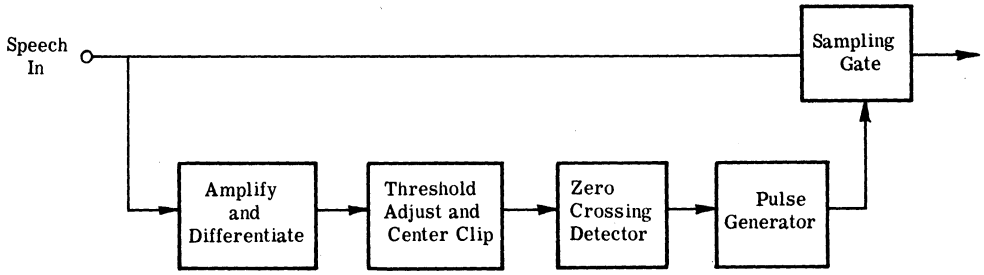

Fig. 31. Functional block diagram of analog extremal coder.

32. Basically, the circuit contains an input amplifier driving a differentiating circuit, certain threshold and bias adjustments, a zero-crossing detector, and a pulse generator driving a sampling gate. In addition, there is a capacitor holding circuit on the output of the sampling gate which acts as a "boxcar" circuit. This circuit simulates a particular kind of decoding or receiving circuit which might be used with extremum coding and transmission systems.

Basically the operation of the circuit is as follows. The input amplifier drives an RC differentiating network, the output of which is amplified and fed to a clipping circuit. By means of the Bias control (see circuit diagram), it is possible to adjust the zero clipping level of the clipping circuit. The clipper produces a rectangular wave whose transistions occur at the zero-crossings of the differentiated signal. Thus a zero-crossing with a positive slope produces the positive portion of the rectangular wave, and a negative-going zero-crossing produces the negative portion of the wave. In addition, by means of the Hysterisis and Balance controls, it is possible to spread the clipping points so that a positive-going slope through the zero level will not result in the clipper operating until the positive-going voltage has reached a certain value above zero. Similarly, the curve will not produce a negative-going transition until the differentiated signal has passed through zero, and past a certain negative voltage level. The spreading of these transition levels from zero to points on either side of zero allows the elimination of small fluctuations around zero of the derivative which correspond to small "bumps" and noise in the original inputs.

The rectangular wave output of the clipper is passed through a phase inverter and a differentiating circuit which feeds a diode gate, with the result that a negative pulse is produced for each transistion of the clipper. Thus a pulse is produced at the extreme points of the original input signal. These negative pulses are fed to the blocking oscillator and an amplifier-inverter. The amplifier-inverter produces 20-volt pulses suitable for triggering a digital counter or other external equipment. The blocking oscillator provides the properly shaped sampling pulse to the sampling gate.

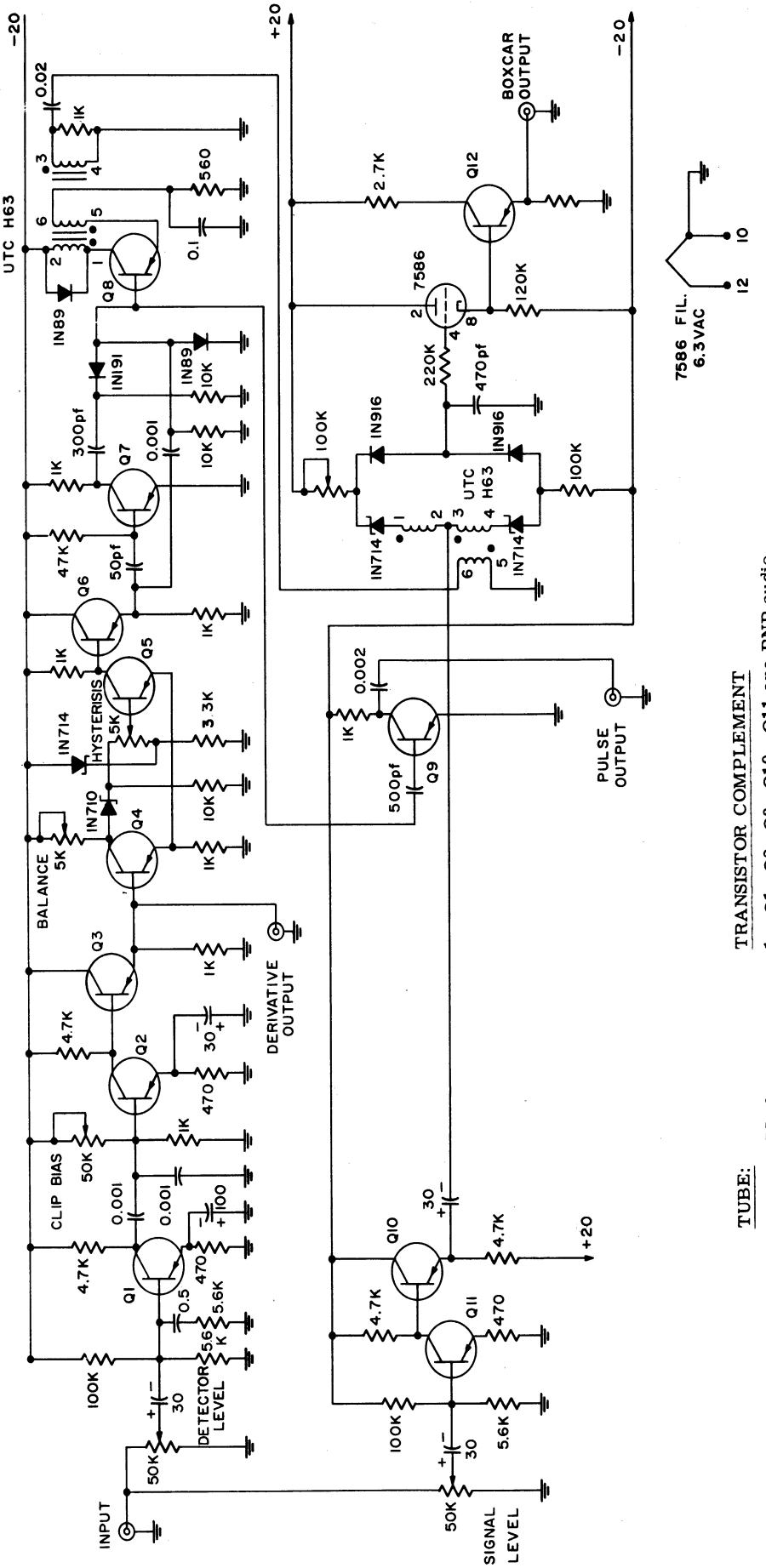

TUBE:

1. Type 75B6 Nuvistor

TRANSISTOR COMPLEMENT

1. Q1, Q2, Q3, Q10, Q11 are PNP audio transistors, 2N369, 2N526, or equiv.
2. Q4, Q5, Q6, Q7, Q8, Q9 are PNP switching transistors, 2N404 or equiv.
3. Q12 is an audio, NPN, Germanium, 2N336 or equiv.

Fig. 32. Analog extremum detector and boxcar receiver.

The original input signal is fed, through an amplifier and emitter follower driver, to the sampling gate. By means of the input sampling pulses from the detection circuit, the audio-input signal then is sampled at the extreme points of the wave. The output of the sampling gate, then, is a very narrow pulse of amplitude equal to the value of the input signal at the sampling time. At this point the sample would be set over a transmission link in an actual system. To implement the "receiver" a capacitor on the output of the sampling gate is then charged to the value of the sample amplitude, and holds this value until the next sampling pulse arrives. This implements the circuit commonly called "boxcar," since the output is a rectangular wave with varying amplitudes.

A nuvistor tube operated in a cathode follower configuration (Harris, Ref. 10) provides the necessary isolation between the "boxcar" circuit and the output circuits. This is necessary to keep the capacitor from being discharged between sampling times. The input impedance of the nuvistor is sufficiently high so that essentially a voltage reading is made of the capacitor output, thus keeping the output circuit sufficiently isolated.

The circuit described above was used in the experimental procedure depicted in Fig. 33. The speech input was first filtered by a lowpass 4 kc filter. The signal was then sent to the input of Fig. 32. Extrema rate was monitored by a counter, and scope pictures of input and output were taken. Provision was also made to switch from actual speech to extremal coded speech.

4.2.1 Experimental Results. The general results obtained in these experiments can be stated as follows: for rates of about 2000 extrema per second the quality with the boxcar receiver had noticeable noise which could not be entirely removed. Nevertheless there was entire intelligibility and speaker recognizabiltiy, etc. When we got to about 2800 extrema per second the quality was quite good. We feel that improvements on this circuit would result in an improved quality at rates of about 2000 extrema per second. Thus this would realize the previous computer results.

Our conclusion is that the number of permutations in the operation of this circuit were so great that we did not achieve a satisfactory peaking of the experimental results in the time available. It should be possible to improve this circuit so that a better quality extremal coded channel could be obtained for a lower (than 2800) extrema rate. We are sure that this process using this particular type of circuit has not yet been pushed to its optimum output.

4.3 Summary of Implementation Results

In summary the computer extremal coded experiments of the prior section were aimed at providing a method of finding good operating techniques and experimental bounds for extremal coding. Based on the time available, and with the methods used in this work, we were

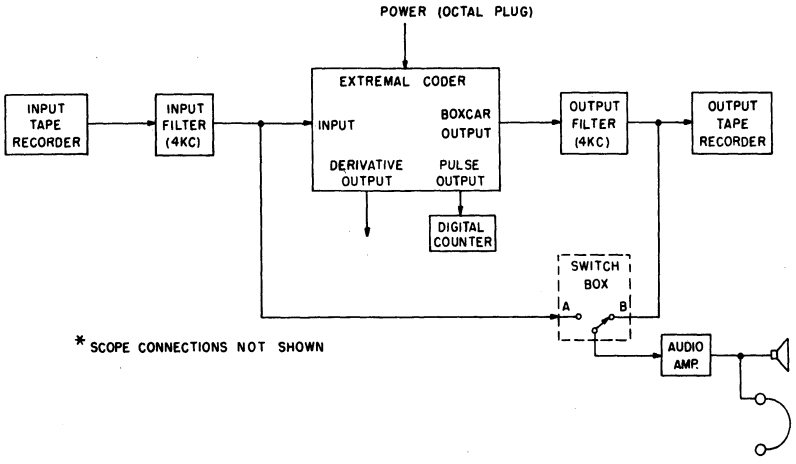

Fig. 33. Typical operating configuration

able to achieve quality comparable with good telephone quality at rates of the order of 2100 extrema per second (on the level of a talkspurt) which corresponds to an estimated 2300 extrema per second for a talk burst. Although this is the quality that we have been able to achieve in the time available here, we do not feel that this is the end or upper limit for this type of procedure. We estimate that something like 2000 extrema per second (talk burst) will be required for operating an extremal coded situation with sufficient quality and sufficient simplicity to warrant its practical implementation.

In the analog method just described, it was the intention to demonstrate that the equipment to implement such extremal coders is not very complex. Also, it was intended to use this analog system to implement the results of the computer experimentation. The results obtained via the analog method required higher extrema rates than those that were obtained with the computer method. Rates of the order of 2800 extrema per second (talk burst) were required in order to get acceptable quality. Although this is greater than the 2300, we believe this is due to circuit imperfections.

PART II. PERFORMANCE OF HIGH SPEED DIGITAL COMMUNICATIONS OVER TROPOSCATTER LINKS

It will be the objective in this section to study the critical issues when sending high speed digital data over troposcatter radio links. Although the sending of digital data over troposcatter links is not new, the particular aspect here is the high bit rate. This treatment will be somewhat general, but will emphasize the case where the data is sent via FM modulation.[5]

When a digital communication system is in the presence of fading, there are two basic issues to consider. The first issue is the "probability of error," assuming that the link is synchronized. The second issue deals with how the fading affects the digital synchronization. The determination of the probability of error under fading has been studied fairly extensively in the past; in our work here effort was spent in ascertaining the results of this work, and will be reported below.

The major effort here was spent investigating the effect of the fading on the synchronization. This is a crucial aspect for all time-multiplexed digital systems, especially at high data rates.

In the following section I will first report the collected results on the expected behavior of the probability of error. In reporting these predictions, we will first discuss the issue when there is no fading. There are a number of issues concerned with sending data that are profitably discussed before considering the effect of fading. Section 1 then will consider first the probability of error for systems without fading, and then for systems with fading.

Section 2 is concerned with evaluating the effect of the fading on the sync. The basic method utilized here consists of using data from a simulation to estimate the fading conditions under an actual Rayleigh fading link. This data will be applied to two different diversity models in an attempt to obtain a range of realistic estimates of expected performance.

1. THEORETICAL PREDICTIONS FOR PROBABILITY OF ERROR ASSUMING SYNCHRONIZATION

We are here dealing with the issue of sending digital data over a communication link and considering the probability of error, assuming synchronization. When the link has fading conditions, one both has to worry not only about the effect of the fading on the probability of error itself, but also how the fading affects the ability to keep the system synchronized.

[5]The Signal Corps is effecting a high speed (576 kc) digital troposcatter link which uses FM modulation. The video signal is time-multiplexed PCM voice samples. The link operates between Tobyhana, Pa. and Fort Monmouth, N. J. The link is operated by the Radio Relay Branch in USAELRDL at Fort Monmouth.

As mentioned above, we will first consider the sending of digital data without fading to establish some fundamentals involved. Therefore this section will consider first the case without fading and then the case with fading.

When considering sending digital (PCM) signals over radio links, it is first necessary to note whether the system is digital throughout, or whether the RF link is basically analog. It is clear that a digital signal can modulate an analog signal, and thus send the data over an analog system.

For a number of reasons, to be discussed below, it would be desirable to send digital data over strictly digital channels. There are two major reasons for sending digital data over analog links. First of all, most of the RF links across the country employ analog modulation. This is because the major communication signals in the past have been voice and television. However, the ever-growing use of digital computers means that digital signals will become increasingly important in the future.

Secondly, analog modulations must be used if one wishes to send both digital and analog signals. Many times one avoids digitizing an analog signal, and the signal must be sent analog. For these reasons, then, digital signals are often sent via analog modulations.

It is of interest to note any differences between sending data over digital systems and sending it over analog systems.

1.1 Digital Systems Versus Analog Systems.

First of all, in a digital system the object of the receiver is to make a decision. For this purpose the receiver must be synchronized, and any distortion of the waveform is important only to the extent that it affects the decision. In analog systems, on the other hand, it is the objective of the receiver to extract the modulating signal with as much accuracy and signal fidelity as possible. Here noise enters into the system in a different way, since any change of waveform is direct noise.

Thus if one sends digital data over an analog modulation it is not clear that one gets the same noise properties as if one used a digital modulation (or receiver). However, one might be able to get equivalent noise properties. Consider as an example the use of FSK versus FM. If an FM signal is modulated by a binary video, the resulting transmitted signal is similar to an FSK signal. The receiver, however, is an analog discriminator receiver rather than a digital FSK one.

It is of interest also to compare the performance measures for the digital system with that of the analog system. In the digital system one carries out a probability of error calculation wherein one evaluates the probability of making a correct decision in the presence of distorting noise. To do this one must make assumptions about the coherence of the signal, the

synchronization (to coordinate sampling time), and properties of the noise. Using these one in effect evaluates the probability densities of both "correct signal-plus-noise" and "incorrect signal-plus-noise," to arrive at a probability of error. A very important item here is that one always has both the signal and noise present in the calculation. The analog method on the other hand is concerned with the usual calculation of audio-like signal-to-noise ratios. Here one usually treats the signal and the noise separately. The signal-to-noise ratio is presumably well correlated with the deteriorating effect (to an observer) of a speech (or a video) signal. For these calculations the signal is assumed to be either a sine wave or a random signal with an assumed power spectrum. The noise is treated in terms of its power spectrum. One then evaluates the effect of the system on both the signal and the noise. Note that here the signal and the noise are treated separately. It is well-known that for large signal-to-noise ratios this separate treatment is comparable to the simultaneous treatment.

The point here is to note a basic difference between a digital and an analog evaluation. It has long been recognized that there is a certain arbitrariness about analog signal-to-noise ratios. This aspect introduces some complexity when evaluating digital data over analog modulations.

The above are the basic differences encountered when considering sending data over digital systems as compared to analog systems.

1.2 Probability of Error Comparison with no Fading

We now wish to protray both theoretical and experimental probability of error results (without fading) for various methods of sending digital data. Both digital and analog modulations will be assumed; the first four curves will be theoretical results, while the fifth is experimental.

The comparative results are depicted in Fig. 34, and the discussion here will center around this figure. Curve A on this figure refers to the digital PSK case. If one has available complete RF coherence, then the best binary system that one can construct in the presence of white Gaussian noise is the "phase shift keyed" system. A block diagram of a PSK system corresponding to this curve is shown in Fig. 35. Here it is seen how the coherence and synchronization enter in. One must have the coherence in order to be able to multiply by a signal of exactly the correct phase, and one must be synchronized in order to sample at exactly the right point.

The next case (curve B of Fig. 34) refers to the "differentially coherent" case, which is a slight modification of the coherent case. Here it is assumed that one uses the phase of the previous "signal" as reference, so that one can make the decision based on the change of phase. Curve B of Fig. 34 depicts the theoretical probability of error for a binary differentially coherent case. It is seen that this performance is only about 1 db worse than the coherent ideal.

Curves C and D on Fig. 34 represent two theoretical predictions for sending digital data via an FM (analog) modulation. The curves are different because different models are

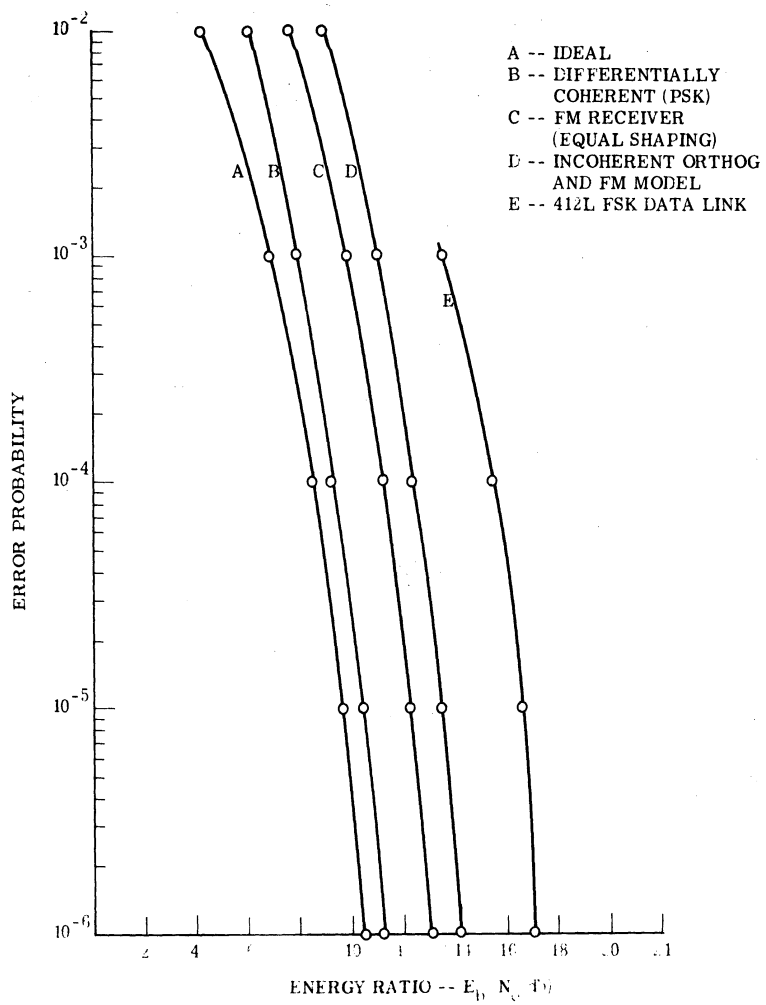

Fig. 34. Probability of error versus E_b N_o for nonfading conditions.

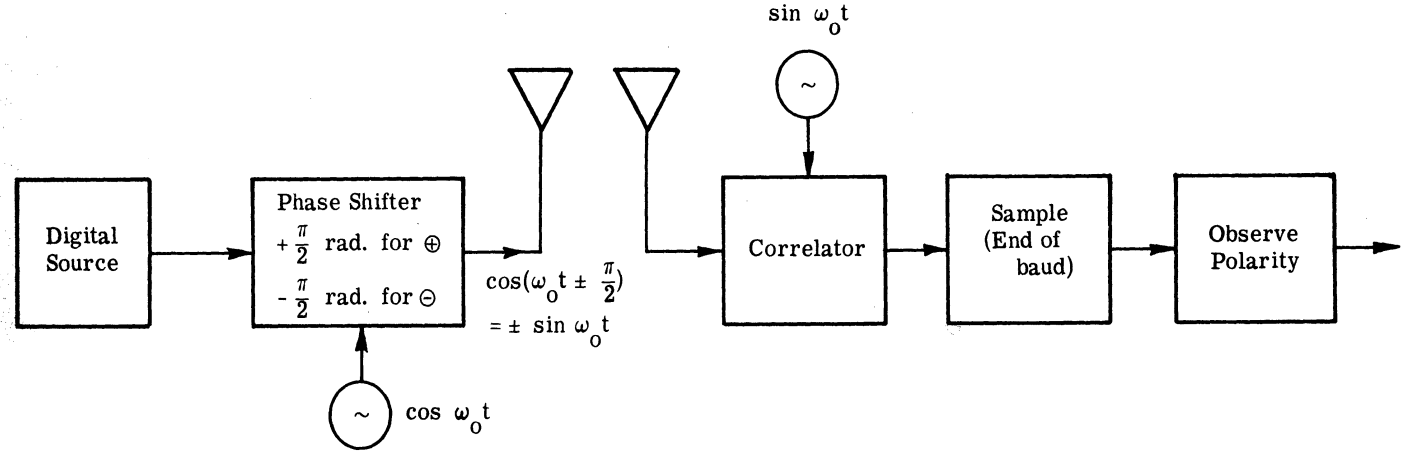

Fig. 35. Block diagram of PSK digital system (coherent)

used for the theoretical prediction. FM is often used as the RF modulation for sending digital data both because it is a fairly efficient method (similar to FSK) and because so many existing RF link-terminals have FM as their modulation.

Curve C of Fig. 34 is derived by Meyerhoff and Mazer, Ref. 12, and gives the result when an FM modulation under certain conditions is used for digital data. The important assumption here is that both the transmitter and the receiver have a Gaussian-shaped filter. The transmitter has a low pass Gaussian filter to do the video shaping so that the modulating pulse (and hence frequency variation) is Gaussian. In the receiver the IF bandpass is assumed to have a Gaussian frequency response. Also, it is assumed that the noise is white Gaussian, and that one has perfect video synchronism. In Ref. 12 it is stated that about 1 db should be allowed for intersymbol influence from the results depicted here. However since all system calculations have idealizations, we did think it necessary to alter the stated results for comparative purposes. Therefore curve C represents the predicted results when sending data over FM under the conditions stated above.

Curve D on Fig. 34 shows the prediction for binary data over FM using a different model. This case is evaluated by Montgomery, Ref. 11. Since the analysis there was in terms of S/N, it was necessary to assume a TW to plot the error probability, P_E, as a function of E_b/N_o.[6] In accordance with the TW factors treated in Ref. 1 (p. 16), a TW factor of 2 was used here. This is the factor associated with "incoherent FSK," and appears suitable here. This TW factor is the "occupancy" factor, and is determined by how close one can place two frequencies and not cause interference if integrating over a time T (band length).

Using 2 for TW then, the results of Ref. 11 appear as shown on Curve D. These results are achieved by a fairly simple vector diagram depicting the role of signal and noise. It is assumed that the undeviated carrier frequency is the reference, and that the center frequency has been subtracted from the frequency to be measured so that one needs to confine attention only to the difference. The decision device then depends upon deciding whether the "phase" advances or recedes during one binary interval. The vector diagram analysis then reduces to two cases:

1. No errors can occur as long as S exceeds N
2. If N exceeds S, errors occur for half the time.

This analysis of course ignores those cases where the noise changes status during a bit interval (baud). Thus it is assumed that the noise remains constant during a baud. In a non-fading situation the FM signal can of course be assumed constant.

[6] S/N is defined as the r.m.s. signal power to noise power ratio. E_b/N_o is defined as the ratio of signal energy to noise power per cycle. S/N is related to E_b/N_o by the equation E_b/N_o = TW S/N. (see Ref. 1)

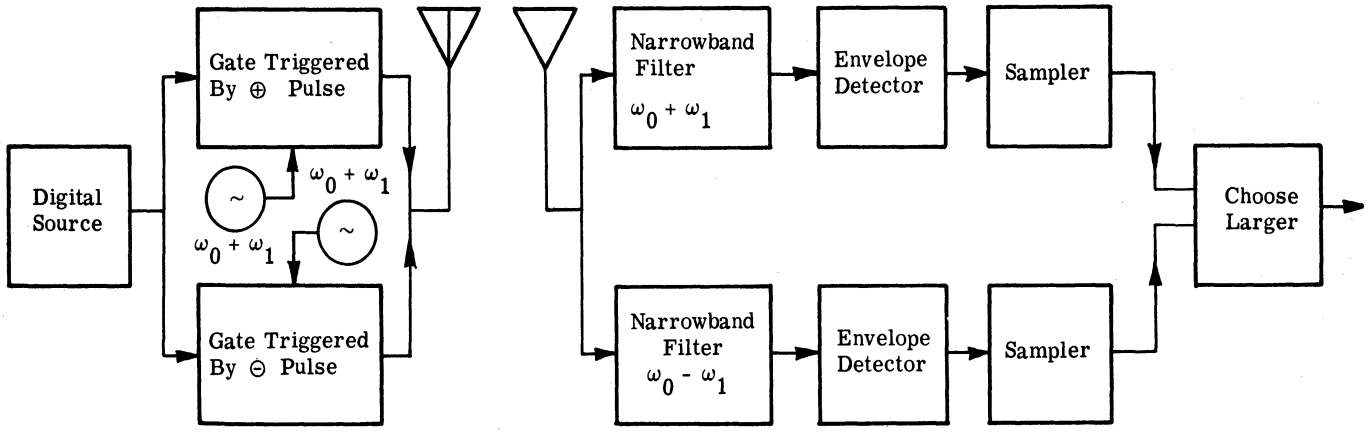

Fig. 36. Block diagram of incoherent FSK system.

We consider that Curves C and D on Fig. 34 indicate the range of probability of error for sending digital data via FM.

Curve D in Fig. 34 also results if one evaluates an incoherent FSK (incoherent orthogonal) digital system (Ref. 1). A block diagram of this system is shown in Fig. 36. This curve is achieved by the methods depicted in Ref. 1, and these methods are standard for digital systems.

From the above theoretical predictions we conclude that an FM modulation should be able to perform about as well as an incoherent FSK digital system when sending digital data. Curve E on Fig. 34, represents the measured results for the performance of the Air Force 412L FSK Data Link (Ref. 19). Our purpose in noting this result is to depict the measured results for an entirely digital system. Of course, each system has its particular goals and problems. The objective of this system is to implement a digital data system for transmitting over a narrowband voice channel at a bit rate of 750 or 1500 bits per second, where the typical link is a telephone line.

Thus this system was not designed to be optimized against white Gaussian noise, but rather in terms of impulse noise and envelope delay distortion. The results here simply state the performance when the system was evaluated in the presence of white Gaussian noise; the system was optimized in terms of the above goals.

It is of interest to note that the effective TW here is 2.54. We use a theoretical value of 2 when considering an incoherent FSK system.

In conclusion, in comparing the situation for sending data over non-fading links it appears that theoretically one should be able to operate an analog FM signal at about the same performance as a digital incoherent FSK system. This implies that a discriminator-plus-sampler receiver is fairly efficient for sending data. Also, it appears that one can in practice achieve a digital system which is within 3 db of the theoretical incoherent performance. This comparison holds when the disturbance is white Gaussian noise.

1.3 Probability of Error Behavior with Rayleigh Fading

In this section we wish to depict those theoretical results which have been predicted for the probability of error behavior when sending digital data over Rayleigh fading links. These results, of course, assume that the system is synchronized. The Rayleigh probability density function appears to fit actual measured fading statistics for observation times in the order of minutes. The effect of fading on synchronization will be considered in the next section.

We will depict the probability of error results both for no-diversity and with diversity for three cases. The three cases are: (1) differentially coherent phase shift keyed; (2) an FM time multiplexed case; and (3) an FM frequency multiplexed case. The reasons for discussing these three cases are of interest. First of all, on fading links it is impractical to operate with complete coherence. Differential coherence, however, should be possible. When considering the FM case, it will be remembered that the FM case in the previous section included both the coherent FSK case and the case of modulating an FM signal with a binary train. Here we wish to note that either of these cases also includes time multiplexed FSK or FM cases. It makes no difference, so far as the link is concerned, whether the binary train comes from a simple source or from interleaved sources. Since frequency multiplexing is another common way of multiplexing this case has been included here.

The theoretical probability of error curves, both for no-diversity and with dual diversity, for these three cases are shown in Fig. 37. The first set of curves of Fig. 37 refers to the differentially coherent PSK in the presence of fading. Curve A refers to the situation with a single channel and Curve A' when maximal ratio diversity is included. These theoretical results have been taken from Voelcker, Ref. 20. The major assumptions used in this work are: (1) the interference is white Gaussian noise; (2) fading and this white Gaussian noise are assumed to be the only forms of disturbance; (3) the communication system is assumed to be time synchronous, and (4) the results shown here apply to an "optimum receiver." In applying the results here it was again necessary to assume a TW factor. A TW factor of 1 was assumed, which is justified in Ref. 1 (p. 16). Of course the link conditions and the equipment stabilities have to be sufficient to prevent the level of coherence required for the differentially coherent PSK. Fading will generally preclude the operation of any coherent communication system except for this DCPSK.

The next set of curves (to the right) on Fig. 37 refer either to the FSK case or the case where an FM modulator is modulated by a binary signal. Curve B refers to the fading single channel case and Curve B' states the corresponding case with dual diversity.

Curve B, for no-diversity, is obtained by simply treating E_b/N_o as a random variable. Thus, both for incoherent FSK and for FM modulated by a binary train, the predicted

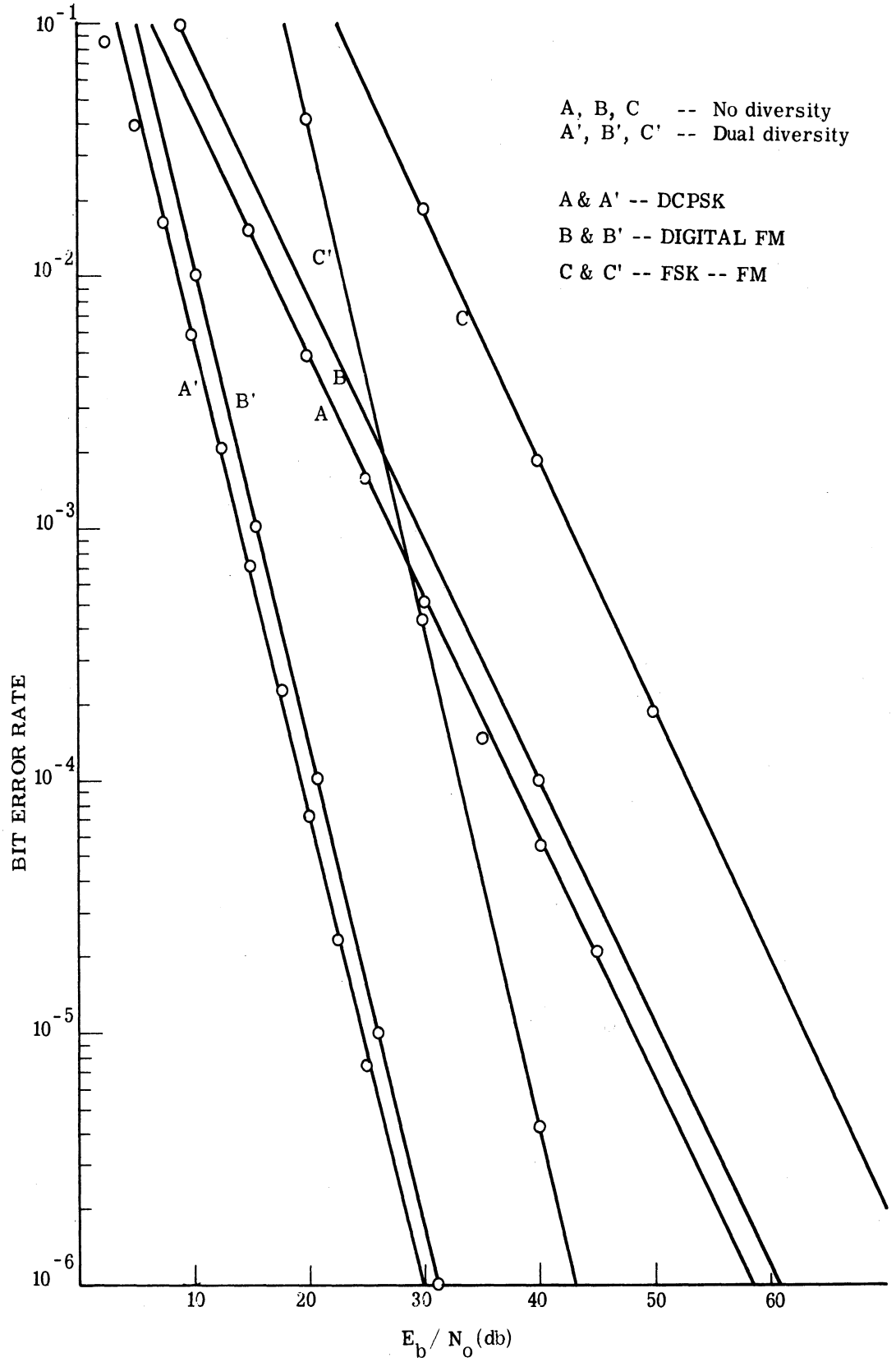

Fig. 37. Probability of Error versus E_b/N_o for fading cases.

probability of error (Ref. 1 and 11) is:

$$P_E = \frac{1}{2} e^{-E'_b/2N_o} = \frac{1}{2} e^{-R} \tag{23}$$

where: $R \triangleq \frac{1}{2} E'_b/N_o$

E'_b = short time average signal energy

The P_E for fading (with no-diversity) can be estimated by leting $\sqrt{E'_b/N_o}$ have a Rayleigh distribution. We can now use the expression for finding the expected value of a random variable:

$$P_{EF} = \int_o^\infty P_E(R)\, p(\sqrt{R})\, dR \tag{24}$$

where: P_{EF} = probability of bit error with fading

$P_E(R)$ = probability of bit error for a given E'_b/N_o (equals the no-fading error result)

$p(\sqrt{R})$ = probability density (assumed Rayleigh) of $\sqrt{R}$

$$= \frac{\sqrt{R}}{R_{ave}} e^{-R/2\, R_{ave}}$$

in which $R_{ave} = E_b/2N_o$ = mean signal energy/$2N_o$. Using this equation, we have:

$$P_{EF} = \int_o^\infty \frac{1}{2} e^{-R} \frac{1}{R_{ave}} e^{-R/R_{ave}} dR$$

$$= \frac{1}{2(R_{ave} + 1)} = \frac{1}{2(E_b/2N_o + 1)} \tag{25}$$

Curve B then, is the result of plotting Eq. 25.

The case for dual diversity for this FM or FSK case was obtained by a simple approximation. If the two channels in a diversity reception are independent, and if an ideal diversity circuit can be implemented, then we can argue as follows. The error probability is dominated by the time when the input is below threshold. If we over simplify the situation by saying that few errors occur above threshold, and that the error rate is 50% below threshold, then an overall error probability of P_1 indicates the input is below threshold $2P_1$ of the time. A number, n, of independent similar inputs will be simultaneously below threshold $(2P_1)^n$ of the time, and the resultant overall error probability will be $.5(2P_1)^n$. Barrow (Ref. 14) obtains the identical expression by a more careful derivation. Further, since the equal gain and switched diversity results are close for two channels (Brennan, Ref. 22) this approximate result can be regarded as applicable to either.

As mentioned before, this set of curves notice includes the time multiplex case. In other words if one is modulating the FM situation with a binary case it does not matter whether

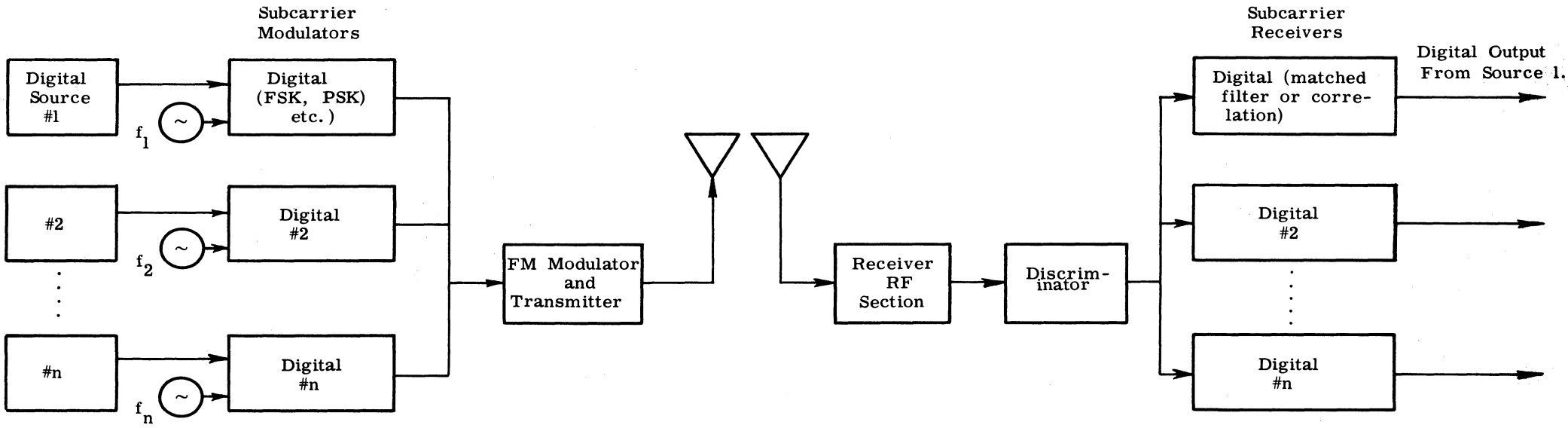

Fig. 38. Block diagram of FSK-FM system.

the binary signals are being time multiplexed or not. Since another quite common way of multiplexing multiple sources is to use frequency multiplexing, it is of interest to consider this method with FM under fading. This area has been the subject of a good deal of theoretical work (Castel and Magnen, Ref. 13; Barrow, Ref. 14; Johansen, Ref. 15).

Curve C shows the theoretical prediction for no-diversity, and C' for maximal ratio dual diversity. When frequency multiplexing digital signals over FM one is in effect combining FSK signals of differing frequency, and using the result to modulate an FM signal. Thus such a system is called FSK-FM. A block diagram of such a system is shown in Fig. 38.

The analysis of frequency division multiplexed-FM systems is complicated because the results depend upon the particular subcarrier channel, the duty factor associated with the participating channels, what steps are taken against cross-talk, whether or not pre-emphasis is used, and many other factors. Therefore this is one of the most complex cases to handle and possibly one of the least reliable in its theoretical predictions. We notice on Fig. 37 that there is a great deal of difference between the frequency multiplex and the time multiplexed performance of FM systems. Possibly one of the reasons for this great difference is that there is no clean-cut theory here, but one must repeatedly make estimates of the actual parameters that are in force. For example the width and shape of the IF bandpass will effect the results, and this must always be estimated.

We will briefly indicate the method used to obtain the results in curves C and C'. For the digital part of the system one obtains the probability of error via the probability calculation of the type treated extensively in Ref. 1. For systems where one is multiplexing and sending the multiplexed data over an analog system, one in addition has to derive a curve for the signal-to-noise ratio at the input to the digital receiver versus the IF E_b/N_o of the composite RF signal. It is this curve which requires a great deal of effort to derive.

Curves C and C' in Fig. 37 show the plot of Eq. 33 of Ref. 15. This equation is:

$$P_{EF} = \frac{\sqrt{\pi}\ (20.8)^m}{2\ \Gamma\left(\frac{m+1}{2}\right)}\left(\frac{N_o}{E_b}\right)^m \qquad (26)$$

where: m = order of diversity

$\Gamma(x)$ = Gamma function

Some of the assumptions implied by this result are:

(1) An FSK-FM system using ideal (matched filter) incoherent FSK receivers for the individual data channels.

(2) Maximal-ratio IF combining of signals from diversity arms, done before FM detection.

(3) White Gaussian noise over RF bandwidth.

(4) The FM detector (a discriminator) is described below FM threshold by the formula:

$$[\text{SNR after discriminator}] = \left[3.4\,\frac{(\delta f)^2}{B}\,\tau\right][\text{SNR before discriminator}]^2 \qquad (27)$$

where: δf = rms frequency deviation produced by a single channel about its particular binary subcarrier

B = IF bandwidth (before discriminator)

τ = baud time (duration of telegraph waveform)

This description is for below threshold behavior, but is extended to above threshold to simplify analytical procedures, with resultant error estimate slightly optimistic. It should be noted that virtually all but errors will occur when the IF SNR is below the "threshold" of the discriminator, a nominal and loosely defined number below which, for decreasing SNR, discriminator performance degrades at a faster rate than it does above the threshold. This being the case, the performance of the discriminator below threshold is considerably more important than that above threshold, and the fact that nothing much goes wrong above threshold will enable us to make the approximation that the below threshold operation curve extends through the region of high SNR also. The error rates calculated from this approximation will be very slightly optimistic.

(5) No pre-emphasis, and every data channel occupies the same amount of bandwidth in the baseband.

(6) An rms load capacity defined as:

$$L = \frac{\frac{1}{\sqrt{2}} D f_o}{\Delta F} = \frac{\text{rms peak allowable frequency dev. of FM carrier}}{\text{rms frequency dev. of FM carrier}}$$

$$= 3.7 \qquad (28)$$

where: f_o = highest frequency in FM baseband

D = deviation ratio

ΔF = rms frequency deviation of FM carrier.

To summarize the above it is necessary to derive an effective "signal-to-noise ratio" between the digital situations, since one first performs an analog demodulation. The results as shown on Fig. 37 indicate that the frequency division multiplexing for sending data over FM situations is fairly poor. It is about 12 db poorer than the prediction when sending a time multiplexed binary signal over the FM channel. For this reason (assuming the model here to be reasonable) we conclude that frequency multiplexed-FM is fairly poor.

It appears that the composite frequency multiplexed signal does not permit one to optimize use of the FM signal in the manner possible with the binary modulated signal (curves

B and B'). Consequently when using an FM modulation for a multiplexed data signal, one should either use time multiplexing, or use the frequency multiplexed signal with single sideband modulation (see Ref. 15).

The above then, represent the theoretical predictions for sending digital data via FM modulation, and via a digital differentially coherent (DCPSK) system. According to these estimates one can only gain about 3 db by using DCPSK instead of an optimized use of an FM modulation.

2. EVALUATION OF SYNC BEHAVIOR UNDER FADING

Section 1 above depicted the probability of error estimates for various modulations in the presence of fading, assuming system synchronization. As noted before, this is only one of the two basic aspects to consider. The second aspect, the one being dealt with here, concerns the maintaining of synchronism during the fade. It will be the purpose here to ascertain the effect of the fading on the ability to retain the bit synchronization of the equipment.

Whereas the probability of error problem treated above has been widely studied and reported, this second problem dealing with the synchronism is more tailored to the individual system and consequently a relative lack of knowledge exists on this matter, especially for speed data systems over troposcatter links.

The essential idea in evaluating the effect of fading on synchronism is to relate the fading conditions presented by the channel to the circuit behavior exhibited by the sync circuits. For many purposes it is of interest to have this analysis available theoretically, in order to compare with any experimental results. This analysis should both help to uncover malfunctions in the existing operation, and also suggest improvements and their potential advantage.

In the following we will be trying to estimate the theoretical behavior of bit synchronism when sending digital data over troposcatter links. The basic approach to be used here will be as follows. First of all we will try to find, based on various physical situations, the value of a "critical fade." A critical fade is of such a length that if this length is exceeded the particular circuit being considered will lose absolute bit synchronism after a fade. We will evaluate a number of critical fade lengths, based on various assumptions and conditions assumed for the equipment operation.

Then using these critical fades, we will evaluate the probability of exceeding these critical fades, for given signal parameters. This will be done by assuming that a fade corresponds to crossing a given threshold. This is essentially a "level crossing" problem in which we will evaluate the probability of a "level crossing" exceeding the length of time of the critical fade. Note that this implies the presence of a fairly sharp threshold in the equipment performance at the given fade "level."

As in Section 1.2, the random signal amplitude at the receiver input for all cases considered will be assumed to be Rayleigh. The probability of obtaining a fade length exceeding the critical fade length, at a given fade level (threshold), will be obtained making use of computer-generated experimental results of a Rayleigh process. Since the parameters available from these results are valid for a single channel Rayleigh fading case (without diversity) we

have had to extend this basic method to the diversity cases. In the following we will investigate an equal gain diversity and an idealized switched diversity.

2.1 Selection of Critical Fade Length

As mentioned before the general idea involved in the investigation here is to assume that a certain power level represents a threshold or fade level, and we wish to know how often fades below this level will exceed a critical length. In general this procedure assumes that all signals above this threshold or fade level are satisfactory, while all those below are not satisfactory. Simplifications of this nature are necessary in order to proceed with any evaluation.

The first issue is to ascertain the length of critical fades below this threshold. A fade is "critical" if the receiver does not properly locate a framing digit at the end of a fade. In any time-multiplexed digital system it is necessary to have both a bit synchronism and a "frame" synchronism. Frame synchronization refers to grouping the bits in the proper way so that each "channel" gets its proper sample. If a scrambling security device were to be added to the system, one would in addition need "absolute" bit sync. Thus a critical fade will be determined both by what sync is required, and how it is accomplished.

The length of the critical fade in any particular system will be determined by whichever of the following three items first ceases to operate correctly:

1. The bit synchronization circuits and methods
2. The frame synchronization circuits and methods
3. The physical propagation factors combined with limiting equipment factors (such as clock stabilities).

In terms of optimizing the "critical" fade length, it is desirable to cause all three factors to cease operating at about the same time (after beginning a fade). It is useful to consider the basic aspects of each of these.

Bit synchronization should be relatively easy so long as signal is present. After the signal has faded, we will assume that the circuit can be adjusted so that it locks onto the nearest bit position when the signal returns.

The frame sync situation is more difficult. The basic reason for this is that there is ambiguity between the following two states:

1. The system is still frame synchronized, but the signal is sufficiently bad so that the "decision making" device contains many errors.
2. The system has lost frame sync, so that whether or not there is a good signal present is not pertinent.

It is clear that one has to select a "decision rule" with respect to when the system is in frame sync or out of sync. After a string of errors one will decide that frame synchronism

is lost, and will proceed to search for the new sync (called "frame search"). The length of the string of errors which will be permitted until this is done is the factor that determines whether frame sync will limit or control the critical fade.

In digital systems one usually uses an overt frame sync signal; the receiver then correlates with this known signal to detect proper frame position. There are basically two ways to approach the frame sync ambiguity problem. One way is to set a "threshold" on the correlator output for both lock-in (frame lock) and to initiate "frame search." This system would work as follows (with respect to framing). Assuming initially the system is out of frame sync, there will be zero average correlator output until sync is achieved. When correct frame is achieved (by stepping the receiver relative to transmitter) the correlator will begin to integrate away from zero. The system will recognize correct frame sync when the "lock-in" threshold is reached.

Assume now that frame sync is achieved, and a substantial string of errors occurs. The frame correlator output will drop accordingly. When it reaches the "frame search" threshold, the system will decide it has lost frame sync.

As mentioned, this threshold concept is one way to implement the frame sync function. It has the ambiguity disadvantage (mentioned above) that there is no way to distinguish between loss of frame sync and errors due to temporary loss of signal. In this method the actual threshold level, and the relative levels of lock-in and frame search thresholds are parameters which may be adjusted to give the best performance.

A second method, and one more appropriate for fading situations, (really an alteration of the first), consists of incorporating a "signal present" detection and a "hold clock" function. The object is to separate the two ambiguous situations mentioned above. In other words, one will not change the frame sync situation as long as the signal has faded. Also, when the signal does fade, the frame circuits go into a "hold" status which will retain the precise frequency (and phase) that existed prior to fade. The operation envisaged is then as follows. The frame lock-in is controlled by a threshold on a correlator output, as before. When the signal fades the signal detector will cause the "hold" status to go into effect. If the frame signal correlates when the signal returns the system returns to normal operation. If errors continue after the signal has revived, then a "frame search" procedure is initiated.

If the first method is used on a fading link, the frame sync is very likely to control the critical fade (assuming that bit sync does not disappear before this). If the second method is used, then the critical fade should be controlled by the third factor mentioned above: the combination of propagation considerations plus limiting equipment factors such as clock stabilities.

We will now discuss the propagation factors and related equipment parameters. The ability to recover the correct frame position after the signal has revived from a fade is

ultimately limited by the possible "phase" changes during a fade. The two major limiting factors here are: (1) the possible phase changes (phase in terms of "bits") during a fade, and (2) the equipment clock stabilities for the function of clock "holds" as described above.

The possible phase changes depend primarily on the data rate and the physical link-plus-terminals. In a troposcatter link, one can estimate the possible (bit) phase changes by considering the time difference between the extremity path lengths of the "common volume." The common volume, in turn is dependent on the beamwidth of the antenna, and the distance of the link.

If one is performing a "hold" operation during a fade, then the above phase changes must be combined with possible clock stabilities. At data rates of interest here (about 500 kc) it will be seen later in an example that present state-of-the-art clock stabilities do not limit the critical fade. Therefore, ultimate limitation on critical fade will be the signal phase changes during a fade, combined with sufficient attention to equipment development to ensure the indicated operation during fade.

The above then represent the items which will control the length of critical fades. We will now consider one example. For purposes of experimentation, the AN/TCC-44 PCM multiplexing equipment is being operated over an experimental troposcatter link. The data rate used here is 576 kc. We will use this situation as an example of the factors which determine the length of a critical fade.

Since this PCM equipment was designed for non-fading applications, its performance with respect to critical fades is of interest only as an example. It in no way represents a state-of-the-art position, since it was not designed with fading in mind.

First of all, some basic tests (Ref. 21) have indicated that the bit synchronism will cease to function about 0.3 milliseconds after the input signal is interrupted (faded). Thus the bit sync contributes a critical fade length of 0.3 milliseconds.

The frame sync for this equipment, assuming bit sync would still be present (i.e., a clock was being generated) should operate for 3.75 milliseconds after a fade began (Hatton Ref. 18). The frame sync situation uses the threshold method described above. The 3.75 milliseconds applies to particular parameters (see Ref. 18) and essentially states the time which will elapse, between the beginning of 50 percent errors and initiation of the frame search. Thus the frame sync portion of the equipment here, in theory, affords a critical fade length of 3.75 milliseconds. Based on some laboratory tests of the AN/TCC-44 (Ref. 21) it was found that the frame sync critical fade is actually about 2.0 milliseconds.

The remaining factors to consider in this example are the physical propagation

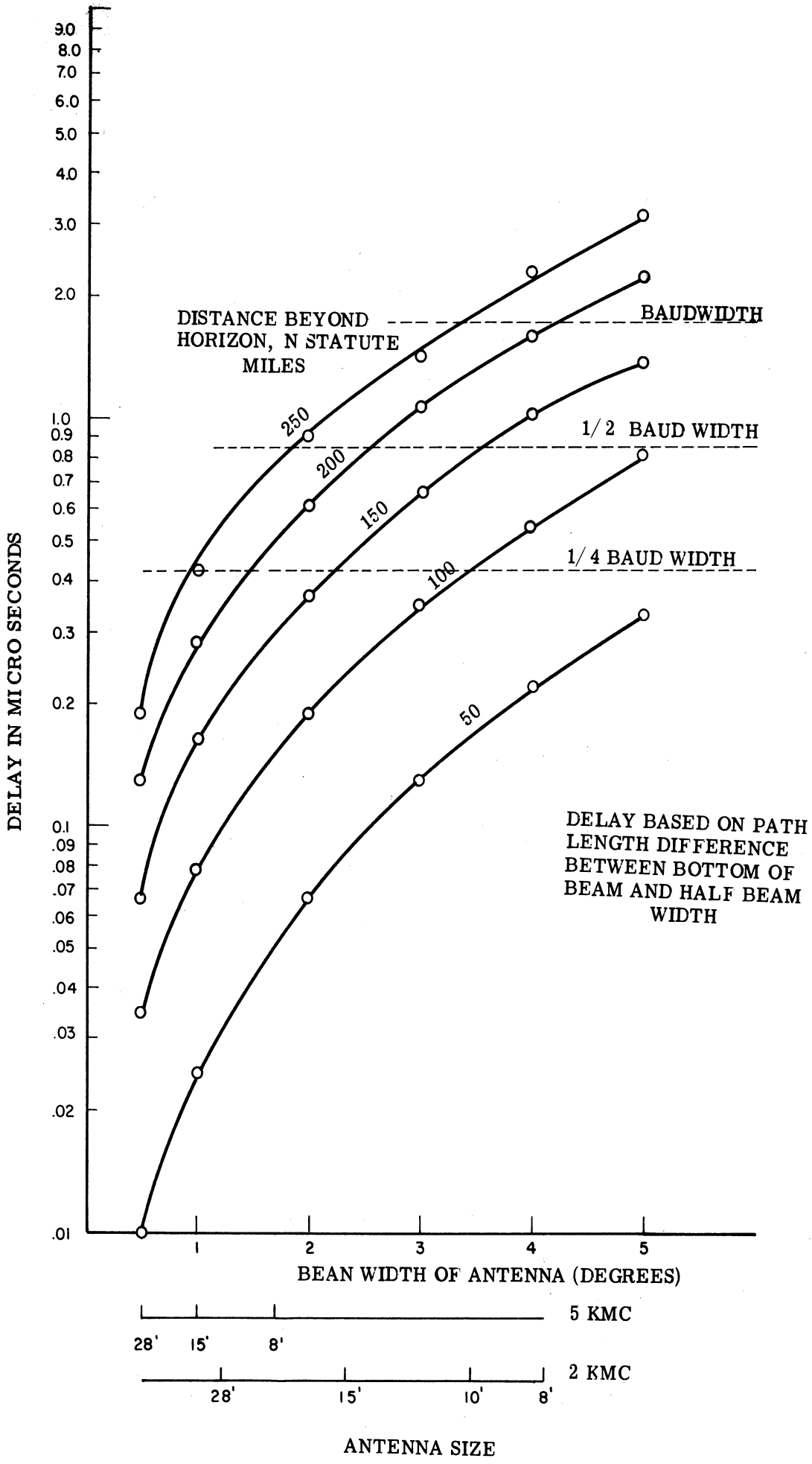

Fig. 39. Delay difference of troposcatter paths.

factors, and the related effect of clock stabilities. Figure 39 shows a plot[7] of the path length delay between the bottom of the "common volume" beam and a path in the middle of the beam. The abscissa is in terms of parabolic antenna size for two different frequencies. At a given data rate this plot shows how much the bit phase could change, during a fade if the path moved from the bottom of the beam to the middle.

In the example of the experimental troposcatter of interest here, the frequency is 5 kMc with 15' antennas. The distance is about 100 miles. From Fig. 39 the delay to half-beam path is 0.08 μ seconds. Thus the total time excursion, from extremity to extremity could be as great as 0.16 μ seconds. From this it appears that movement of bit phase during a fade can never exceed one-half a baud length at the baud rate of 576 kc. Therefore this aspect alone cannot determine a critical fade length.

If, during a fade, clock stabilities were inadequate, this would contribute to the bit phase change during the fade. However, with clock stabilities of about 1 part in 10^8 per second, it is easily seen that a critical fade of 5 seconds permissible (at 576 kc) even if only 1/10 of the baud is available for clock drift. Thus this will not limit the critical fade length under the conditions of this example.

In conclusion, we first considered those items which determine critical fade length. We then used as an example the AN/TCC-44 equipment over an experimental troposcatter link. With this example we have found the following:

1. With the equipment as originally designed for non-fading conditions, the critical fade length is 0.3 milliseconds, and is determined by loss of bit sync clock.
2. If bit sync clock were improved (for the fading situation), the critical fade length would then be 2.0 milliseconds (in practice) or 3.75 milliseconds by design, which is determined by the frame sync operation. This would be the time from occurrence of 50 percent errors to initiation of "frame search."
3. If the sync circuits were to be changed to operate on a "hold while fade" principle, the critical fade could be extended beyond 3.75 milliseconds. We found above that worst case path length change and available clock stabilities will not permit bit phase changes over half a baud at 576 kc. If perfect equipment operation were possible, critical fades could go as high as 5 seconds. For our purposes, however, we will investigate the situation for a more modest number: 50 milliseconds. We will assume this number to be a conservative representative of the range of critical fades if an attempt is made to design the sync circuits for fading conditions.

In order to study the effort of fading or synchronization, then, we will use the above

[7]This curve was supplied by the Radio Relay Branch of USAERDL, Fort Monmouth, N. J.

values of length (t_o) of critical fades in the next section. We will be able to see how much one can improve the situation by increasing the critical fade length.

2.2 Probability of a Critical Fade without Diversity

Having now dealt with the problem of specifying the critical fade lengths, we will depict the method of arriving at the probability of achieving such critical fades. Since the basic fading model and the signal parameters are in terms of a single channel (without diversity) we will first treat the case for no diverstiy. These results will then be extended to include both an "equal gain" diversity model, and an ideal "switched" diversity model.

The essential problem, when ascertaining the probability of exceeding a certain critical fade, is identical to the classical "level crossing" problem. Although level crossing problems can be expressed in terms of classic probability equations, it is exceedingly difficult to obtain practical solutions via this method.

An alternative to this classical procedure is the following. The statistical phenomena being studied can be generated on a computer. Then, various properties of this statistical model can be "measured" in an experimental fashion via the computer. This procedure results in a quasi-theoretical result, since one "theorizes" that the practical situation of interest is correctly represented by the test statistical model.

We will use this method here to "predict" the fade results for the experimental troposcatter link used as an example in the previous section. Although the particular parameters here will apply to this link, the method used here should have general utility for evaluating the effect of fading on synchronization.

For the troposcatter link example we will use the computer results for a Rayleigh fading signal as depicted by Favreau (Ref. 16). The work reported there used an electronic analog computer to measure (among other things) the "level crossing" probabilities of a Rayleigh fading signal. In this work the Rayleigh signal was generated by linear envelope detection of a narrowband Gaussian noise. It is well known that the envelope of a band of normally distributed noise approaches a true Rayleigh distribution as the bandwidth approaches zero. Essentially the experiment is run for intervals of length T; the level crossing probability is obtained by repeatedly running these experiments and counting the number of times in which a fade greater than a length t_o occurs.

To use these level crossing results the following are required as input parameters:

f_b = fading bandwidth (approximately the average fading rate; assumed 10 cps in example here)

T = observation time over which one observes the waveform

k = fading level (threshold), expressed as fraction of voltage mean.

In terms of these parameters, the precise level crossing probability measured in

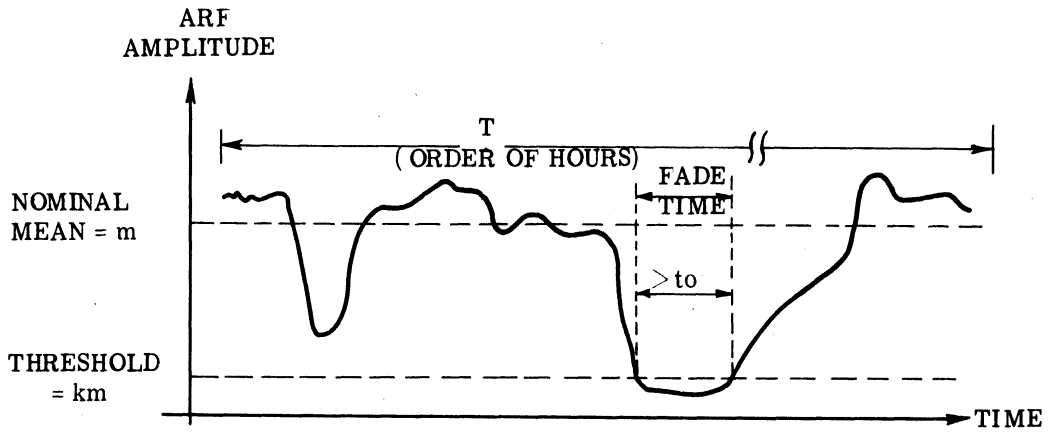

Fig. 40. Sample waveform of a typical fade.

Ref. 16 is $P(f_bT, f_bt_o, k)$, and is defined as follows:

$P(f_bT, f_bt_o, k) \equiv$ the probability that there are one or more fades of length greater than or equal to t_o during an observation period T.

It is clear that, if we let t_o equal a critical fade, that the above provides the probability of obtaining a critical fade. The above terminology can be clarified by referring to Fig. 40.

When measuring the level crossing situation for a Rayleigh distributed waveform (under the given conditions), Favreau found that an expression which fits the data quite well is:

$$P(f_bT, f_bt_o, k) \cong 1 - e^{-P'(0)f_bT} \tag{29}$$

where $P'(0)$ = average time density of occurrence of events (fades exceeding or equal to t_o).

Since Eq. 29 is in the form of the cumulative distribution for an event whose probability $P'(0)$ in an independent sample time $\frac{1}{f_b}$ is small, one result of the measurements is as follows: the level crossing situation in a Rayleigh case can be considered as taking independent samples at time intervals $T = 1/f_b$. As noted before, f_b is the bandwidth of the Rayleigh signal. Note that we can now interpret $P'(0)$ as being the probability of a fade in the interval $\frac{1}{f_b}$. This result simplifies the level crossing analysis.

Furthermore, the experimental measurements mentioned found the value of $P'(0)$ versus k. $P'(0)$ can be expressed as:

$$P'(0) = I(k)\, e^{-f_bt_o/r(k)} \tag{30}$$

where: $I(k)$ = intercept of Eq. 30 at $f_bt_o = 0$

$r(k)$ = reciprocal of slope of Eq. 30 on log-log paper.

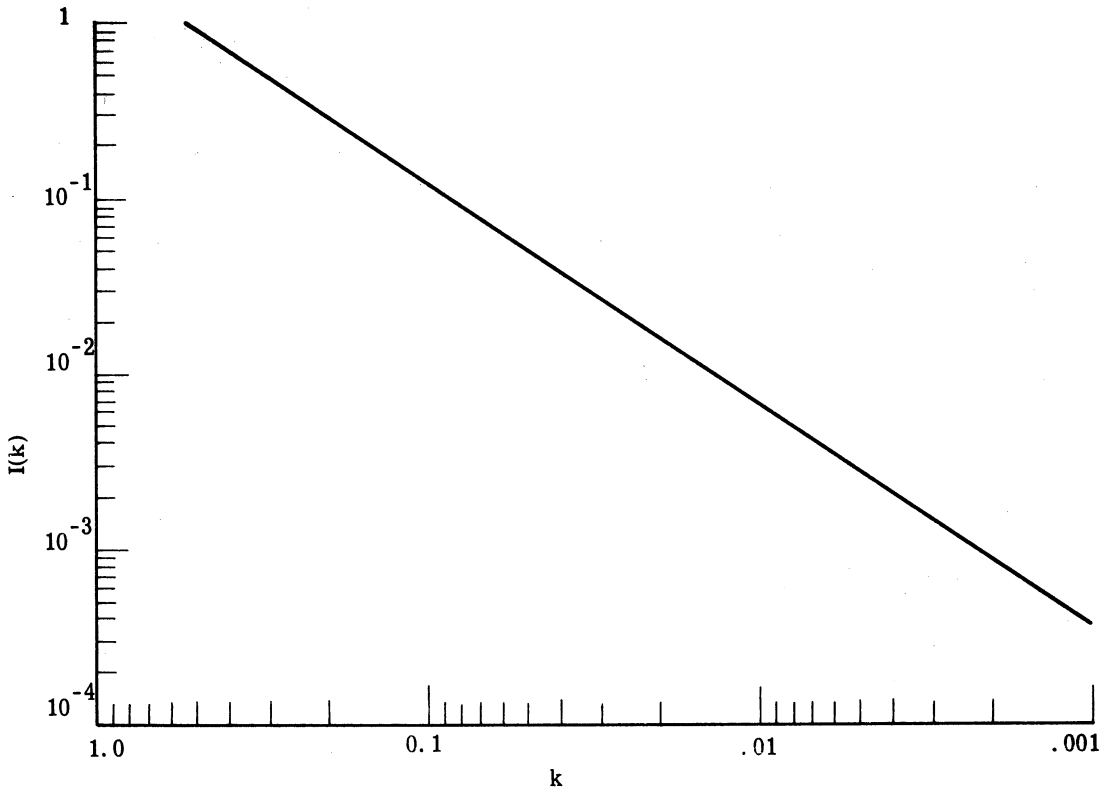

Fig. 41. Plot of I(k) versus k.

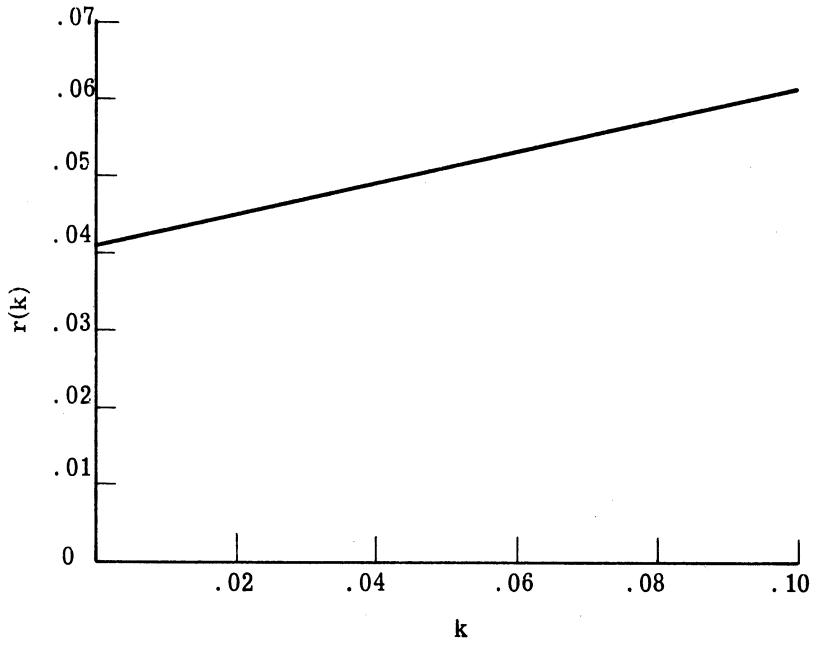

Fig. 42. Plot of r(k) versus k.

Using the resulting functions I(k) and r(k), we can find values of $P'(0)$ for any combination of the parameters f_b and t_o. The functions I(k) and r(k) are plotted versus k in figures 41 and 42.

We can now depict the fading prediction for a single channel troposcatter link with no diversity by applying the results of Ref. 16. In the next two sections we will extend this procedure to diversity cases.

First we must adopt values for the input parameters k and f_b, and values for the

System	t_o	P = .01	P = .095	P = .632
Single Channel	3.75 50	.04 3.44×10^{2}	.4 3.44×10^{3}	4.0 3.44×10^{4}
Equal Gain	3.75 50	3.21 2.5×10^{5}	32.1 2.5×10^{6}	321 2.5×10^{7}
Switch Diversity	3.75 50	20 2×10^{8}	200 2×10^{9}	2000 2.0×10^{10}

Table III. Table of observation times (T) for $t_o = 3.75$ msec. compared to $t_o = 50$ msec. $k_1 = .05$

critical fades (t_o). The following values have been selected on the basis of information from the Radio Relay Branch of USAERDL at Fort Monmouth:

f_b = 10 cps

k = 0.1 and 0.05. The 0.1 figure (20 db) roughly corresponds to the evident "fading margin" for the worst month of the year. The 0.05 figure (26 db) corresponds roughly to the margin with respect to the average of all months.

t_o = critical fade lengths = 0.3 milliseconds, 2.0 msec, 3.75 msec, and 50 msecs. These numbers are obtained from the example used in the preceding section.

The three left-most curves of Fig. 43 show the results of using Eq. 29 and some of the above parameters. Here the k = 0.05, which corresponds to a voltage difference of 26 db between the mean signal level and the fading threshold. The t_o's shown here are 0.3 msec, 2 msec and 3.75 msec. The 50 msec t_o is too far out of range to be plotted here, and is shown in a table form in Table III.

Assume for a moment that 3.75 msec is the critical fade length. In a 1 second observation interval the probability of one or more fades exceeding 3.75 msec is 0.2. On the average one would expect at least 1 fade every five seconds. It is obvious that such a situation is unacceptable. In the next section we will see how diversity improves the situation.

Figure 44 shows the same curves, but for a k of 0.1. This refers to 20 db, which is roughly the fade margin relative to the worst month of the year. It can be seen that the results are quite sensitive to k, as would be expected.

Having presented the results, it is necessary to consider the inaccuracies involved. Routhly speaking the fading situation can be thought of as follows. The average fading rate (f_b) can be visualized roughly as providing the "opportunity" for a fade of a certain length. In other words, the average number of times in which the signal is "down" is given by this average f_b. Then, in evaluating P, one is in effect evaluating the joint probability of both being down and of staying below a certain level for a given amount of time. As would be expected such a result

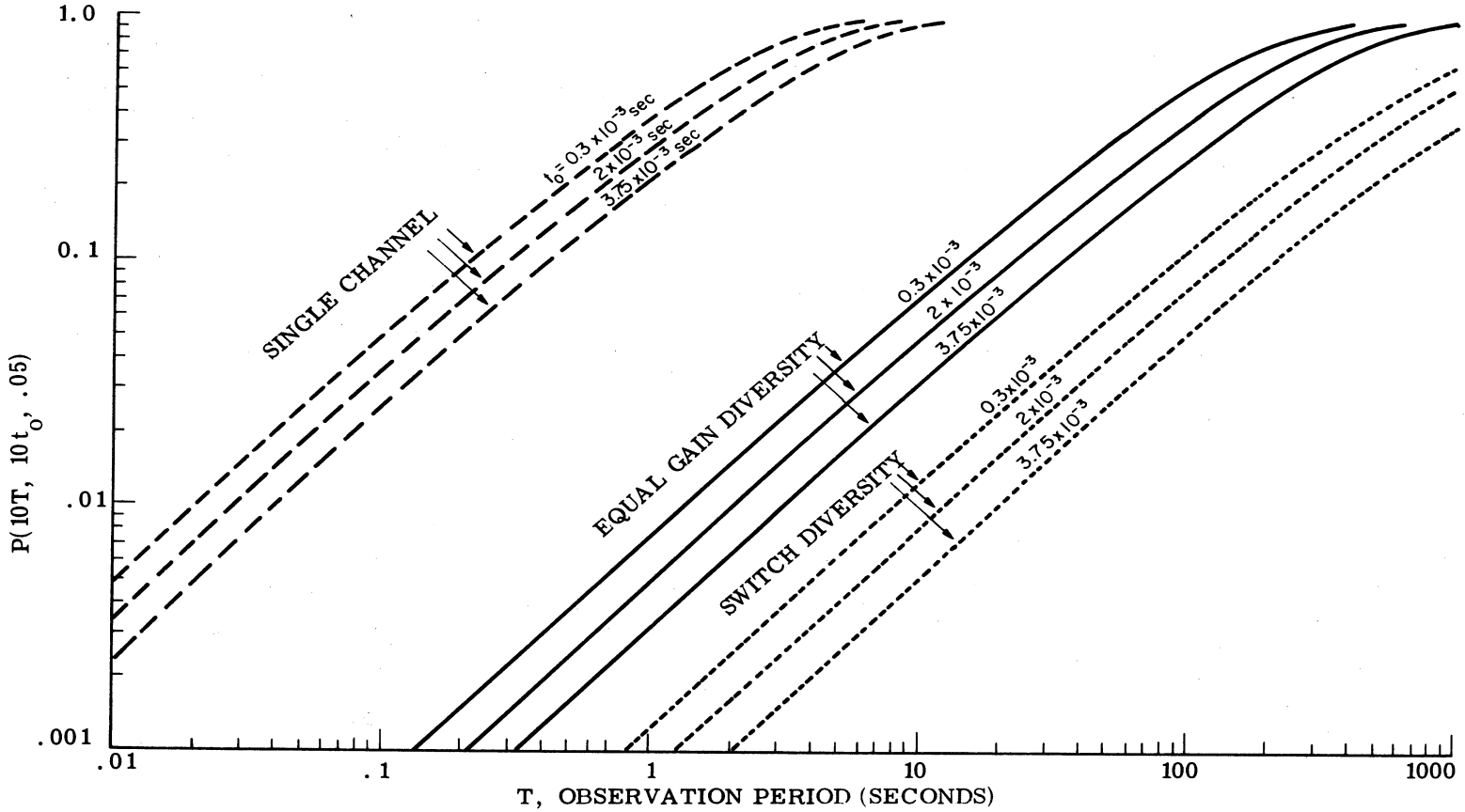

Fig. 43. Fade probability versus observation period threshold ratio $k_1 = .05$

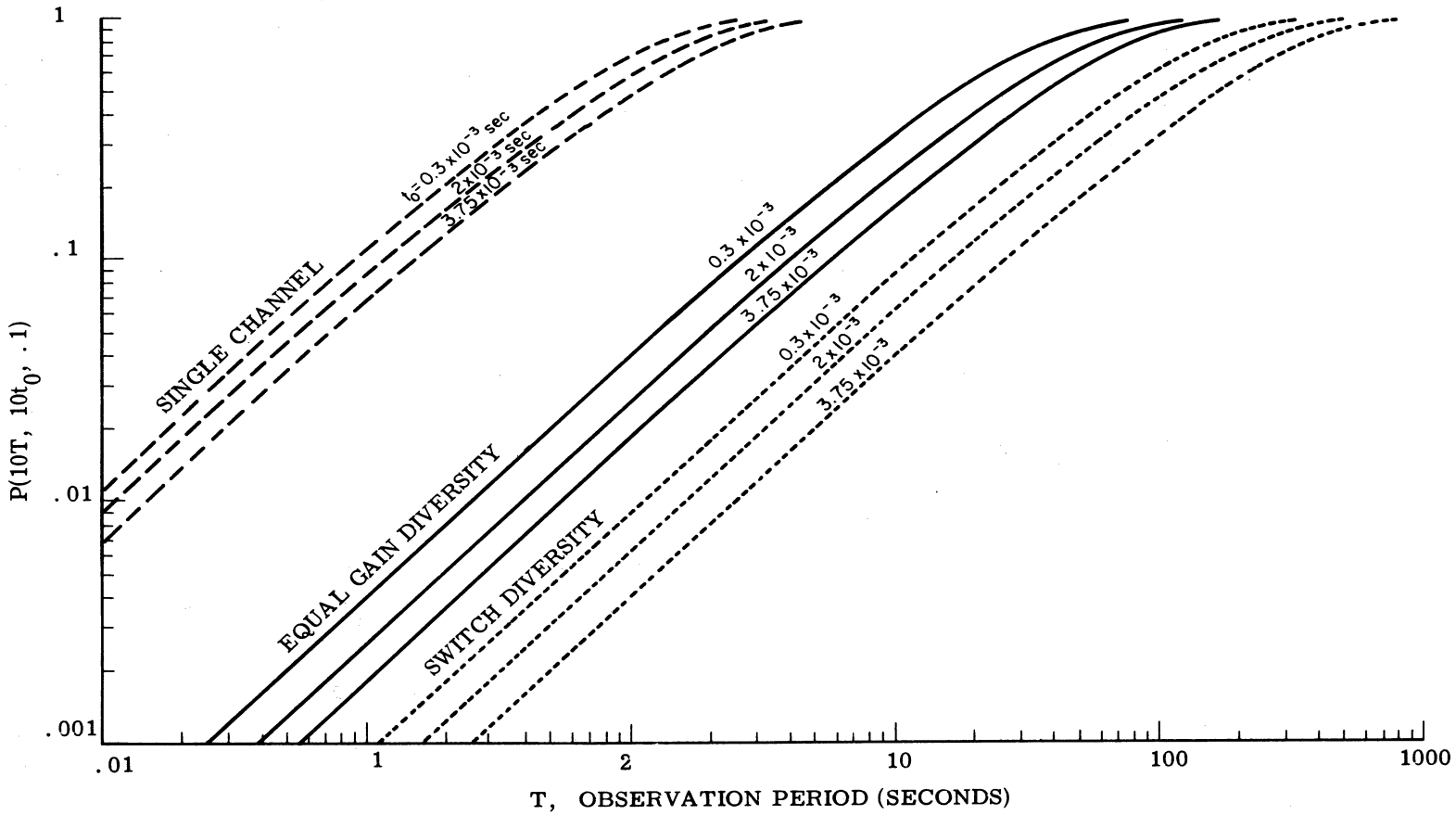

Fig. 44. Fade probability versus observation period.
Threshold ratio $k_1 = 0.1$

is highly dependent on the fine detail of the spectrum. This is probably the greatest inaccuracy in applying the data derived from the assumed statistical model to the physical troposcatter link. It is not clear that the actual frequency spectrum used in this experiment is a valid representation of that which occurs on the actual link. This would mean that the value of P'(0) may be somewhat inaccurate.

2.3 Probability of a Critical Fade with Equal Gain Diversity

Any communication system operating over a fading link, such as troposcatter, will use some type of diversity to offset the fading effects. In this section we will investigate the probability of exceeding a critical fade when an "equal gain diversity" (Ref. 22) is used. This type of diversity is widely used; in particular, it is the diversity used on the experimental troposcatter link mentioned above.

To accomplish this, the chief problem is to relate the single channel aspects to the diversity aspects. The initial input conditions (Rayleigh fading, threshold level, etc.) are all available in terms of a single channel; further, the simulation results (of a computer simulation) described in the previous section are also single channel results. Consequently, in the following, we must first note how the equal-gain diversity alters the single channel result; then, to relate this to the simulation result (for probability of fade) we will need to establish an equivalence between the equal gain behavior and a single channel behavior.

The first step then will be to calculate how the "k" changes when going from a single channel situation to an equal gain diversity situation. It is remembered that k is the ratio of the fading threshold to the signal mean (voltage). Naturally k will decrease with diversity since the mean will increase while the threshold remains constant. This step will of course require introducing a model for the equal-gain diversity behavior.

After this, we will need to relate the new k situation back to the single channel Rayleigh simulation results. We will do this by equating areas under the left-hand tail of two distributions: the first distribution will be the diversity output distribution and the second will be the Rayleigh distribution. By equating these two areas one in effect establishes a third k, or "mean to threshold" ratio. This new k_3 will enable us to use the single channel simulation data for finding probabilities for this diversity case.

2.3.1 Signal-to-Noise Ratio with Equal Gain Diversity. As noted above, we will here calculate how the ratio of threshold to signal mean (k) changes when equal gain diversity is used. Since the threshold may actually be expressed as a certain signal-to-noise ratio, as is the signal mean, we are actually dealing with a change in signal-to-noise ratio.

Figure 45 shows a simple block diagram of the equal gain diversity model. The $x_1(t)$ and $x_2(t)$ represent the amplitude variations caused by the fading. The m(t) represents the basic received carrier signal. It will of course be the same for all diversity channels since the fading is accounted for in the x's. The noise is typically contributed by thermal receiver

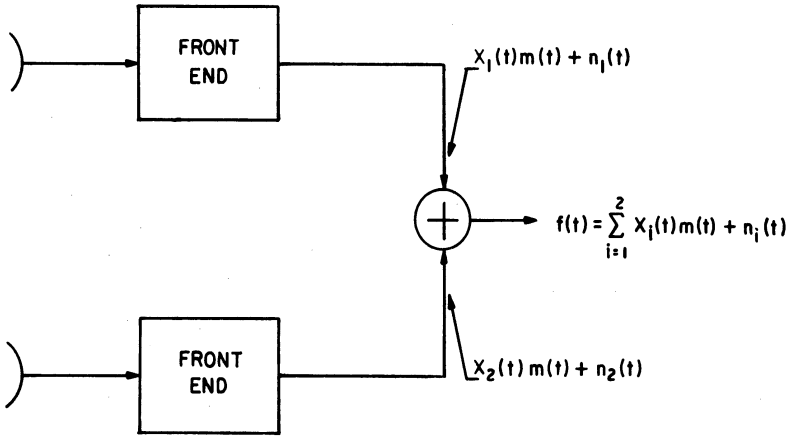

Fig. 45. Equal-gain diversity receiver.

(including antenna) noise. We wish then to compare the signal-to-noise ratio of the two-channel system of Fig. 45 to the signal-to-noise ratio of a single channel system. We may then derive a threshold ratio for the two-channel system, k, in terms of the single channel k.

To derive the new k_2, the following assumptions will be made:

1. $x_1(t)$ and $x_2(t)$ are independent random variables with identical Rayleigh distribution functions.

$$p[x_1(t)] = p[x_2(t)] = \frac{x}{V_x^2} e^{-x^2/2V_x^2} \tag{31}$$

where p[x(t)] is the probability density of the signal amplitude x.

$$V_x^2 = \text{mean of } x^2$$

$$\text{Mean of x is } \bar{x} = \int_{V_x^2}^{x^2} e^{-x^2/2V_x^2}\, dx = V_x \sqrt{\frac{\pi}{2}} \tag{32}$$

2. The bandwidth of signals, f_b, is small compared to the mean frequency of the information carrying signals, m(t).
3. $n_1(t)$ and $n_2(t)$ are uncorrelated internal noise signals with zero means, bandwidths of f_b, and equal rms values of $\sigma_n = \sqrt{\langle n^2 \rangle}$.

The instantaneous power output of the summing device in Fig. 45 is;

$$f^2 = \left\{[x_1(t)\, m(t) + n_1(t)] + [x_2(t)\, m(t) + n_2(t)]\right\}^2 \tag{33}$$

where: $x_1(t)$, $x_2(t)$ = positive real numbers that vary with time because of fading (Rayleigh)

$m(t)$ = originally transmitted signal

$n_1(t)$, $n_2(t)$ = receiver internal noise sources.

From assumptions (1) and (3), the time average power output (f^2) is;

$$\langle f^2 \rangle = \langle \Big[x_1(t)^2 \, m(t)^2 + 2x(t) \, x_2(t) \, m(t)^2 + x^2(t)^2 \, m(t)^2 + n_1(t)^2 + n_2(t)^2 \Big] \rangle$$

$$= \langle [x_1(t) + x_2(t)]^2 \, m(t)^2 \rangle + 2 \langle n^2 \rangle \tag{34}$$

If the average is taken over a small enough time interval, $x_1(t)$ and $x_2(t)$ will be constant; then in view of assumption (2) we get

$$\langle f^2 \rangle = [x_1(t) + x_2(t)]^2 \langle m^2 \rangle + 2\sigma_n^2 \tag{35}$$

where: $\sigma_N^2 = \langle n^2 \rangle$

The power signal-to-noise ratio, $p_2(t)$, for this two-channel system is then;

$$p_2(t) = \frac{[x_1(t) + x_2(t)]^2 \langle m^2 \rangle}{2\sigma_n^2} \tag{36}$$

where: $p_2(t)$ = power signal-to-noise ratio for equal gain diversity system.

The signal voltage-to-rms noise ratio, $v_2(t)$, is

$$v_2(t) = \frac{[x_1(t) + x_2(t)] \langle m^2 \rangle^{1/2}}{\sqrt{2}\,\sigma_n} \tag{37}$$

where: $v_2(t)$ = voltage signal-to-noise ratio for equal gain diversity systems.

The expected value for this signal voltage-to-rms noise ratio is

$$\overline{v_2(t)} = \frac{\sqrt{2}\ \overline{x_1(t)}\ \langle m^2 \rangle^{\frac{1}{2}}}{\sigma_n} \tag{38}$$

For the single channel case without diversity, the average power output is:

$$\langle f^2 \rangle = [x_1(t)]^2 \langle m^2 \rangle + \sigma_n^2 \tag{39}$$

The signal voltage-to-rms noise power for this single channel case is then

$$v_1(t) = \frac{x_1(t) < m^2 >^{1/2}}{\sigma_n} \tag{40}$$

and the expected value is

$$\overline{v_1(t)} = \frac{\overline{x_1(t)} < m^2 >^{1/2}}{\sigma_n} \tag{41}$$

We may now relate the threshold value for the single channel system, k_1, to the resulting threshold value for the two-channel system, k_2. If we denote the absolute voltage signal-to-noise threshold as α, we have

$$\alpha = k_1 \overline{v_1} \tag{42}$$

Substituting $\overline{v_2}$ for $\overline{v_1}$ from Eqs. 38 and 41, we get

$$\alpha = k_1 \frac{\overline{v_2}}{\sqrt{2}} = \left(\frac{k_1}{\sqrt{2}}\right) \overline{v_2}$$

$$= k_2 \overline{v_2} \tag{43}$$

Thus

$$k_2 = \frac{k_1}{\sqrt{2}} \tag{44}$$

which is the desired relationship. Thus, if a system has a "fading margin" between threshold S/N and mean S/N of k_1 db, for a single channel, then this margin should increase by 3 db if an equal gain diversity is used. This 3 db change in fade margin makes a substantial change in probability of exceeding a critical fade, as we shall see below.

2.3.2 Probability of Exceeding Critical Fade. In order to relate the above change in fading margin to the simulated experimental results of Ref. 16, which pertain to single channel Rayleigh fading, we need to find an equivalence between a point on the actual non-Rayleigh distribution of the diversity output and a point on a Rayleigh distribution. The method of analysis below assumes that $p_2(t)$ can be replaced (in this one aspect) by some Rayleigh random process whose distribution matches in the area of interest. It may be noted that the probability density of $p_2(t)$ is equal to the convolution of two Rayleigh functions, assuming that $x_1(t)$ and $x_2(t)$ are independent. Our problem, then, reduces to fitting a convoluted Rayleigh distribution with a Rayleigh one, at some point.

We will do this by equating the amount of time spent below the threshold α in each case. That is, we calculate the cumulative probability that $p_2(t)$ is less than or equal to α. Then we will take a Rayleigh density of the same mean, and find a new k_3 (or threshold) so that the cumulative probability of being below this threshold equals the previous probability. In this way, the simulated data will be used to approximate the probability of exceeding a critical fade when equal gain diversity is used.

From equations (36) and (37) it is evident that the probability that $v_2(t) \leq \alpha = k_2 \overline{v_2}(t)$ is equivalent to the probability that $x_1(t) + x_2(t) \leq k_2 2x_2(t)$. Since $x_1(t)$ and $x_2(t)$ are independent Rayleigh distributions, the probability that

$$P(x_1(t) + x_2(t) \leq k_2 2x_2(t) = P(v_2(t) \leq \alpha)$$

$$= \int_0^{k_2 2\overline{x_2(t)}} \int_{x_1=0}^{x_1=k_2 2\overline{x_2(t)}-x_2(t)} \frac{x_1}{V_x^2} e^{-x_1^2/2V_x^2} \frac{x_2}{V_x^2} e^{-x_2^2/2V_x^2} dx_1 dx_2 \tag{45}$$

where k_2 is the threshold ratio for the equal gain diversity system $V_x = \overline{x}_2 \sqrt{\frac{2}{\pi}}$ from equation 32.

After some algebra, we get;

$$P(v_2(t) \leq \alpha) = 1 - e^{-[k_2 2\overline{x_2(t)}]^2/2V_x} - \sqrt{\frac{\pi}{4V_x}} k_2 2\overline{x_2(t)}\, e^{-[k_2 2\overline{x_2(t)}]^2/4V_x} H\left(\frac{k_2 2\overline{x_2(t)}}{4V_x}\right)$$

$$= 1 - e^{-k_2^2\sqrt{\pi}} - \frac{\pi k_2}{\sqrt{2}} e^{-k_2^2 \frac{\pi}{2}} H\left(k_2\sqrt{\frac{\pi}{2}}\right) \tag{46}$$

where the absolute threshold level $\alpha = k_2 \overline{v_2}$ and the error function, H, is

$$H(x) = \frac{2}{\sqrt{\pi}} \int_0^x e^{-z^2} dz$$

An equation similar to equation 46 has been used by other authors and results from convoluting two Rayleigh distributions.

Using Eq. 44, we can express $P(v_2 \leq \alpha)$ in terms of k_1;

$$P(v_2 \leq \alpha) = 1 - e^{-\frac{k_1^2 \pi}{2}} - \pi \frac{k_1}{2} e^{-k_1^2 \frac{\pi}{4}} H\left(\frac{k_1\sqrt{\pi}}{2}\right) \tag{47}$$

We now define a new Rayleigh random variable, y, whose mean value is equal to that of $v_2(t)$. To do this, let:

$$p(y) = \frac{y}{V_y^2} e^{-\frac{y^2}{2V_y^2}} \tag{48}$$

where: V_y^2 is the mean value of y^2.

The mean of y is;

$$\bar{y} = \int_0^\infty \frac{y^2}{V_y^2} e^{-\frac{y^2}{2V_y^2}} dy = \overline{V_2} = V_y\sqrt{\frac{\pi}{2}} \tag{49}$$

We now want to find a new threshold α', for the equivalent Rayleigh case, so that

$$P(v_2 \leq \alpha) = P(y \leq \alpha') \tag{50}$$

To do this define a k_3 so that:

$$\alpha' = k_3 \bar{y} \tag{51}$$

The probability that y is less than or equal to the new thresold level α' is given by

$$P(y \leq \alpha') = \int_0^{\alpha'} \frac{y}{V_y^2} e^{-\frac{y^2}{2V_y^2}}$$

$$= 1 - e^{-k_3^2 \frac{\pi}{4}} \tag{52}$$

where: $\alpha' = k_3 \bar{y}$.

Using Eqs. 46 and 52, the equation to evaluate k_3 can then be expressed as:

$$1 - e^{\frac{k_1^2\pi}{2}} - \frac{\pi k_1}{2} e^{-\frac{k_1^2\pi}{4}} H\left(\frac{k_1\sqrt{\pi}}{2}\right) = 1 - e^{-\frac{k_3^2\pi}{4}} \tag{52a}$$

We have in effect found a threshold ratio, k_3, for a Rayleigh process which is in some sense equivalent to the threshold ratio for the non-Rayleigh process of $v_2(t)$. We may now use these resultant values of k in the simulation data technique (i.e., Eqs. 29 and 30) directly in order to get approximate equal gain diversity results for the probability of fade. For the two values of k_1 of interest here, namely $k_1 = 0.1$ and $k_1 = .05$, $k_3 = .00721$ and .00181 respectively (from Eq. 52a).

Thus, with the new threshold established this way, we have found that Rayleigh

distribution which spends the same amount of time below the threshold α' as does the actual diversity output distribution below the threshold α. This is one way to approximate the effect of the diversity so that the single channel simulation data can be used to obtain an estimated probability of exceeding a critical fade.

The middle set of curves on Figs. 43 and 44 give the probability results using this method. Critical fade lengths of 0.3 milliseconds, 2.0 millisecond, and 3.75 milliseconds are shown. Consider the 3.75 millisecond case; in an interval (T) of 1 second, the probability of exceeding a fade drops from 0.21 to 0.0033 for k = 0.05 in going from single channel to equal gain diversity. This is a ratio of 640 in probability.

We will now consider another model for a diversity calculation which will use the Rayleigh simulation technique to find the probability of exceeding a critical fade.

2.4 Probability of Critical Fade with Switched Diversity

A two-channel diversity system is here considered in which that channel with the largest signal level at any given time is used as the receiver. Thus a fade occurs only when both channels are below the threshold. This type diversity is basically a "switched" type and corresponds to the "selection" type of switched diversity described in Ref. 22. This type of diversity is considered the classical type. Although the diversity method here is different than that for the equal gain diversity system, the simulation results used before are still employed here. They are used in a somewhat different way, as will be seen.

Again we assume that the single channel signal has a Rayleigh fading characteristic of bandwidth f_b. Here we will again assume independent "samples" (observation periods) every $1/f_b$ seconds. As mentioned before, the simulation results of Ref. 16 demonstrated that this observation period may allow us to assume independent samples.

In addition we will again assume that the probability of a fade in this interval $1/f_b$ seconds is much less than 1, so that we may use equations equivalent to (29) and (30) above. Instead of using P'(0) however, we will have to find the corresponding $P'_{1,2}(0)$ which results from the switched diversity. Thus, the probability of exceeding a critical fade will be given by:

$$P_{1,2}(f_bT, f_bt_o, k_1) \cong 1 - e^{-P'_{1,2}(0)f_bT} \tag{53}$$

where: $P_{1,2}(f_bT, f_bt_o, k_1)$ = probability of exceeding a critical fade t_o in observation time T

T = an arbitrary observation interval greater than $1/f_b$.

The $P'_{1,2}(0)$ will be evaluated by using an observation interval of $1/f_b$ (0.1 seconds). All we need is to find an expression for $P'_{1,2}(0)$. The essential idea is to use the simulated measurements of $P(f_bT, f_bt_o, k)$ from Ref. 16 to achieve a switched diversity $P'_{1,2}(0)$ to use in Eq. 53.

This will be done in the following manner. We can find a $P'_{1,2}(0)$ by letting the fade period t_{01} of the first channel be the observation interval for the possible fades of channel 2. Further, since the basic simulation data (for $P(f_bT, f_bt_o, k)$) is "cumulative" in type, we can form a probability density by differentiating with respect to t_0.

We will now derive the $P'_{1,2}(0)$.

Let $P_1(f_b \cdot 1/f_b, f_bt_{01}, k_1)$ be the probability that 1 or more fades of length $\geq t_0$ occur in an observation time $1/f_b$ on channel 1. Since the observation time equals $1/f_b$, we can assume that the above probability is the probability of just 1 fade of length $\geq t$, i.e., more than one independent fade can never occur in a time $1/f_b$.

Since P_1 is essentially a cumulative distribution the probability density, $\frac{-\partial P_1}{\partial t_{01}}$ is the probability that a fade of length exactly t_{01} occurs in an observation time $1/f_b$ seconds.

Let $P_2(f_bt_{01}, f_bt_0, k)$ be the probability that 1 or more fades of length $\geq t_0$ occur in an observation time t_{01}. Note that the observation time t_{01} here was the "fade length" for channel 1.

Now combining the above comments it is evident that when channel 1 experiences a fade of length t_{01}, and channel 2 experiences a fade of length $\geq t_0$ in this interval t_{01}, the entire two-channel system experiences a fade $\geq t_0$ seconds. Assuming that the fades on each channel are independent, the probability that such a situation will occur is given by:

$$P_{t_{01}}(1, f_bt_0, k) = -\frac{\partial P_1}{\partial t_{01}} \times P_2(f_bt_{01}, f_bt_0, k) \times \Delta t_{01} \tag{54}$$

where: $P_{t_{01}}$ = probability that one or more fades of length $\geq t_0$ occurs in an observation time between t_{01} and $t_{01} + \Delta t_{01}$ in the switched diversity situation.

The total probability that a system fade occurs is then clearly obtained by integrating $-P_{t_{01}}$ over the limits from t_0 to $1/f_b$. The lower limit t_0 is set since the observation period t_{01} cannot be smaller than the fade length of interest t_0. The upper limit $1/f_b$ is set since we chose this as the smallest independent time for P_1 (above) in order to eliminate the occurrence of more than one fade (observation time) of t_{01}. Hence:

$$P_{1,2}(1, f_bt_o, k) = \int_{t_0}^{1/f_b} \frac{-\partial P_1}{\partial t_{01}} \times P_2(f_bt_{01}, f_bt_0, k)\, dt_{01} = P'_{1,2}(0) \tag{55}$$

This integration may be approximated, in the usual manner, by:

$$P'_{1,2}(0) = \sum_{t_0}^{1/f_b} \Delta P_1 \times P_2(f_b t_{01}^*, f_b t_0, k) \qquad (56)$$

where: ΔP_1 = change in P_1 over interval Δt_{01}

t_{01}^* = a median value of t_{01} in Δt_{01}.

As noted before P_1 and P_2 may be found by using the simulation results of Ref. 16, as described in Section 2.2. Then approximate values of $P'_{1,2}(0)$ can be calculated for given values of k. Finally, using these values for $P_{1,2}(0)$, we get from equation (30),

$$P_{1,2}(T, t_0, k_1) \cong 1 - e^{-P'_{1,2}(0) f_b T} \qquad (57)$$

This is the estimated probability of exceeding a critical fade (t_0) when using this idealized switched diversity on a Rayleigh fading link.

It may be noted that, in addition to the assumptions mentioned earlier, this treatment implies an instantaneous switch operation.

The dotted curves of Fig. 43 are plots of $P_{1,2}(f_b T, 10t_0, k_1)$ for $k_1 = 0.05$ and $t_0 = 3.75$ msec, 2.0 msec, and 0.3 msec. The dotted curves of Fig. 44 are similar except that $k_1 = 0.01$.

Consider the improvement of the idealized switched diversity over equal gain diversity for $t_0 = 3.75$ msec at T = 10 seconds. For a k = 0.05 in Fig. 43 it is seen that the probability of a critical fade is reduced from 0.033 to 0.005 in going from equal gain to switched diversity. This is a factor of improvement of about 6.5.

Although the switched diversity model used here indicates an improvement over the equal gain case, it is still true that the system must tolerate fade lengths much greater than 3.75 msec. Immediately below we will indicate the results if the critical fade length was of the order of 50 msec. The change in probability is so great that the results could not be plotted conveniently on Fig. 43 and Fig. 44. A table with these results will be shown in the next section.

2.5 Conclusions

The main concern in this section has been with the influence of fading on the maintenance of synchronization. This synchronization problem becomes more severe as the data rate is increased.

The method used here was to first ascertain the critical fade length, and then to evaluate the probability of exceeding the critical fade length under given conditions. With the method of analysis used here both an equal gain diversity and a switched diversity model were evaluated. Both of these models incorporated data which resulted from a simulation of a single

channel Rayleigh fading.

As sample values for critical fades, we have used some parameters which apply to a digital communication system designed for nonfading conditions. It is not the point here to evaluate this equipment, but rather to simply note the relation between the length of critical fade and the probability of the fade occurring. Also it is useful to establish what order of magnitude is required to get acceptable results.

It was condcluded in Section 2.1 that it is reasonable to consider that critical fades of as long at 50 milliseconds would be tolerable if equipment is designed with this purpose in mind. We could not plot critical fade lengths of 50 milliseconds on Figs. 43 and 44 because of the vast change in scale. Therefore Table III compares the lengths of observation intervals T required to achieve specific probabilities of fade. A comparison is shown for the critical fade lengths of 3.75 milliseconds and 50 milliseconds. For example, with an equal gain diversity, at the level where the probability of a critical fade is .01, the observation interval changes from 3.21 seconds with an equal gain diversity to 2.5×10^5 for the 50 millisecond critical fade. For the switched diversity the numbers change from 20 seconds to 2×10^8 seconds. Since the critical fade was changed by a factor of 10, these great changes in observation interval for an equal probability of fade signify the importance of increasing the tolerable (critical) fade time under Rayleigh fading conditions.

It is pertinent to review again the various assumptions and the conditions that have gone into both the results of Figs. 43 and 44 and those of Table III above. First of all in using the simulation data of Ref. 16 one source of error might be due to the fact that one assumes that the frequency spectrum present in the actual Rayleigh link corresponds to that spectrum which was present in the simulation. The value of P'(0) is a function of this frequency spectrum. In addition the simulated data was not very accurate for k's in the range that we used here.

Another source of error is the assumption that the signals involved in the diversity model are independent. In practice it is known that signals do have some dependence; correlation gets as high as 0.3 in actual cases. This is a source of error in any theoretical evaluation of fading conditions.

In addition to the above assumptions which apply to both diversity models, each diversity model, had its own particular assumptions which are described in the respective section. For example, the switched diversity system required an instantaneous switching action. In practice one would have an averaging time before making a decision to switch the system.

It may also be noted that the switched diversity system can be considered as an idealization of a diversity model. It is clear that the switched diversity results will be better than the equal gain ones. One reason for this is the fact that, if one channel is quite low, and the other slightly above threshold, the equal gain model may cause the resultant to be below

threshold. In the ideal switched case, of course, the fact that one of the channels was slightly above threshold would allow the channel to keep operating. This is sound intuitive reason for expecting that the switched diversity case would show better results.

This concludes the study of the influence of fading on synchronization.

APPENDIX A: COMPUTER PROGRAM, PROBABILITY DISTRIBUTION OF EXTREMA

Main Program

The entire voice tape specimen consisted of 216,000 samples. Each of the 216,000 intervals between samples, corresponding to a clock pulse interval, τ, contained either one extremum or no extremum. A separate program examined these 216,000 intervals and computed whether or not an extremum occurred in a given interval. This information was then punched out on binary cards. The computer program, whose flow diagram is shown, accepts as input this set of binary cards. The data from these cards are read, by a subroutine called READCD, into a vector 6000 computer words long (i.e., 216,000 bits). Each sample (or bit) is either a 0, signifying no extremum at the corresponding time interval on the voice tape specimen, or a 1, signifying an extremum at that time.

Let $\underline{N'}$ be the number of parallel channels, in talk burst $0 < N' \leq 24$; $\underline{\ell}$ be the length, in bits or samples, of a channel, $\ell = 216{,}000/N'$; Δ_i be the ith clock pulse interval for the N' parallel channels, $1 \leq k \leq N'$. The main program computes t_k by a subroutine, COUNT 1. The subroutine counts the number of extrema, $\underline{k}$, in each Δ_i, from i = 1 to $i = \ell$. A running sum, $t_k = t_k + 1$, is kept for each occurrence of k and the final sums, t_k, are returned to the main program.

The following quantities are then computed and printed out:

1. The observed frequency of occurrence, r(k), of $\underline{k}$ extrema:

$$r(k) = \frac{t_k}{\ell} = \frac{N' t_k}{216{,}000}, \qquad 0 \leq k \leq 24$$

2. $\lambda = \dfrac{N' \times T}{216{,}000}$, where $T = \sum_{k=0}^{N'} k t_k$, i.e., T is the total number of extrema on the tape.

3. The Poisson values, $p(k, \lambda)$, for $\underline{k}$ extrema:

$$p(k, \lambda) = e^{-\lambda} \frac{\lambda^k}{k!}, \qquad 0 \leq k \leq 24$$

4. The discrepency, pe(k)

$$pe(k) = 1. - \frac{r(k)}{p(k, \lambda)}, \qquad 0 \leq k \leq 24$$

Standard Deviation Program

The above program average all distributions r(k) over 216,000/N' equivalent clock pulse intervals. Here groups of 900 consecutive Δ's each (equivalent to $\omega = 25$ computer words) are examined. There are $v = 216{,}000/N \times 900$ such groups.

Letting $v = \ell/900$; $\bar{x}(k) = r(k)$, $0 \leq k \leq 24$, the main program calls on the subroutine COUNT 2. repeatedly, specifically v times. COUNT 2. is the same as COUNT 1. except for the new size of the groups over which the t_k's are computed, i.e., groups of $m = 25$ words instead of $m = \ell/36$ words. For each value of N', a set of relative frequencies, $r_m(k)$, are computed and printed out:

$$r_m(k) = \frac{t_{k_m}}{900} \qquad \begin{matrix} 0 \leq k \leq 24 \\ 1 \leq m \leq v \end{matrix}$$

The standard deviations of k, $\sigma(k)$, are computed and printed out before returning to the beginning of the program for a new N'.

$$\sigma(k) = \sqrt{\frac{\sum_{m=1}^{v} [r_m(k) - \bar{x}(k)]^2}{v}} \qquad 0 \leq k \leq 24$$

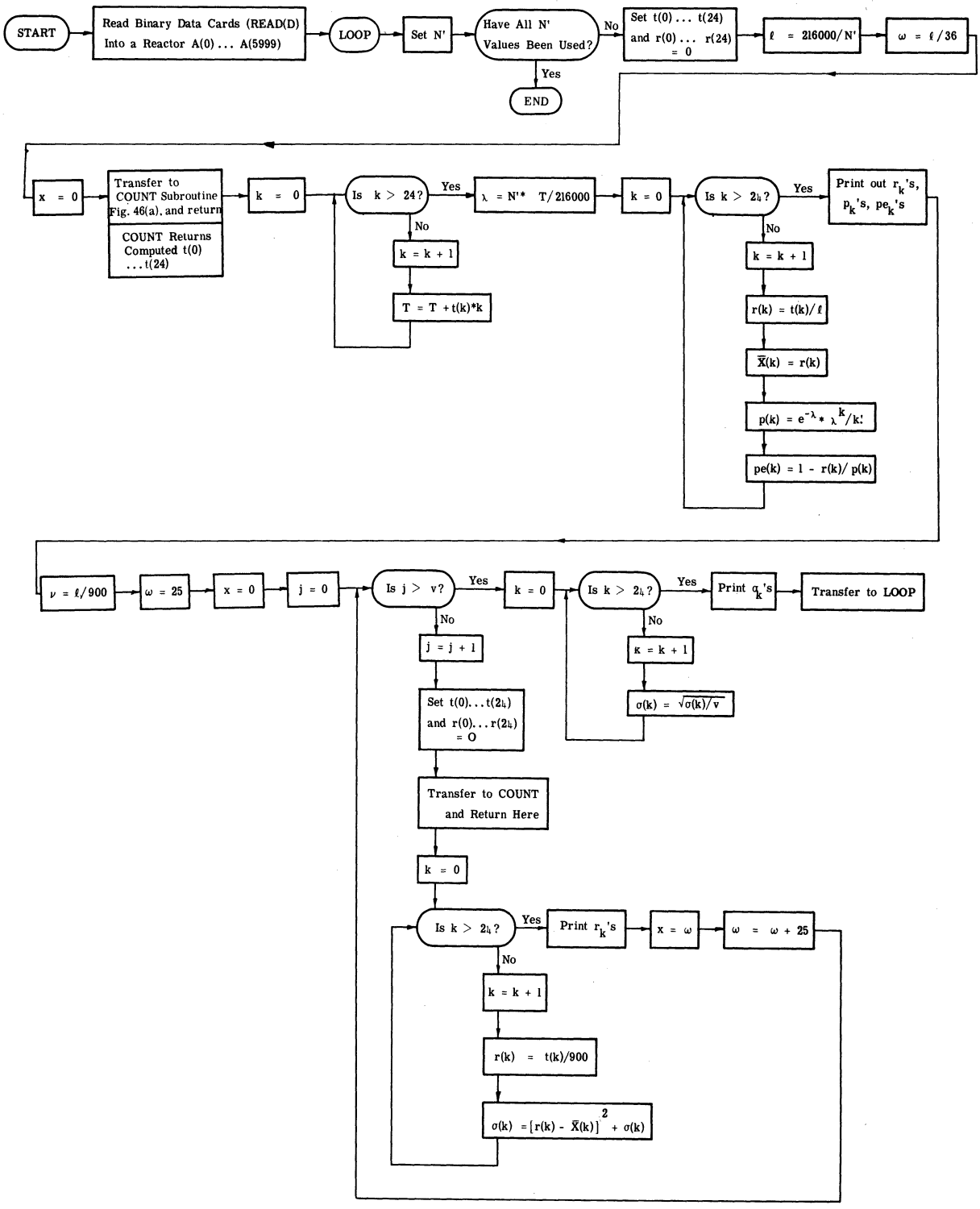

Fig. 46. Computer flow diagram for Probability distribution of extrema.

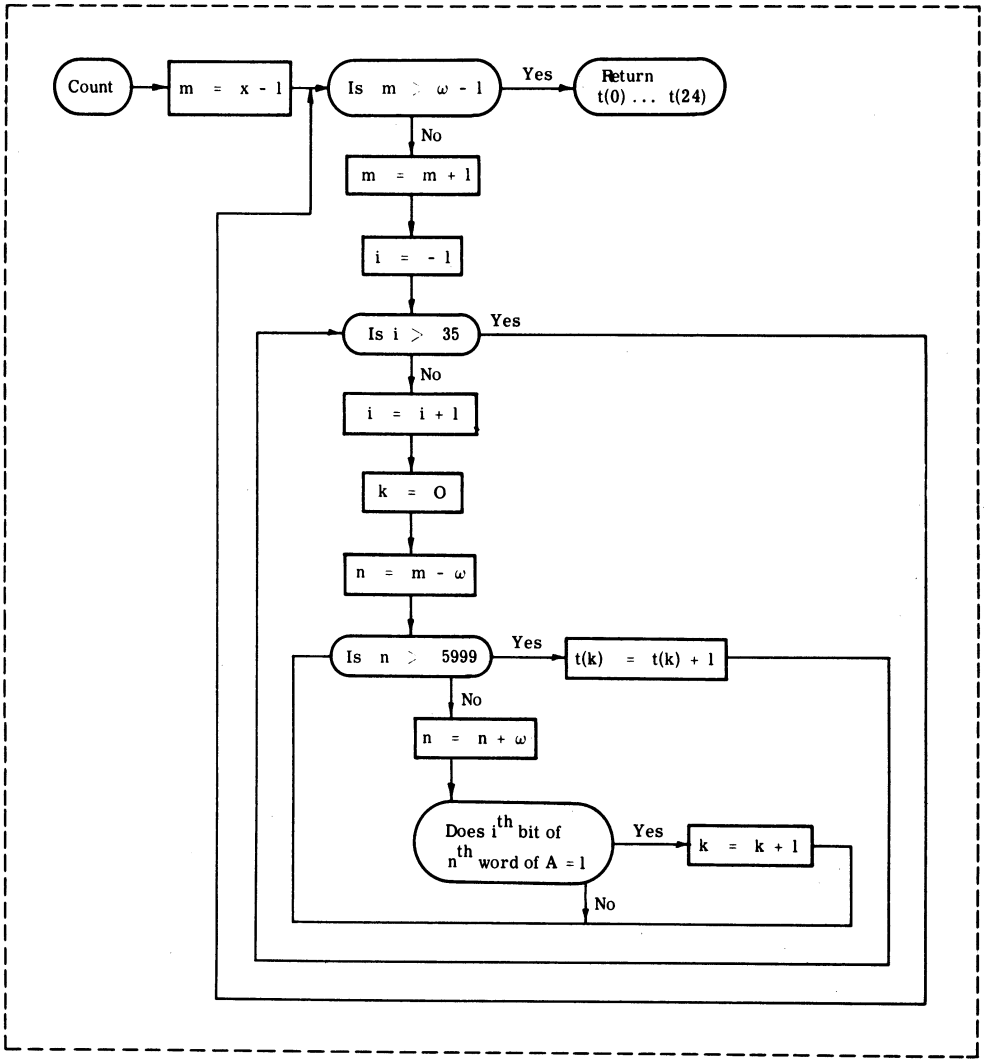

Fig. 46(a). COUNT subroutine.

APPENDIX B: COMPUTER PROGRAM FOR A MULTICHANNEL SYSTEM SIMULATION

A computer program is here described for testing a 24 channel system using the techniques of Section 3.3. The simulation of 23 channels is performed for 10 seconds before the 24th channel, the voice channel, is added to the system. This insures that the starting conditions of the 23 channels will not affect the analysis. The 23 channel simulation was discussed before in Section 3.3.1 and is here elaborated on. After deleting several extrema from the voice tape, as determined by the computer run, the remaining extrema are put onto a new tape. This new tape may then be processed in the usual manner to retrieve an audio reproduction of the original speech with the effect of the buffer included.

The input tape for this program is a high density tape, each record of which corresponds to approximately 14,000 25 μsec samples of the original low density voice tape. Each of these records consists of the location and amplitude of the extrema points on the original voice tape. The location is an interger count of the corresponding 25 μ-second interval. One record at a time is read into computer storage and processed. These records correspond to the actual voice channel, while 23 other voice channels are simulated by the program.

This simulation begins by assuming that 13 percent of the 23 channels are in resumption pauses; 13 percent are in type II talk bursts; and the remaining 74 percent are in type I talk bursts. This assumption means that we use the functions, $p_1(x)$, $f_2(x)$ and $f_1(x)$ respectively, to compute the starting time lengths or intervals which are stored appropriately in T(1) . . . T(23). Another starting assumption is to look at half of these channels, T(1) . . . T(12); and let N' (the number of channels in simultaneous talk bursts) equal the number of this half which were computed by $f_2(x)$ or $f_1(x)$. Thus only half of the talkers are transmitting information in the direction of interest.

Having initialized in the above manner, successive talk and pause times are then computed on the simulated channels in accordance with the method illustrated in Fig. 17 of the text. As new values of time are computed, they are placed in T(1), T(2), etc. so that T(1) . . . T(23) is always an up-to-date record of when the next changes will occur on all channels. These changes may be from talk bursts to a pause, or from a pause to a talk burst. This is illustrated by the following statement. Given the initial set of time values and the above method the following three operations are performed: 1) search for smallest current value of T(1) . . . T(24), called T(ℓ); 2) subtract T(ℓ) from all T's', and 3) compute a new time by the appropriate function for this $\underline{\ell}$ channel. This process is repeated until the delay time (DELAY) has been exceeded. At this point the main section of the program (LOOPA) is entered.

LOOPA: Again the simulated channel with the smallest time interval is found, $T(\ell)$, and the rest of the program runs for this number of clock pulses. (A running count (CP) of clock pulses is kept.) N', the number of channels in talk bursts, is computed for each new $T(\ell)$.

For each clock pulse the number of extrema, k, existing on the simulated channels is selected from a Poisson-distribution stored in a matrix, called Table. N' is used as the raw index on the matrix. A random number, r, is generated, $0 \leq r \leq 1$ and this number is located as an element of the N' raw, i.e., $T_{N'(k-1)} < r \leq T_{N'K}$. K, the upper column index, is taken as the number of extrema on the simulated channels. The buffer state, B, is computed, i.e., $B = B + k$. In order that an extremum on the voice channel be deleted, three conditions must be met:

1) The clock pulse count, CP, must match the location of an extremum on the voice channel. If this is true, $B = B + 1$.
2) The buffer state B must be greater than 16: $B > 16$.
3) $\frac{(B - 16)}{k + 1}$ must be $>r$, where r is a random number generated at this point each time.

When all of these conditions are met, the current extremum on the voice channel is frozen out. Otherwise the buffer state is recomputed by equations:

1) If $B > 16$, $B = 15$
2) If $1 \leq B \leq 16$, $B = B - 1$
3) If $B = 0$, no change.

This main section is continued for a time equal to $T(\ell)$. $T(\ell)$ is then subtracted from all other channel times and a new time interval computed and stored in $T(\ell)$. Then a return is made to LOOPA, i.e., a new smallest time interval, or $T(\ell)$, is found. The process is continued until all input records have been examined or, equivalently, until we have simulated a run of the same time span as the original voice tape.

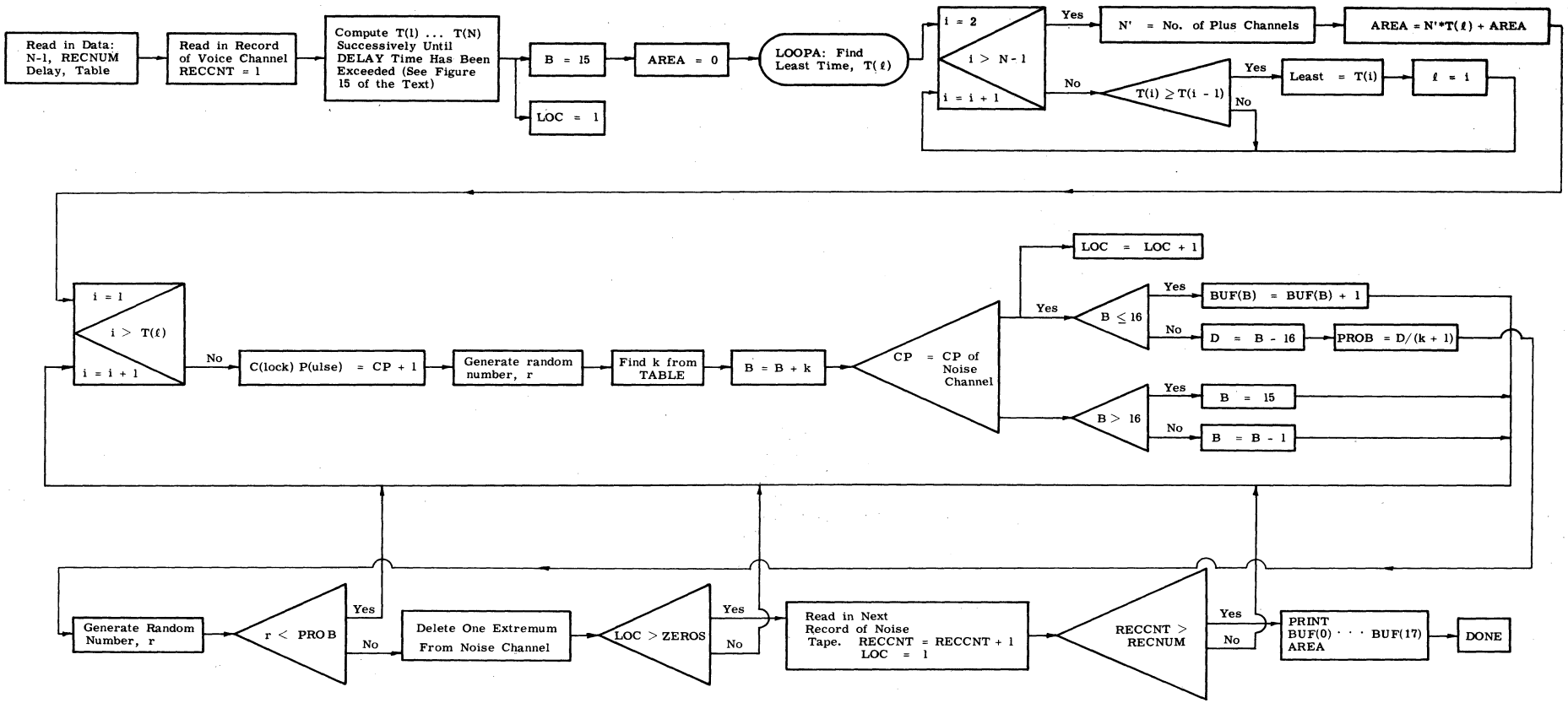

N' = Number of Channels to be Simulated
RECNUM = Number of Records on Noise Tape
ZEROS = Number of Extrema per Record
DELAY = Number of .001 Seconds Intervals to Delay (10 Seconds or 10000 intervals)
TABLE = Matrix of Poisson Values: N rows and 10 columns, $0 \leq k \leq 10$.

Fig. 47. Computer flow diagram for 24 channel system test.

APPENDIX C: COMPUTER PROGRAM FOR EXTREMAL CODING SYSTEM SIMULATION

This appendix describes the computer program for the single channel extremal coded experiments described in Section 4.1.

1. Variable Initialization

This section clears or initializes various storage areas which will be used during the computation phase (i.e., sets the initial conditions for the program.). Initial conditions are set for the following variables: PRINT (N), PLOT (N), FREQ (N), PLIM, WRDCNT, SAMPLE, ZEROS, RECNUM, SKPRCD, SKIPFL, and QUAN(N). Note: QUAN(N) is used to quantize the extrema after the location has been determined by FINXT. Initially the quantization law is set such that no quantization occurs, i.e., QUAN(O) = 0, QUAN(1) = 1, . . . , QUAN(511) = 511. It is this initial law which is placed in storage during the variable initialization.

If the output record is to be quantized by a different table, it will have to be submitted as data.

2. Input Data

The following variables must always be supplied as data: STOP = $ YES $

This will stop the computer so the operator can mount the data tape and output tape.

RECCNT = n

This is the count of the number of records on the data tape. $0 < n \leq 60$

KC = n

The sampling rate in samples/sec.

The following variables are optional:

PRINT(1) = $ YES $, PRINT(5) = $ YES $, . . . , PRINT(n) = $ YES $

The packed samples, unpacked samples, and calculated samples of any record n whose PRINT(n) = $ YES $ will be printed.

PLOT(1) = $ YES $, PLOT(9) = $ YES $, . . . , PLOT(n) = $ YES $

A printer plot will be given of any record n whose PLOT(n) = $ YES $.

PLIM = n

n will be number of samples on each end of record that will be plotted. If PLOT(n) = $ YES $ is given and PLIM is not given the first and last 400 samples will be plotted.

SKIPFL = n

The output tape is normally started at the beginning, but if for some reason there is information on the beginning of the tape (recorded by files) that must be saved, this will skip n files. One run through this program of n records will produce n records on the program output tape and one (1) file.

SKPRCD = n

The data input tape may be positioned to the nth record if desired. The records 1 through n - 1 will be counted but not processed.

QUAN(0) = 0, 2, 2, 4, 4, 4, 4, 8, . . .

If need be the QUAN table can be changed. In the previous example an extrema with a value of 3 will be recoded with a value of 4, 4 → 4, 5 → 4, 6 → 4, 7 → 8, etc. The original signs will be retained automatically.

3. READTP

Reads one record of data from the program input tape, unpacks and converts the data from the format of the A to D Unit to an equivalent computer representation. Various checks are made on the data to insure reliable operation of the A to D converter and recording of the data. If a data record is unacceptable an appropriate comment is printed.

4. DERIV

This section of program determines the bounds in which an extrema lies. The entire record is scanned and areas in which extremum lie are saved for further processing. The methods for determining these bounds make use of the "center window" discussed in Section 4.1 of this report. (See also Figure 24)

5. FINXT

The "extrema bounded area" is scanned for the actual value and location of the proper extrema. The largest numerical sample is chosen if the general trend of the curve is approaching a maximum or the smallest value if the trend is toward a minimum. If more than one sample could be considered the extrema, the location of the first possible extrema will be used. That is, if in the range determined by DERIV, the maximum (or minimum) value is attained by several samples, the extrema location is chosen to correspond with the first possible extrema.

6. CURVE

The extrema are quantized using the QUAN table and the samples between two consecutive extrema are filled in by the following relationship; $f(x) = x^2 (3 - 2x)$ where the amplitude has been normalized to 1 and x is the normalized time $\left(\text{i.e., } x = \frac{t - t_1}{t_2 - t_1}\right)$.

7. PACKWT

Converts and repacks the samples into the proper D to A format and writes the record onto the program output tape.

8. S/N

Calculate signal/noise ratio

$$S/N = 10 \log \frac{\sum_i \hat{f}_{in}^2(t_i)}{\sum_i \left[f_o(t_i) - f_{in}(t_i)\right]^2}$$

9. PACKX

Writes onto the program output tape an equivalent length record of no signal. This will occur if a data record cannot be processed or if no extrema exist in the record (i.e., pause in the speech).

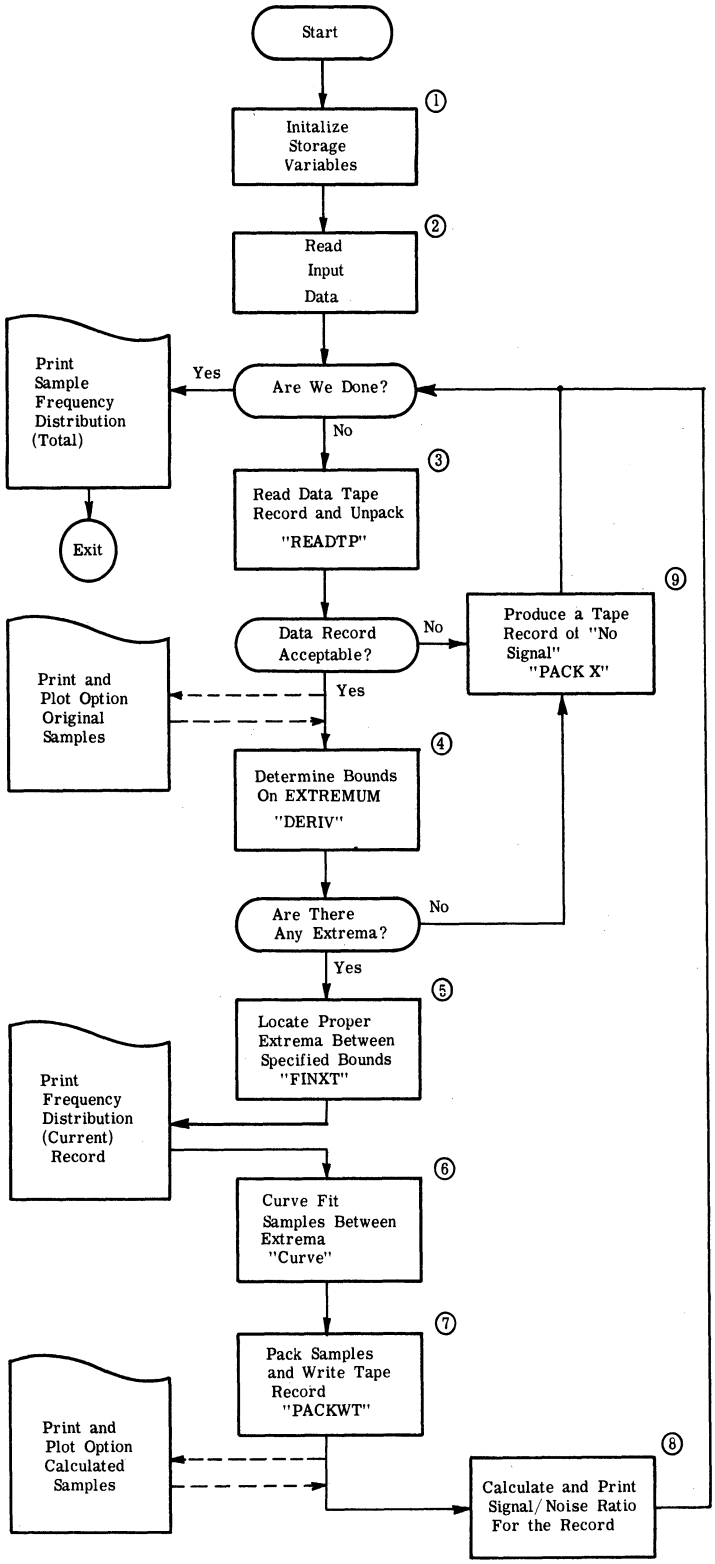

Fig. 48. Computer flow diagram for Extremal coding system simulation.

LIST OF REFERENCES

1. M. P. Ristenbatt, T. G. Birdsall, T. Felisky and S. B. Weinstein, Digital Communication Studies, Cooley Electronics Laboratory Technical Report No. 133, The University of Michigan, Ann Arbor, Michigan, April 1962.
2. R. Filipowsky, "Ein Mehrkanal-Impülsubertragungsverfahren mit automatisch veränderlicher Impulszahl," Österreichische Zeitschrift für Telegraphen-Telephon-, Funk- und Fernsehtechnik, Vols. 9-10, 11-12, pp. 113-129, pp. 147-158; September-October, November-December, 1955.
3. R. J. Filipowsky, "Digital Data Transmission Systems of the Future," IRE Trans. on Communications Systems, Vol. CS-9, March 1961, pp. 88-96.
4. M. V. Mathews, "Extremal Coding for Speech Transmission," IRE Trans. on Information Theory, Vol. IT-5, September 1959, pp. 129-136.
5. L. R. Spogen, et al., "Speech Processing by the Selective Amplitude Sampling System," J. Acoust. Soc. Am., Vol. 32, December 1960, pp. 1621-1625.
7. T. G. Birdsall, M. P. Ristenbatt, and S. B. Weinstein, "Analysis of Asynchronous Time Multiplexing of Speech Sources," IRE Trans. on Communications Systems, Vol. CS-10, December 1962, pp. 390-397.
8. K. Bullington and J. M. Fraser, "Engineering Aspects of TASI," AIEE, July 1959.
9. O. J. Murphy and A. C. Norvine, "Characteristic Time Intervals in Telephone Conversation," Bell System Technical Journal, April 1938, pp. 281-291.
10. P. E. Harris, "Radar Boxcar Circuits Using Nuvistors," Electronics, September 15, 1961, pp. 66-67.
11. G. F. Montgomery, "A Comparison of Amplitude and Angle Modulation for Narrow-Band Communication of Binary-Coded Messages in Fluctuation Noise," Proc. IRE, February 1954, pp. 447-454.
12. A. A. Meyerhoff and W. M. Mazer, Microwave Radio Relay Systems Study, Final Report, Task II, Radio Corporation of America, New York, New York, August 31, 1959.
13. du Castel and Magnen, "Etude de la Qualite Telegraphique dans les Faisceaux Hertzians Transhorizons," Ann Telecommun, Vol. 14, March-April 1959, pp. 99-108.
14. B. B. Barrow, "Error Probabilities for Telegraph Signals Transmitted on a Fading FM Carrier," Proc. IRE, Vol. 18, September 1960, pp. 1613-29.
15. D. E. Johansen, "Binary Error Rates in Fading FDM-FM Communications," IRE PGCS, September 1961, pp. 206-214.
16. R. R. Favreau, H. Low and I. Pfeffer, "Evaluation of Complex Statistical Functions by an Analog Computer," IRE Nat. Conv. Record, Computers, 1956, pp. 31-37.
18. W. Hatton, et al., Second Semi-Annual Progress Report for Pulse Code Modulation Systems, Vol. 1, Raytheon Company, Waltham, Massachusetts, 15 June 1959 to 14 December 1959.
19. Defense Systems Dept., General Electric Co., "Introduction to FSK Data Transmission System," AD 272108.

20. H. B. Voelcker, "Phase-Shift Keying in Fading Channels," I.E.E., January 1960, pp. 31-38.

21. Letter from Lt. A. W. Drake, Communications Security Branch of USAELRDL, Fort Monmouth, N. J.

22. D. G. Brennan, "Linear Diversity Combining Techniques," Proc. I.R.E., June 1959, pp. 1075-1102.

DISTRIBUTION LIST

(One copy unless otherwise noted)

OASD (R&E), Rm 3E1065
ATTN: Technical Library
The Pentagon
Washington 25, D.C.

Chief of Research and Development
OCS, Department of the Army
Washington 25, D.C.

Commanding General
U. S. Army Materiel Command
ATTN: R&D Directorate
Washington 25, D.C.

Commanding General
U. S. Army Electronics Command
ATTN: AMSEL-AD
Fort Monmouth, N. J. (3 copies)

Commander, Armed Services Technical Information Agency
ATTN: TISIA
Arlington Hall Station
Arlington 12, Virginia (10 copies)

Commanding General
USA Combat Developments Command
ATTN: CDCMR-E
Fort Belvoir, Virginia

Commanding Officer
USA Communication and Electronics Combat Development Agency
Fort Huachuca, Arizona

Commanding General
U. S. Army Electronics Research and Development Activity
ATTN: Technical Library
Fort Huachuca, Arizona

Chief, U. S. Army Security Agency
Arlington Hall Station
Arlington 12, Virginia (2 copies)

Commanding Officer
U. S. Army Electronics Materiel Support Agency
ATTN: SELMS-ADJ
Fort Monmouth, New Jersey

Director, Fort Monmouth Office
USA Communication and Electronics Combat Development Agency
Fort Monmouth, New Jersey

Corps of Engineers Liaison Office
U. S. Army Electronics Research & Development Laboratory
Fort Monmouth, New Jersey

Marine Corps Liaison Office
U. S. Army Electronics Research & Development Laboratory
Fort Monmouth, New Jersey

AFSC Scientific/Technical Liaison Office
U. S. Army Electronics Research & Development Laboratory
Fort Monmouth, New Jersey

Commanding Officer
U. S. Army Electronics Research & Development Laboratory
ATTN: Logistics Division (Mr. A. Boniello, SELRA/ND-4)
Fort Monmouth, New Jersey (7 copies)

Commanding Officer
U. S. Army Electronics Research & Development Laboratory
ATTN: Director of Research/Engineering
Fort Monmouth, New Jersey

Commanding Officer
U. S. Army Electronics Research & Development Laboratory
ATTN: SELRA/ND-4
Fort Monmouth, New Jersey

Commanding Officer
U. S. Army Electronics Research & Development Laboratory
ATTN: Technical Information Division
Fort Monmouth, New Jersey (3 copies)

Director
National Security Agency
ATTN: R12 (M. Klein)
Fort George Meade, Maryland

Deputy President
U. S. Army Security Agency Board
Arlington Hall Station
Arlington 12, Virginia

Director, U. S. Naval Research Laboratory
ATTN: Code 2027
Washington 25, D.C.

Commanding Officer and Director
U. S. Navy Electronics Laboratory
San Diego 52, California

Aeronautical Systems Division
ATTN: ASAPRL
Wright-Patterson Air Force Base, Ohio

Air Force Cambridge Research Laboratories
ATTN: CRZC
L. G. Hanscom Field
Bedford, Massachusetts

Air Force Cambridge Research Laboratories
ATTN: CRXL-R
L. G. Hanscom Field
Bedford, Massachusetts

Hq, Electronic Systems Division
ATTN: ESAI
L. G. Hanscom Field
Bedford, Massachusetts

Rome Air Development Center
ATTN: RAALD
Griffiss Air Force Base, New York

Commanding Officer
U. S. Army Electronics Research & Development Laboratory
ATTN: Technical Documents Center
Fort Monmouth, New Jersey

AFSC Scientific/Technical Liaison Office
U. S. Naval Air Development Center
Johnsville, Pennsylvania

U. S. National Bureau of Standards
Boulder Laboratories
ATTN: Library
Boulder, Colorado